Iranian Journal of Numerical Analysis and Optimization

Volume 4 , Number 1

Winter 2014

Ferdowsi University of Mashhad, Iran

In the Name of God

Iranian Journal of Numerical Analysis and Optimization (IJNAO)

This journal is authorized under the registration No. 174/853 dated 1386/2/26, by the Ministry of Culture and Islamic Guidence.

Volume 4, Number 1, Winter 2014

ISSN: 1735-7144

Publisher: Faculty of Mathematical Sciences, Ferdowsi University of Mashhad

Published by: Ferdowsi University of Mashhad Press

Circulation: 250

Address: Iranian Journal of Numerical Analysis and Optimization

Faculty of Mathematical Sciences, Ferdowsi University of Mashhad

P.O. Box 1159, Mashhad 91775, Iran.

Tel-Fax: +98-511-8828606

E-mail: mjms@um.ac.ir

Website: http://jm.um.ac.ir/index.php/math

This journal is indexed by:

• Mathematical Review

• Zenteralblatt

• ISC

به اطلاع کلیه محققان، پژوهشگران، اساتید ارجمند، دانشجویان تحصیلات تکمیلی و نویسندگان محترم می رساند که IJNAO طبق مجوز شماره ۳/۱۸/۵۴۸۹۱۳/ مورخه ۱۳۹۲/۱۰/۲۵ مدیر کل محترم سیاست گذاری و برنامه ریزی امور پژوهشی وزارت علوم، تحقیقات و فناوری، علمی – پژوهشی میباشد.
بر اساس نامه شماره ۹۲/۱۵۳۶/پ مورخه ۱۳۹۲/۱۱/۲۱ سرپرست محترم معاونت پژوهشی وفناوری پایگاه استنادی علوم جهان اسلام، مجله ایرانی آنالیز عددی و بهینه سازی در پایگاه ISC نمایه شده است.

Iranian Journal of Numerical Analysis and Optimization

Volume 4, Number 1, Winter 2014

Ferdowsi University of Mashhad - Iran

Iranian Journal of Numerical Analysis and Optimization

University of Technology, Tehran.
e-mail: nezamm@sina.sharif.edu
Salehi Fathabadi, H.*
(Operations Research)
School of Mathematics, Statistics and Computer Sciences,
University of Tehran, Tehran.
e-mail: hsalehi@ut.ac.ir
Soheili, A.*
(Numerical Analysis)
Department of Applied Mathematics,
Ferdowsi University of Mashhad, Mashhad.
e-mail: soheili@um.ac.ir
Taghizadeh Kakhki, H.**
(Operations Research)
Department of Applied Mathematics,
Ferdowsi University of Mashhad, Mashhad.
e-mail: taghizad@math.um.ac.ir
Toutounian, F.*
(Numerical Analysis)
Department of Applied Mathematics,
Ferdowsi University of Mashhad, Mashhad.
e-mail: toutouni@math.um.ac.ir

This journal is published under the auspices of Ferdowsi University of Mashhad

---

* Full Professor

** Associate Professor

We would like to acknowledge the help of Narjes khatoon Zohorian in the preparation of this issue.

Letter from the Editor in Chief

I would like to welcome you to the Iranian Journal of Numerical Analysis and Optimization (IJNAO). This journal is published biannually and supported by the Faculty of Mathematical Sciences at the Ferdowsi University of Mashhad. Faculty of Mathematical Sciences with three centers of excellence and three research centers is well-known in mathematical communities in Iran.
The main aim of the journal is to facilitate discussions and collaborations between specialists in applied mathematics, especially in the fields of numerical analysis and optimization, in the region and worldwide.
Our vision is that scholars from different applied mathematical research disciplines, pool their insight, knowledge and efforts by communicating via this international journal.
In order to assure high quality of the journal, each article will be reviewed by subject-qualified referees.
Our expectations for IJNAO are as high as any well-known applied mathematical journal in the world. We trust that by publishing quality research and creative work, the possibility of more collaborations between researchers would be provided. We invite all applied mathematicians especially in the fields of numerical analysis and optimization to join us by submitting their original work to the Iranian Journal of Numerical Analysis and Optimization.

Mohammad Hadi Farahi

Contents

Iranian Journal of Numerical Analysis and Optimization
Vol 4, No. 1, (2014), pp 1-24

High order immersed interface method for acoustic wave equation with discontinuous coefficients

J. Farzi* and S. M. Hosseini

Abstract

This paper concerns the numerical solution of the acoustic wave equation that contains interfaces in the solution domain. To solve the interface problems with high accuracy, more attention should be paid to the interfaces. In fact, any direct application of a high order finite difference method to these problems leads to inaccurate approximate solutions with high oscillations at the interfaces. There is however, the possibility of deriving some high order methods to resolve this phenomenon at the interfaces. In this paper, a sixth order immersed interface method for acoustic wave equation is presented. The order of accuracy is also maintained at the discontinuity using the jump conditions. Some numerical experiments are included which confirm the order of accuracy and numerical stability of the presented method.

Keywords: Interface methods; High order methods; Lax-Wendroff method; Discontinuous coefficients; Jump conditions.

1 Introduction

In this paper we develop a class of high order numerical methods for wave equations with discontinuous coefficients. The class of interface problems involves many problems of real world applications in Science and Engineering, such as Seismology, Ocean acoustics, and Electromagnetic. A nave implementation of high order methods fails to achieve high order accuracy and

* Coresponding authour
Received 24 September 2013; revised 2 December 2013; accepted 11 December 2013
J. Farzi
Department of Mathematics, Tarbiat Modares University, P.O. Box 14115-175, Tehran, Iran.
Department of Mathematics, Sahand University Of Technology, P.O. Box 51335-1996, Tabriz, Iran. e-mail: farzi@sut.ac.ir

S. M. Hosseini
Department of Mathematics, Tarbiat Modares University, P.O. Box 14115-175, Tehran, Iran. e-mail: hossei_m@modares.ac.ir

produces some spurious oscillations (Gibbs phenomenon) near the discontinuity. There are several approaches to deal with such a problem of accuracy loss. An efficient method for the simulation of these equations should be able to reduce dispersion and dissipation errors in the propagation of the solution [16]. Many researchers are interested in high order methods for hyperbolic problems. Long time behavior of the solution of these problems is an important challenge to the numerical simulation of such problems.

A good deal of literature exists on the numerical solution of interface problems. Two traditional methods are adding viscosity to the problem and using flux limiters [5]. A recent approach is using essentially nonoscillatory (ENO) or weighted ENO methods [6]. We distinguish the interface methods in two sets with or without use of jump conditions. The first set consists of those methods, such as the recent works of Gustafsson and his coworkers [3, 4] and Leveque [8] that do not impose jump conditions in the formulation of the numerical solution of these equations. These methods are based on shock capturing methods and Riemman solvers for conservation laws. The second set, whose history goes back to the pioneering work of Peskin [11] for the simulation of blood flow in the heart, consists of those methods that use some sort of jump condition in their formulation. In fact, to achieve high order results, it is recommended to use a special high order method in the vicinity of the discontinuity. Derivative matching methods is a related issue and have been developed by Driscoll and Fornberg [1] for one and two dimensional Maxwell equations and followed by many others researcher such as Zhao and Wei [19], which derived a derivative matching approach based on the FDTD schemes for Maxwell equations. This scheme is based on fictitious point method and in a vicinity of the interface they introduce original points in one side and ghost or fictitious points (unknown values) in the other side of the interface. Using the derivative matching conditions the values at the ghost points are evaluated. The emphasis in this paper is on the second set of methods that use physical jump conditions at the interface which are usually easily accessible from the physical properties of the problem. Therefore, we perform the numerical solutions to satisfy these jump conditions. The immersed interface method (IIM) considers a standard method for the regular points and imposes a new method for the irregular points to update the solution at the next time level with the same accuracy as the standard method. The implementation of this new method requires the solution of several small linear systems to obtain coefficients of the difference method on the irregular points, without imposing any significant computational cost on the calculations. The explicit relations between two media (in heterogeneous media) through jump conditions eliminate the role of the fictitious points and therefor, this method attains the high order results without ghost points. There is a related class of methods, known as simplified immersed interface methods, that modify explicitly the numerical values at the irregular points [12, 17].

The immersed interface method has been discussed for various kinds of partial differential equations and its implementation to many real world ap-

plications has been successful. A full review of this method for interface problems of parabolic and elliptic type is available in the recent book of Li and Ito [10].

In this paper, a sixth order method for the acoustic wave equation with discontinuous coefficients is presented. This higher order method in some sense is an improvement on the works of Zhang and LeVeque [18] and Farzi and Hosseini [2]. There are several methods for the simulation of the time evolution for the wave equation. The Lax-Wendroff method is a simple time discretization method for implementation. However, to reduce possible dispersion and dissipation errors one can invoke TVD and WENO methods to avoid oscillations near the discontinuity [6, 9]. In this paper, we consider a coupled application of Lax-Wendroff and the immersed interface method on the interface. The contribution of this paper is given in the next sections. The extension of this method to any order is direct and is given in Section 4. The stability analysis and implementation of the method for two dimensional problems is presented in Section 5. Physical jump conditions are demonstrated for the one dimensional acoustic wave equation.

The explicit and closed form discretization formula is obtained in Section 2. The theory and numerical results are also developed for piecewise smooth coefficients (Sections 3, 4 and 5). The numerical results reported in Section 5 confirm the efficiency of the method to approximate the solution with a well presented behavior of wave propagation and also a high order accuracy at the interfaces. The long time behavior of the method is illustrated by Test problem 3 in numerical results. The order of the new immersed interface method is justified in Test problem 4 with numerical order of accuracy. Numerical stability of the method is addressed in Test problem 5.

2 Acoustic Wave Equation

Let $u(x,t)$ and $p(x,t)$ be the acoustic velocity and acoustic pressure, respectively. Then the one-dimensional wave equation can be written as the following model problem

$$U_t + AU_x = 0, \tag{1}$$

where,

$$U(x,t) = \begin{pmatrix} u \\ p \end{pmatrix}, \quad A(x) = \begin{pmatrix} 0 & \frac{1}{\rho} \\ \kappa & 0 \end{pmatrix}, \tag{2}$$

and $A(x)$ is a function of position consisting of physical quantities such as density $\rho(x)$, sound speed $c(x)$ and $\kappa = \rho c^2$. We first focus mainly on problems in which the density and sound speed are piecewise constant functions and have a jump discontinuity at the point $x = \alpha$, which we call the interface,

$$(\rho, c) = \begin{cases} (\rho^-, c^-),\ x < \alpha, \\ (\rho^+, c^+),\ x > \alpha, \end{cases} \tag{3}$$

Then application of our formulation for problems with more general piecewise smooth coefficients will be addressed. Typical applications in which this assumption is appropriate include long range underwater acoustics, various seismological problems as well as electromagnetic problems. Throughout the paper we use the symbol A^+ for $A(x)$ with $x > \alpha$ and A^- for $A(x)$ with $x < \alpha$. The same meaning will apply to other matrices.

In this part, we derive a high order method for this equation and we postpone the treatment of the nonsmooth solution at the interface to the next sections, where we discuss and derive jump conditions and give an approximation that extends the high accuracy of the solution, obtained for the smooth regions, to the interface. At the left or right of the point of discontinuity we can use any standard method. The Lax-Wendroff method is a simple time evolution explicit method for implementation which uses the values at the current time level and does not need any knowledge of previously calculated values. This method is based on Taylor series expansion in time and substitution of the time derivatives with space derivatives using (1). We consider

$$\begin{aligned} U(x_j, t_{n+1}) \approx U(x_j, t_n) &+ \frac{k}{1!}\frac{\partial U}{\partial t}(x_j, t_n) + \frac{k^2}{2!}\frac{\partial^2 U}{\partial t^2}(x_j, t_n) \\ &+ \frac{k^3}{3!}\frac{\partial^3 U}{\partial t^3}(x_j, t_n) + \frac{k^4}{4!}\frac{\partial^4 U}{\partial t^4}(x_j, t_n) + \frac{k^5}{5!}\frac{\partial^5 U}{\partial t^5}(x_j, t_n) \\ &+ \frac{k^6}{6!}\frac{\partial^6 U}{\partial t^6}(x_j, t_n) \end{aligned} \tag{4}$$

where k is the length of the time steps. Replacing the time derivatives by the space derivatives and discretizing the space derivatives we get

$$\begin{aligned} U(x_j, t_{n+1}) \approx U(x_j, t_n) &- \frac{1}{1!}kA_jQ_6^{(1)}U(x_j, t_n) + \frac{1}{2!}k^2c_j^2Q_6^{(2)}U(x_j, t_n) \\ &- \frac{1}{3!}k^3c_j^2A_jQ_4^{(3)}U(x_j, t_n) + \frac{1}{4!}k^4c_j^4Q_4^{(4)}U(x_j, t_n) \\ &- \frac{1}{5!}k^5c_j^4A_jQ_2^{(5)}U(x_j, t_n) + \frac{1}{6!}k^6c_j^6Q_2^{(6)}U(x_j, t_n), \end{aligned} \tag{5}$$

where $A_j = A(x_j)$ and $c_j = c(x_j)$, $Q_p^{(q)}$ is central difference formula of order p for $\frac{\partial^q}{\partial x^q}$ [5] and we have used the relation $A^2 = c^2 I$, in which I is the 2×2 identity matrix.

Substitution of $Q_p^{(q)}$ as explained in [2], which deals only with the advection equation, gives a fully discretized representation of the acoustic equation by the following matrix-vector equation

$$U_j^{n+1} = U_j^n + \sum_{l=1}^{7} \Gamma_{j,l} U_{j+l-4}^n \tag{6}$$

where the $\Gamma_{j,l}$'s are two by two matrices (coefficient matrices) and can be expressed as

$$\Gamma_{j,l} = w_l A(\lambda A + (4-l)I), \qquad j,l = 1,2,...,7, \tag{7}$$

with

$$\begin{aligned} w_1 &= \tfrac{1}{6!}\lambda((2-\lambda^2c^2)^2 - \lambda^2c^2), \\ w_2 &= -\tfrac{1}{5!}\lambda((3-\lambda^2c^2)^2 - 4\lambda^2c^2), \\ w_3 &= -(\tfrac{1}{3!}\lambda(7-\lambda^2c^2))^2, \\ w_4 &= \tfrac{1}{2\times 4!}\lambda((6-\lambda^2c^2)^2 - \lambda^2c^2), \end{aligned}$$

and $w_7 = w_1, w_6 = w_2, w_5 = w_4$. h is the spacial grid step length and $\lambda = \frac{k}{h}$.

In fact, the high order derivatives are not valid at the interface and consequently the obtained results are of first order or even less. A detailed discussion of this phenomenon of losing the accuracy has already been presented by Sei and Symes [14]. So, obviously, on each side of the discontinuity of $A(x)$ the method is of order six for the acoustic equation, while at the grid points near to the discontinuity the method fails to maintain this order of accuracy.

More precisely, suppose that the interface lies between two adjacent grid points with indices J and $J+1$, i.e. $x_J < \alpha < x_{J+1}$, then this method works well at those grid points at which all the required points to update them are located completely on the left or right of the interface, but it fails to be accurate at the grid points (irregular points) $J-2, J-1, \ldots, J+3$. So, we need a new scheme to maintain the same order of accuracy at these irregular points.

For a general piecewise smooth coefficient problem we can derive the same method, but in this case the derivatives of the coefficient $A(x)$ will come into the difference equation. It should be noted, however, that the coefficient matrices are not as simple as those appearing in (7), but we can follow the same procedure to provide a sixth order method for this case as well. Here with an efficient derivation of these formulas we can save more in computations. In the following, we present the time derivative approximations in (4) and approximations of the corresponding space derivatives

$$
\begin{aligned}
&(U_t)_j^n \approx -AQ_6^{(1)}U_j^n,\\
&(U_{tt})_j^n \approx B^{(1)}Q_6^{(1)}U_j^n + B^{(2)}Q_6^{(2)}U_j^n,\\
&(U_{ttt})_j^n \approx C^{(1)}Q_4^{(1)}U_j^n + C^{(2)}Q_4^{(2)}U_j^n + C^{(3)}Q_4^{(3)}U_j^n,\\
&(U_{tttt})_j^n \approx D^{(1)}Q_4^{(1)}U_j^n + D^{(2)}Q_4^{(2)}U_j^n + D^{(3)}Q_4^{(3)}U_j^n + D^{(4)}Q_4^{(4)}U_j^n,\\
&(U_{ttttt})_j^n \approx E^{(1)}Q_2^{(1)}U_j^n + E^{(2)}Q_2^{(2)}U_j^n + E^{(3)}Q_2^{(3)}U_j^n + E^{(4)}Q_2^{(4)}U_j^n\\
&\qquad\qquad +E^{(5)}Q_2^{(5)}U_j^n,\\
&(U_{tttttt})_j^n \approx F^{(1)}Q_2^{(1)}U_j^n + F^{(2)}Q_2^{(2)}U_j^n + F^{(3)}Q_2^{(3)}U_j^n + F^{(4)}Q_2^{(4)}U_j^n\\
&\qquad\qquad +F^{(5)}Q_2^{(5)}U_j^n + F^{(6)}Q_2^{(6)}U_j^n,
\end{aligned}
\tag{8}
$$

where,

$$
\begin{aligned}
&B^{(1)} = AA',\\
&B^{(2)} = A^2,\\
&C^{(1)} = -B^{(1)}A' - B^{(2)}A'',\\
&C^{(2)} = -B^{(1)}A - 2B^{(2)}A',\\
&C^{(3)} = -B^{(2)}A,\\
&D^{(1)} = -C^{(1)}A' - C^{(2)}A'' - C^{(3)}A''',\\
&D^{(2)} = -C^{(1)}A - 2C^{(2)}A' - 3C^{(3)}A'',\\
&D^{(3)} = -C^{(2)}A - 3C^{(3)}A',\\
&D^{(4)} = -C^{(3)}A,\\
&E^{(1)} = -D^{(1)}A' - D^{(2)}A'' - D^{(3)}A''' - D^{(4)}A'''',\\
&E^{(2)} = -D^{(1)}A - 2D^{(2)}A' - 3D^{(3)}A'' - 4D^{(4)}A''',\\
&E^{(3)} = -D^{(2)}A - 3D^{(3)}A' - 6D^{(4)}A'',\\
&E^{(4)} = -D^{(3)}A - 4D^{(4)}A',\\
&E^{(5)} = -D^{(4)}A,\\
&F^{(1)} = -E^{(1)}A' - E^{(2)}A'' - E^{(3)}A''' - E^{(4)}A'''' - E^{(5)}A'''''',\\
&F^{(2)} = -E^{(1)}A - 2E^{(2)}A' - 3E^{(3)}A'' - 4E^{(4)}A''' - 5E^{(5)}A'''',\\
&F^{(3)} = -E^{(2)}A - 3E^{(3)}A' - 6E^{(4)}A'' - 10E^{(5)}A''',\\
&F^{(4)} = -E^{(3)}A - 4E^{(4)}A' - 10E^{(5)}A'',\\
&F^{(5)} = -E^{(4)}A - 5E^{(5)}A',\\
&F^{(6)} = -E^{(5)}A.
\end{aligned}
$$

A similar standard method has been addressed by Qiu and Shu [13], in which the finite difference WENO schemes with Lax-Wendroff time discretization for solving nonlinear hyperbolic conservation law systems was developed. It uses a WENO scheme instead $Q_6^{(1)}$ in (8) and proceeds to the final formulations.

3 Jump Conditions

We study the jump conditions for a piecewise coefficient problem and then consider a general variable coefficient wave equation. A test problem for this case is also given in the section on numerical results.

3.1 Piecewise constant coefficient

In this section we introduce some jump conditions to serve as a tool for developing a new method for the irregular points. By irregular points, we mean those grid points that in the process of updating to the next time level, use grid points on both sides of the interface. If the interface $x = \alpha$ lies in the interval (x_J, x_{J+1}) then the irregular points for the given method (6) are the grid points $J-2, J-1, \ldots, J+3$. So, there exist six irregular points and the method (6) fails to be accurate at these points.

For the acoustic wave equation we impose the jump conditions $[u] = 0$ and $[p] = 0$ that can be denoted by a single statement

$$[U] = 0. \tag{9}$$

Using these conditions and the wave equation (1), we obtain the following relations at the interface [12],

$$\frac{\partial^k U(\alpha^+, t)}{\partial x^k} = D_k \frac{\partial^k U(\alpha^-, t)}{\partial x^k}, \quad k = 0, 1, 2, ... \tag{10}$$

where,

$$D_{2k} = (\frac{c^-}{c^+})^{2k} \begin{bmatrix} 1 & 0 \\ 0 & 1 \end{bmatrix}, \qquad D_{2k+1} = (\frac{c^-}{c^+})^{2k} \begin{bmatrix} \frac{\kappa^-}{\kappa^+} & 0 \\ 0 & \frac{\rho^+}{\rho^-} \end{bmatrix}.$$

3.2 A general piecewise smooth coefficient

For a general piecewise smooth coefficient, by using again the condition $[U] = 0$ and imposing the relations $[U_t] = 0, \ldots, [U_{ttttt}] = 0$, we obtain

$$
\begin{aligned}
&U_x^+ = Q_1 U_x^-,\\
&U_{xx}^+ = Q_2 U_x^- + Q_3 U_{xx}^-,\\
&U_{xxx}^+ = Q_4 U_x^- + Q_5 U_{xx}^- + Q_6 U_{xxx}^-,\\
&U_{xxxx}^+ = Q_7 U_x^- + Q_8 U_{xx}^- + Q_9 U_{xxx}^- + Q_{10} U_{xxxx}^-\\
&U_{xxxxx}^+ = Q_{11} U_x^- + Q_{12} U_{xx}^- + Q_{13} U_{xxx}^- + Q_{14} U_{xxxx}^- + Q_{15} U_{xxxxx}^-,\\
&U_{xxxxxx}^+ = Q_{16} U_x^- + Q_{17} U_{xx}^- + Q_{18} U_{xxx}^- + Q_{19} U_{xxxx}^- + Q_{20} U_{xxxxx}^-\\
&\qquad\quad + Q_{21} U_{xxxxxx}^-
\end{aligned}
\tag{11}
$$

where

$$
\begin{aligned}
&Q_1 = -GA^-,\\
&Q_2 = G^2\Big(- B_+^{(1)} GA^- + B_-^{(1)}\Big),\\
&Q_3 = G^2 B_-^{(2)},\\
&Q_4 = G^3(-C_+^{(1)} Q_1 + C_-^{(1)} - C_+^{(2)} Q_2),\\
&Q_5 = G^3(-C_+^{(2)} Q_3 + C_-^{(2)}),\\
&Q_6 = G^3 C_-^{(3)},\\
&Q_7 = G^4(-D_+^{(1)} Q_1 + D_-^{(1)} - D_+^{(3)} Q_4 - D_+^{(2)} Q_2),\\
&Q_8 = G^4(-D_+^{(2)} Q_3 - D_+^{(3)} Q_5 + D_-^{(2)}),\\
&Q_9 = G^4(-D_+^{(3)} Q_6 + D_-^{(3)}),\\
&Q_{10} = G^4 D_-^{(4)},\\
&Q_{11} = G^5(-E_+^{(1)} Q_1 - E_+^{(2)} Q_2 - E_+^{(3)} Q_4 - E_+^{(4)} Q_7 + E_-^{(1)}),\\
&Q_{12} = G^5(-E_+^{(2)} Q_3 - E_+^{(3)} Q_5 - E_+^{(4)} Q_8 + E_-^{(2)}),\\
&Q_{13} = G^5(-E_+^{(3)} Q_6 - E_+^{(4)} Q_9 + E_-^{(3)}),\\
&Q_{14} = G^5(-E_+^{(4)} Q_{10} + E_-^{(4)}),\\
&Q_{15} = G^5 E_-^{(5)},\\
&Q_{16} = G^6(-F_+^{(1)} Q_1 - F_+^{(2)} Q_2 - F_+^{(3)} Q_4 - F_+^{(4)} Q_7 - F_+^{(5)} Q_{11} + F_-^{(1)})\\
&Q_{17} = G^6(-F_+^{(2)} Q_3 - F_+^{(3)} Q_5 - F_+^{(4)} Q_8 - F_+^{(5)} Q_{12} + F_-^{(2)})\\
&Q_{18} = G^6(-F_+^{(3)} Q_6 - F_+^{(4)} Q_9 - F_+^{(5)} Q_{13} + F_-^{(3)})\\
&Q_{19} = G^6(-F_+^{(4)} Q_{10} - F_+^{(5)} Q_{14} + F_-^{(4)})\\
&Q_{20} = G^6(-F_+^{(5)} Q_{15} + F_-^{(5)})\\
&Q_{21} = G^6 F_-^{(6)}
\end{aligned}
\tag{12}
$$

where $G = (-A^+)^{-1}$ and the other matrices have already been introduced in previous sections.

4 Approximation at the interface for acoustic equation

We first investigate the approximation of the solution at the irregular points for the case of piecewise constant coefficients. At these points we impose the same method as (6) and let the coefficients to be determined appropriately.

Then we obtain seven unknown 2×2 matrices to maintain the sixth order accuracy of the method. The details are presented at x_J and a similar argument is also applied to the other irregular points. The symbol J indicates a fixed number corresponding to the interval (x_J, x_{J+1}) that contains the interface α.

Theorem 4.1. *If the coefficients of (6) satisfy the following linear system of equations*

$$\sum_{l=1}^{4} \alpha_{il}\Gamma_{J,l} + \sum_{l=5}^{7} \alpha_{il}\Gamma_{J,l}D_i = F_i^-, \qquad (i = 0, 1, \ldots, 6) \tag{13}$$

where,

$$\alpha_{il} = (\frac{r_l}{h})^i, \qquad (i = 0, 1, \ldots, 6, \quad l = 1, 2, \ldots, 7) \tag{14}$$

$$F_i^- = (\alpha_{14} - \lambda A^-)^i - \alpha_{14}^i, \qquad i = 0, 1, \ldots, 6. \tag{15}$$

then, the method (6) is of order 6 at the irregular point x_J.

Proof. To prove this result we consider the local truncation error at x_J up to sixth order

$$\begin{aligned} L = \frac{1}{k}\sum_{l=1}^{7} \Gamma_{j,l}U_{j+l-4} + (AU_x - \frac{1}{2}kA^2U_{xx} + \frac{1}{6}k^2A^3U_{xxx} - \frac{1}{24}k^3A^4U_{xxxx} \\ + \frac{1}{120}k^4A^5U_{xxxxx} - \frac{1}{720}k^5A^6U_{xxxxxx})_J + O(k^6). \end{aligned} \tag{16}$$

Using the relation $A^2 = c^2 I$ we get

$$\begin{aligned} L = \frac{1}{k}\sum_{l=1}^{7} \Gamma_{j,l}U_{j+l-4} + (AU_x - \frac{1}{2}kc^2U_{xx} + \frac{1}{6}k^2c^2AU_{xxx} - \frac{1}{24}k^3c^4U_{xxxx} \\ + \frac{1}{120}k^4c^4AU_{xxxxx} - \frac{1}{720}k^5c^6U_{xxxxxx})_J + O(k^6). \end{aligned} \tag{17}$$

Now to proceed with the proof we need to expand each term of (17) up to sixth order about $x = \alpha$. To this end, we distinguish two sets of points in first summation

$$\begin{aligned} U_{j+l-4} = U^- + r_lU_x^- + \frac{1}{2}r_l^2U_{xx}^- + \frac{1}{6}r_l^3U_{xxx}^- + \frac{1}{24}r_l^4U_{xxxx}^- \\ + \frac{1}{120}r_l^5U_{xxxxx}^- + \frac{1}{720}r_l^6U_{xxxxxx}^-, \quad 1 \le l \le 4, \end{aligned} \tag{18}$$

$$U_{j+l-4} = D_0U^- + r_lD_1U_x^- + \frac{1}{2}r_l^2D_2U_{xx}^- + \frac{1}{6}r_l^3D_3U_{xxx}^- + \frac{1}{24}r_l^4D_4U_{xxxx}^- + \frac{1}{120}r_l^5D_5U_{xxxxx}^- + \frac{1}{720}r_l^6D_6U_{xxxxxx}^-) \quad 5 \le l \le 7, \tag{19}$$

where $U^- = \lim_{x\to\alpha^-} U(x,t)$, and

$$r_l = x_{J-4+l} - \alpha, \qquad (l = 1, 2, \dots 7).$$

Note that we have used the jump conditions (10) in (19). If we substitute (18), (19) and similar expansions for other terms into (17) we obtain L as a function of U^-, U_x^-, U_{xx}^-, U_{xxx}^-, U_{xxxx}^-, U_{xxxxx}^- and U_{xxxxxx}^-. Therefore, to achieve sixth order accuracy we have to force the coefficients of these terms to be zero. These systems of matrix equations are exactly the same as (13), (14) and (15). □

In theorem 4.1, the unknown 2×2 matrices $\Gamma_{J,l}, l = 1, 2, \dots, 7$ will be obtained by solving the linear system (13). These linear systems can be easily converted to some lower order linear systems. As the matrices D_j, $j = 1, \dots, 7$, are diagonal it is possible to decouple these systems to four 7×7 linear systems; e.g., the first 7×7 linear system determines the scalar unknowns $(\Gamma_{J,l})_{11}, l = 1, 2, \dots, 7$. In fact, because of this property, there are only two different coefficient matrices in these four systems of linear equations. These properties are valid at all irregular points. It should be mentioned that in the tested numerical problems we did not get any ill-conditioning warning due to the coefficient matrices. On the other irregular points similar relations can be derived. So, at the grid point $J-1$ one obtains,

$$\sum_{l=1}^{5} \alpha_{il}\Gamma_{J-1,l} + \sum_{l=6}^{7} \alpha_{il}\Gamma_{J-1,l}D_i = F_i^-, \qquad (i = 0, 1, \dots, 6)$$

where,

$$\alpha_{il} = (\frac{r_l}{h} - 1)^i, \qquad (i = 0, 1, \dots, 6, \quad l = 1, 2, \dots, 7).$$

At the grid point $J-2$ we have

$$\sum_{l=1}^{6} \alpha_{il}\Gamma_{J-2,l} + \alpha_{i7}\Gamma_{J-2,l}D_i = F_i^-, \qquad (i = 0, 1, \dots, 6)$$

where,

$$\alpha_{il} = (\frac{r_l}{h} - 2)^i, \qquad (i = 0, 1, \dots, 6, \quad l = 1, 2, \dots, 7).$$

At the grid point $J+1$ we have

$$\sum_{l=1}^{3} \alpha_{il}\Gamma_{J+1,l}D_i^{-1} + \sum_{l=4}^{7} \alpha_{il}\Gamma_{J+1,l} = F_i^+, \qquad (i = 0, 1, \ldots, 6)$$

where,

$$\alpha_{il} = (\frac{r_l}{h} + 1)^i, \qquad (i = 0, 1, \ldots, 6, \quad l = 1, 2, \ldots, 7).$$

At the grid point $J + 2$ we obtain

$$\sum_{l=1}^{2} \alpha_{il}\Gamma_{J+2,l}D_i^{-1} + \sum_{l=3}^{7} \alpha_{il}\Gamma_{J+2,l} = F_i^+, \qquad (i = 0, 1, \ldots, 6)$$

where,

$$\alpha_{il} = (\frac{r_l}{h} + 2)^i, \qquad (i = 0, 1, \ldots, 6, \quad l = 1, 2, \ldots, 7).$$

At the grid point $J + 3$ we have

$$\alpha_{i1}\Gamma_{J+3,1}D_i^{-1} + \sum_{l=2}^{7} \alpha_{il}\Gamma_{J+3,l} = F_i^+, \qquad (i = 0, 1, \ldots, 6)$$

where,

$$\alpha_{il} = (\frac{r_l}{h} + 3)^i, \qquad (i = 0, 1, \ldots, 6, \quad l = 1, 2, \ldots, 7).$$

The given formulation of the immersed interface method demonstrates the possibility of the direct extension of these relations to higher orders. The closed form formulas for right hand side matrices (15) are valid for lower and higher order formulations. For higher order methods α_{14} should only be replaced with a new one; for example, this element for fourth order method is α_{13}. The proof of the following theorem is similar to Theorem 4.1 and so we omit it.

Theorem 4.2. *If the coefficient matrices of (6) satisfy the following system of matrix equations*

$$\sum_{l=1}^{m} \alpha_{il}\Gamma_{j,l}D_i^{-1} + \sum_{l=m+1}^{M+1} \alpha_{il}\Gamma_{j,l} = F_i^*, \qquad (i = 0, 1, \ldots, M-1)$$

where for $j \leq J$, $F_i^* = F_i^- D^{-1}$ and for $j \geq J + 1$, $F_i^* = F_i^+$. Then, the method (6) gives a Mth order approximation of the solution of (1) at irregular grid x_j.

Now we extend Theorem 4.1 to the case where the coefficients are piecewise smooth. The local truncation error for a general piecewise smooth co-

efficient at x_J can be represented as follows

$$\begin{aligned} L = \frac{1}{k}\sum_{l=1}^{7}\Gamma_{j,l}U_{j+l-4} \\ -\Big(T^{(1)}U_x + kT^{(2)}U_{xx} + k^2T^{(3)}U_{xxx} + k^3T^{(4)}U_{xxxx} \\ +k^4T^{(5)}U_{xxxxx} + k^5T^{(6)}U_{xxxxxx}\Big)_J + O(k^6). \end{aligned}$$

where

$$\begin{aligned} T^{(1)} &= -A + \frac{1}{2}kB^{(1)} + \frac{1}{6}k^2C^{(1)} + \frac{1}{24}k^3D^{(1)} + \frac{1}{120}k^4E^{(1)} + \frac{1}{720}k^5F^{(1)}, \\ T^{(2)} &= \frac{1}{2}B^{(2)} + \frac{1}{6}kC^{(2)} + \frac{1}{24}k^2D^{(2)} + \frac{1}{120}k^3E^{(2)} + \frac{1}{720}k^4F^{(2)}, \\ T^{(3)} &= \frac{1}{6}C^{(3)} + \frac{1}{24}kD^{(3)} + \frac{1}{120}k^2E^{(3)} + \frac{1}{720}k^3F^{(3)}, \\ T^{(4)} &= \frac{1}{24}D^{(4)} + \frac{1}{120}kE^{(4)} + \frac{1}{720}k^2F^{(4)}, \\ T^{(5)} &= \frac{1}{120}E^{(5)} + \frac{1}{720}kF^{(5)}, \\ T^{(6)} &= \frac{1}{720}F^{(6)}. \end{aligned}$$

To obtain a sixth order method it is required that the matrices $\Gamma_{J,l}$ satisfy the following linear matrix system

$$\sum_{l=1}^{4}\alpha_{i,l}\Gamma_{J,l} + \sum_{l=5}^{7}\alpha_{i,l}\Gamma_{J,l}Q^{(i,l)} = R_i, \quad i = 1, 2, \ldots, 7. \tag{20}$$

where

$$\begin{aligned} Q^{(1,l)} &= I, \\ Q^{(2,l)} &= Q_1 + \frac{1}{2}r_lQ_2 + \frac{1}{6}r_l^2Q_4 + \frac{1}{24}r_l^3Q_7 + \frac{1}{120}r_l^4Q_{11} + \frac{1}{720}r_l^5Q_{16}, \\ Q^{(3,l)} &= Q_3 + \frac{1}{3}r_lQ_5 + \frac{1}{12}r_l^2Q_8 + \frac{1}{60}r_l^3Q_{12} + \frac{1}{360}r_l^4Q_{17}, \\ Q^{(4,l)} &= Q_6 + \frac{1}{4}r_lQ_9 + \frac{1}{20}r_l^2Q_{13} + \frac{1}{120}r_l^3Q_{18}, \\ Q^{(5,l)} &= Q_{10} + \frac{1}{5}r_lQ_{14} + \frac{1}{30}r_l^2Q_{19}, \\ Q^{(6,l)} &= Q_{15} + \frac{1}{6}r_lQ_{20}, \\ Q^{(7,l)} &= Q_{21}. \end{aligned}$$

and

$$
\begin{aligned}
R_1 &= 0,\\
R_2 &= \nu T^{(1)},\\
R_3 &= 2\nu\alpha_{1,4}T^{(1)} + 2\nu^2 T^{(2)},\\
R_4 &= 3\nu\alpha_{2,4}T^{(1)} + 6\nu^2\alpha_{1,4}T^{(2)} + 6\nu^3 T^{(3)},\\
R_5 &= 4\nu\alpha_{3,4}T^{(1)} + 12\nu^2\alpha_{2,4}T^{(2)} + 24\nu^3\alpha_{1,4}T^{(3)} + 24\nu^4 T^{(4)},\\
R_6 &= 5\nu\alpha_{4,4}T^{(1)} + 20\nu^2\alpha_{4,3}kT^{(2)} + 60\nu^3\alpha_{4,2}T^{(3)} + 120\nu^3\alpha_{4,1}T^{(4)} + 120\nu^4 T^{(5)},\\
R_7 &= 6\nu\alpha_{5,4}T^{(1)} + 30\nu^2\alpha_{4,4}T^{(2)} + 120\nu^3\alpha_{3,4}T^{(3)} + 360\nu^4\alpha_{2,4}T^{(4)}\\
&\quad +720\nu^5\alpha_{1,4}T^{(5)} + 720\nu^6 T^{(6)}.
\end{aligned}
$$

We note that the matrices $Q^{(i,l)}$ are diagonal 2×2 matrices and it is possible to solve the linear systems (20) in a similar way as discussed before.

At the irregular point x_{J+1} we have

$$\sum_{l=1}^{3}\alpha_{i,l}\Gamma_{J,l}\hat{Q}^{(i,l)} + \sum_{l=4}^{7}\alpha_{i,l}\Gamma_{J,l} = R_i, \quad i = 1,2,\ldots,7.$$

where

$$
\begin{aligned}
\hat{Q}^{(1,l)} &= I,\\
\hat{Q}^{(2,l)} &= Q_1^{-1} + \frac{1}{2}r_l Q_2^{-1} + \frac{1}{6}r_l^2 Q_4^{-1} + \frac{1}{24}r_l^3 Q_7^{-1} + \frac{1}{120}r_l^4 Q_{11}^{-1} + \frac{1}{720}r_l^5 Q_{16}^{-1},\\
\hat{Q}^{(3,l)} &= Q_3^{-1} + \frac{1}{3}r_l Q_5^{-1} + \frac{1}{12}r_l^2 Q_8^{-1} + \frac{1}{60}r_l^3 Q_{12}^{-1} + \frac{1}{360}r_l^4 Q_{17}^{-1},\\
\hat{Q}^{(4,l)} &= Q_6^{-1} + \frac{1}{4}r_l^4 Q_9^{-1} + \frac{1}{20}r_l^2 Q_{13}^{-1} + \frac{1}{120}r_l^3 Q_{18}^{-1},\\
\hat{Q}^{(5,l)} &= Q_{10}^{-1} + \frac{1}{5}r_l Q_{14}^{-1} + \frac{1}{30}r_l^2 Q_{19}^{-1},\\
\hat{Q}^{(6,l)} &= Q_{15}^{-1} + \frac{1}{6}r_l Q_{20}^{-1},\\
\hat{Q}^{(7,l)} &= Q_{21}^{-1}.
\end{aligned}
$$

Similar formulae can be deduced for other irregular points.

5 Numerical Results

In this section, some test problems are given to show the efficiency of the derived high order method. The simulation results are given for different cases. The test problems Test 1 and Test 2 illustrate general behavior of the solution of the acoustic wave equation at the interface. Also, the numerical results of the test problem Test 4 (in two cases 4-1, 4-2) are given for the acoustic wave equation with piecewise smooth coefficients. The parameter

values, the function $f(x)$, and the CFL number are clearly specified in each test problem. The numerical order of accuracy and L_1 and L_∞ errors are reported for the test problem Test 3, see Table 1, which verifies numerically the long time behavior of this approximation. The test problem Test 5 shows the numerical stability of the method. The computational cost for the calculation of the coefficient matrices at irregular points is independent of N, the number of spatial grid points in the discretization. The coefficient matrices can be computed in a couple of milliseconds on a desktop computer.

The numerical results are given for the following acoustic wave equation problem [3]:
If $x < \alpha$:

$$u(x,t) = \frac{1}{\rho_l c_l}(f(t - \frac{x-\alpha}{c_l}) + \frac{\rho_l c_l - \rho_r c_r}{\rho_l c_l + \rho_r c_r} f(t + \frac{x-\alpha}{c_l})),$$
$$p(x,t) = f(t - \frac{x-\alpha}{c_l}) - \frac{\rho_l c_l - \rho_r c_r}{\rho_l c_l + \rho_r c_r} f(t + \frac{x-\alpha}{c_l}), \tag{21}$$

and if $\alpha \leq x$:

$$u(x,t) = \frac{2}{\rho_l c_l + \rho_r c_r} f(t - \frac{x-\alpha}{c_r}),$$
$$p(x,t) = \frac{2\rho_r c_r}{\rho_l c_l + \rho_r c_r} f(t - \frac{x-\alpha}{c_r}), \tag{22}$$

where, $f(x)$ is a smooth function.

Test 1: In this test, we consider $f(x) = e^{-200(x^2-1/2)^2}$ and the parameters are chosen as $\alpha = 0$, $\rho_l = -1$,$\rho_r = -1.5$, $c_l = 1$, $c_r = 0.5$. Figures 1 and 2 illustrate numerical and exact solutions for u and p with $N = 320$ and $c_{\max}\lambda = 0.8$. There are two gaussian pulses going to the right and a pulse hits the interface and then transmits with a generated reflecting pulse. The CFL number in this case is about one and there is no spurious oscillation.

Test 2: In this test, problem we consider a rather high frequency function $f(x) = \sin(30x)$ with parameters $\alpha = 0$, $\rho_l = 0.5, \rho_r = 1.0, c_l = 0.8, c_r = 1.0$. Figures 3 and 4 illustrate numerical and exact solutions for u and p with $N = 320$ and $c_{\max}\lambda = 0.8$. After hitting the interface the magnitudes of velocity and pressure are changed.

Test 3: To illustrate the long time behavior of this method, we consider the jump $f(x) = \sin(\pi x)$, as initial data for acoustic equations with $\alpha = \frac{\pi}{2}$, and the same parameters as in Test 2. The numerical results are reported in Table 1 for several values of N at $t = 50\pi$. The numerical order of accuracy and L_1 and L_∞ errors are presented in this Table in which LaxW-IIM denotes the Lax-Wendroff immersed interface method.

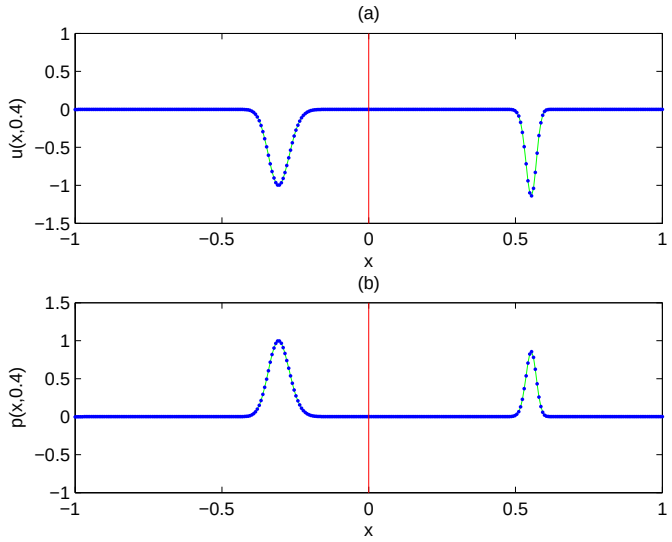

Figure 1: Test 1: Numerical(.) and exact(-) solutions for u and p at $t = 0.4$

It is well known that a typical high order method provides first order results for interface problems[14, 15]. In Table 2, we show the result of eliminating of jump conditions and using the high order numerical method (6) without interface treatment. We can clearly see that the results are at most first order.

Table 1: (Test 3) The L_1, L_∞ errors and the numerical order of accuracy for LaxW-IIM method over the whole interval and the same quantities at irregular points for $f(x) = \sin(\pi x)$ at $t = 50\pi$ are reported

N	**LaxW-IIM**				**Irregular points**			
	L_1 error	order	L_∞ error	order	L_1 error	order	L_∞ error	order
15	8.37E-001		1.56E-001		2.44E-001		1.06E-001	
30	4.03E-002	4.17	3.32E-003	4.89	6.92E-003	4.89	1.81E-003	5.58
60	1.11E-003	5.06	4.14E-005	5.46	1.43E-004	5.46	3.05E-005	5.75
120	3.05E-005	5.12	5.26E-007	5.85	2.37E-006	5.85	4.42E-007	6.04
240	8.90E-007	5.07	7.18E-009	5.98	3.67E-008	5.98	6.54E-009	6.04

Test 4: In this test, problem we consider two variable coefficient problems. Let us define a general form of the variable coefficient,

$$(\rho(x), c(x)) = \begin{cases} (\rho^- + f_1(x), c^- + g_1(x)), & x < \alpha, \\ (\rho^+ + f_2(x), c^+ + g_2(x)), & x > \alpha. \end{cases} \tag{23}$$

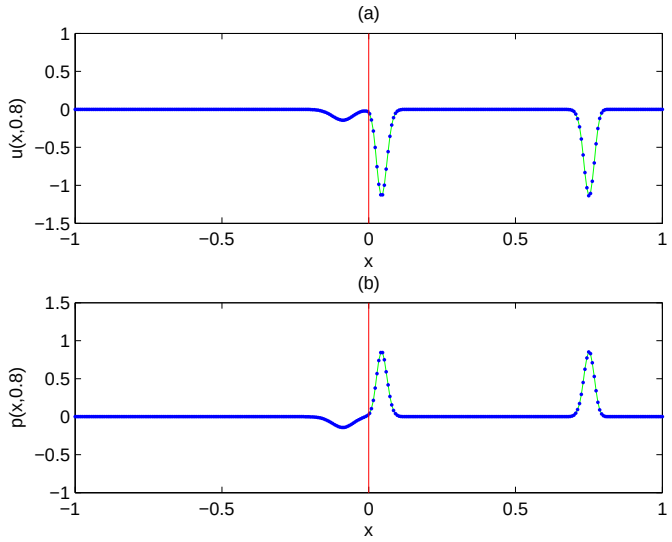

Figure 2: Test 1: Numerical(.) and exact(-) solutions for u and p at $t = 0.8$

Table 2: (Test 3) The L_1, L_∞ errors and the numerical order of accuracy for method in equation (6) over the whole interval and the same quantities at irregular points for $f(x) = \sin(\pi x)$ at $t = 50\pi$, without interface treatment, are reported

N	**LaxW-IIM**				**Irregular points**			
	L_1 error	order	L_∞ error	order	L_1 error	order	L_∞ error	order
15	7.91E+000		2.35E+000		5.17E+000		2.35E+000	
30	3.84E+000	0.99	8.60E-001	1.57	1.65E+000	1.57	8.16E-001	1.45
60	4.19E+000	0.12	3.56E-001	1.14	7.33E-001	1.14	3.56E-001	1.17
120	4.29E+000	0.03	1.84E-001	0.92	3.84E-001	0.92	1.84E-001	0.94
240	4.33E+000	0.01	9.24E-002	0.97	1.95E-001	0.97	9.24E-002	0.99

where f_1, f_2, g_1 and g_2 are arbitrary and smooth functions which vanish at $x = \alpha$ and ρ^-, ρ^+, c^- and c^+ are constants.

To illustrate the behavior of the numerical solution near the interface, we consider the following two sets of functions and we show the numerical quality of solution for the first set through some figures and for the second set of functions Table 4 is given in which the order of accuracy is reported numerically.

1. The first coefficient set:

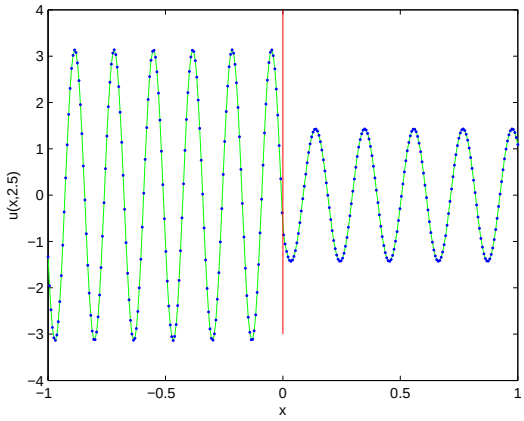

Figure 3: Test 2: Numerical(.) and exact(-) solutions for u at $t = 2.5$

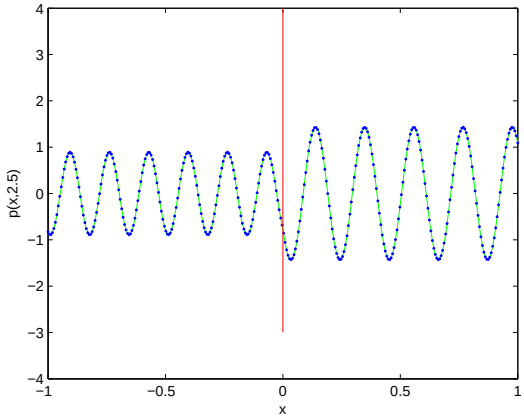

Figure 4: Test 2: Numerical(.) and exact(-) solutions for p at $t = 2.5$

$$
\begin{aligned}
f_1(x) &= (x+1)\sin(x-\alpha), \\
g_1(x) &= (x+1)(x-\alpha), \\
f_2(x) &= (x-1)\sin(x-\alpha), \\
g_2(x) &= (x-1)(x-\alpha).
\end{aligned} \tag{24}
$$

2. The second coefficient set:

$$
\begin{aligned}
f_1(x) &= 0, \\
g_1(x) &= 0, \\
f_2(x) &= 0, \\
g_2(x) &= -6(e^{\frac{x}{c^+}} - 1).
\end{aligned} \tag{25}
$$

Table 3: Jumps in the coefficients of Test 4-1

k	$f_1^{(k)}(0^-)$	$f_2^{(k)}(0^+)$	$g_1^{(k)}(0^-)$	$g_2^{(k)}(0^+)$	$\rho^{(k)}(0^-)$	$\rho^{(k)}(0^+)$	$c^{(k)}(0^-)$	$c^{(k)}(0^+)$
0	0	0	0	0	0.5	1	0.8	1
1	1	-1	1	-1	1	-1	1	-1
2	2	2	2	2	2	2	2	2
3	-1	1	0	0	-1	1	0	0
4	-4	-4	0	0	-4	-4	0	0
5	1	-1	0	0	1	-1	0	0

The parameters for the first set are the same as in Test 2 and for the second one we consider $c^- = 1, c^+ = \frac{1+\sqrt{5}}{2}, \rho^- = 1, \rho^+ = -6$. The details of the jump discontinuities of the first coefficient set (24) are reported in Table 3. From Table 3 it is clearly seen that the first order derivatives of ρ and c are discontinuous and since c is a polynomial, its higher order derivatives become zero while the higher derivatives of ρ are discontinuous.

Figures 5 and 6 for (24) illustrate the quality of the numerical solutions for u and p with $N = 320$ and $c_{\max}\lambda = 0.8$. This behavior confirms that the method has been able to successfully capture the solution near the interface without any spurious oscillations.

The numerical order of accuracy and errors for (25), the second coefficient set, has been shown in Table 4 for the final time $t = 0.5$ with the following initial data,

$$u(x,0) = \begin{cases} 2e^{-x} - e^{x}, & x \le 0, \\ e^{0.8x}, & x > 0 \end{cases}, \quad p(x,0) = \begin{cases} 2e^{-x} + e^{x}, & x \le 0, \\ 3e^{2x}, & x > 0. \end{cases} \tag{26}$$

It should be mentioned that the results of Table 4 have been obtained by implementing our formulations with exact coefficients, confirming that the true order of accuracy of the presented method for this type of coefficients is also 6. Since the computation of jump conditions for the case of piecewise constant coefficients is simple, in practice one might prefer to use some approximation of the exact coefficients in the implementation.

Since the obtained approximation is close to the exact coefficient, the order of accuracy of the numerical results obtained by the method of this paper should be closer to the true 6^{th} order. We have examined the presented method using best uniform approximation of degree zero for the coefficients near the interface and we obtained an order of accuracy of at least 2. We expect to get a solution of higher order of accuracy if the best uniform polynomial approximation of a higher degree is used.

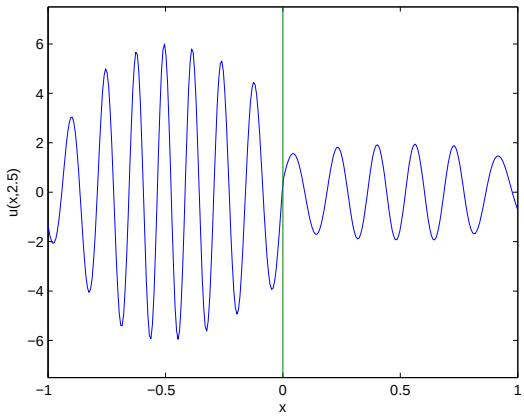

Figure 5: Test 4-1: Quality of the numerical solution for u at $t = 2.5$

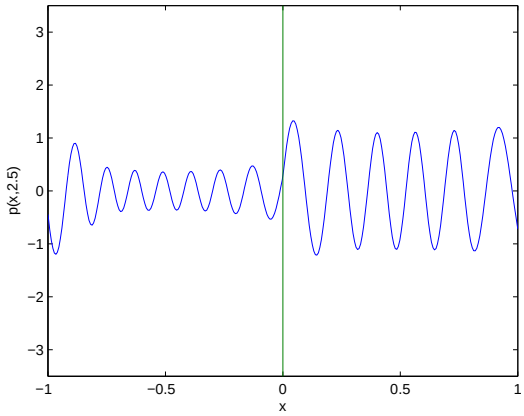

Figure 6: Test 4-1: Quality of the numerical solution for p at $t = 2.5$

Table 4: (Test 4-2) The L_1, L_∞ errors and the numerical order of accuracy for LaxW-IIM method

N	u				p			
	L_1 error	order	L_∞ error	order	L_1 error	order	L_∞ error	order
16	2.45e-006	-	1.35e-006	-	2.66e-005	-	1.35e-005	-
32	2.52e-007	3.28	3.10e-008	5.45	9.21e-007	4.85	2.76e-007	5.61
64	9.69e-009	4.70	4.71e-010	6.04	2.80e-008	5.04	5.09e-009	5.76
128	3.26e-010	4.89	7.10e-012	6.05	8.94e-010	4.97	8.74e-011	5.86
256	1.15e-011	4.82	1.15e-013	5.94	3.09e-011	4.85	1.49e-012	5.87

5.1 Numerical stability

A general stability analysis has no direct answer for the given method. Von Neumann stability analysis does not work in this situation, because the coefficients change in a nonsmooth way. So, we are left as an open problem verifying stability using either the energy method or the GKS theory [3, 7]. But here we illustrate the numerical stability of the method through some numerical experiments. The long time behavior of the method, which is very important factor in real problems has been illustrated for Test 5. The results, also, justify the order of accuracy of the method. In this experiment, we have considered several examples of random initial conditions and reported their results in Figure 7. In this figure the norm of the solutions u and p are given versus $\frac{k}{h}$, showing that they do not increase proportional with $\frac{k}{h}$. So, our method does not show instability, because a relative growth of the solution with respect to this factor is a sign of instability [7].

A Von Neumann stability analysis with frozen coefficients provide a reasonable results on the choice of the Courant number. The influence matrix for stability analysis is the following block toeplitz matrix

$$G = \begin{pmatrix} I+\Gamma_4 & \Gamma_5 & \Gamma_6 & \Gamma_7 & & & & & \\ \Gamma_3 & I+\Gamma_4 & \Gamma_5 & \Gamma_6 & \Gamma_7 & & & & \\ \Gamma_2 & \Gamma_3 & I+\Gamma_4 & \Gamma_5 & \Gamma_6 & \Gamma_7 & & & \\ \Gamma_1 & \Gamma_2 & \Gamma_3 & I+\Gamma_4 & \Gamma_5 & \Gamma_6 & \Gamma_7 & & \\ & \ddots & \ddots & \ddots & \ddots & \ddots & \ddots & \ddots & \\ & & \ddots & \ddots & \ddots & \ddots & \ddots & \ddots & \Gamma_7 \\ & & & \ddots & \ddots & \ddots & \ddots & \ddots & \Gamma_6 \\ & & & & \ddots & \ddots & \ddots & \ddots & \Gamma_5 \\ & & & & & \Gamma_1 & \Gamma_2 & \Gamma_3 & I+\Gamma_4 \end{pmatrix}.$$

Note that with frozen coefficients, the coefficient matrix $A(x)$ is independent of α and therefor the coefficient matrices $\Gamma_{j,l}$ are independent of j and we

eliminate this index for simplicity. For linear stability the eigenvalues of G should lie in the unit circle in the complex plane. We numerically locate the eigenvalues of G. This matrix depends on $A(x)$ and λ. Therefor we report the stability results for several values of these parameters.

Table 5: The norm of eigenvalues of influence matrix for different values of parameters. The letter p denotes the periodic boundary conditions

λ	c	ρ	$\rho(G)$	$\rho(G_p)$
1.000	1.000	-1.000	0.543	1.500
2.000	0.500	-1.500	0.554	0.658
1.250	0.800	0.500	0.837	1.187
1.000	1.000	1.000	0.558	1.500

We remark that the boundary conditions have important role in the stability of the problem. In the case of frozen coefficients, i.e. $A(x) = A^+$ or $A(x) = A^-$, the results are shown in the Table 5. In this case we can choose λ large enough for different values of $A(x)$. While, a comparison between different rows of this table shows that in general the eigenvalues are nondecreasing with variation of parameters. Therefor, for nonsmooth coefficients that the situation is more complicated, the inequality $\max_x\{|c(x)|, 1\}\frac{k}{h} < 1$ is a reasonable criteria and numerical tests confirm that this criteria in our test problems.

Test 5: In this test we consider an initial condition $u(x_j, 0) = R_j e^{-6(\frac{x_j-\alpha}{5h})^2}$ and $v(x, 0) = 2u(x, 0)$, where R_j are uniformly distributed random numbers in the interval $[0, 1]$. This example is a variant of a similar one dimensional case in [7]. The parameters are $c_l = 1.0$, $c_r = 0.5$, $\rho_l = 2.5$, $\rho_r = 10.0$, $N = 1000$ and $c_{\max}\lambda = 0.99$. The results are given in Figure 7, which is a typical test among many other tests. There are no noise generation visible near the interface and the norms of the solutions do not grow with $\frac{k}{h}$.

5.2 Two dimensional problems

Implementation of high order interface method for two dimensional acoustic wave equations requires high order jump conditions on the interface. In most applications the standard jump conditions are available in the literature. Such jump conditions are usually given in the normal and tangential directions to the interface. Therefor, we need to define a local coordinate in a typical point on the interface to obtain the required approximations at the interface(see Figure 8). This is done after transformation of the equation to

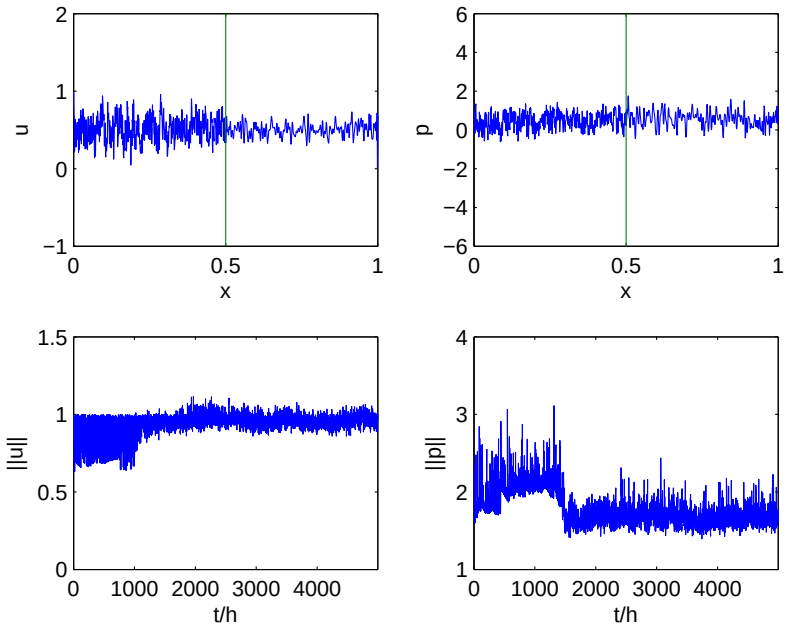

Figure 7: Test 5: The norm and the solution after a long time

the new local coordinate system in $\xi - \eta$ plane. The same formulation in one dimensional case will direct us to the set of equations to be solved for the 2D and 3D cases.

6 Conclusions and discussions

In this paper, we have presented a sixth order immersed interface method for acoustic wave equation with discontinuous coefficient. The effect of piecewise constant and a more general piecewise smooth coefficients on the derived formulations has been investigated. We have also provided different numerical tests which confirm the efficiency of the method and justify their order of accuracy and numerical stability. It should be mentioned that, using jump conditions do not impose a considerable computational cost in the calculations and one should only solve some low order linear systems to obtain the coefficients. In fact, the special treatment of the interface is a preprocessing stage in the implementation of immersed interface method and without loss of overall speed of computation it is also applicable in the parallel computers. In the numerical results, we applied the Lax-Wendroff method for time discretization. However, the weighted essentially nonoscillatory(WENO) and

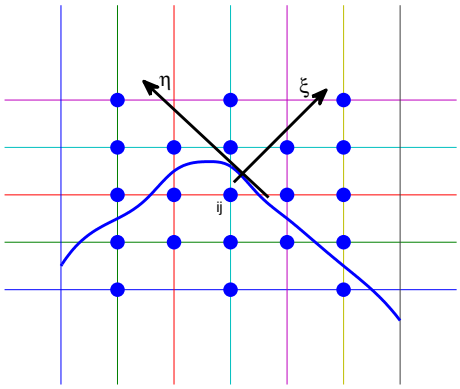

Figure 8: Local coordinates in a two dimensional grid with a curve interface

the total variation diminishing(TVD) methods[6, 9] reduce the possible oscillations in the solution. These methods recently have been added to the CLAWPACK software [9] for numerical solution of conservation laws.

References

1. Driscoll, T. A. and Fornberg, B. *A block pseudospectral method for maxwells equations I. one-dimensional case,* Journal of Comput. Phys. 140 (1998) 47-65.

2. Farzi, J. and Hosseini, S. M. *A high order method for the solution of a one-way wave equation in heterogeneous media,* Far East J. Appl. Math. 36 (3) (2009) 317-330.

3. Gustafsson, B. and Wahlund, P. *Time compact high order difference methods for wave propagation in discontinuous media,* SIAM J. Sci. Comput. 26 (2004) 272-293.

4. Gustafsson, B. and Mossberg, E. *High order difference methods for wave propagation,* SIAM J. Sci. Comput. 26 (2004) 259-271.

5. Gustafsson, B., Kreiss, H. O. and Oliger, J. *Time dependent problems and difference methods,* first ed., John Wiley and Sons, (1996).

6. Jiang, G. S. and Shu, C. W. *Efficient implementation of weighted ENO schemes,* J. Comput. Phys., 126 (1996) 202-228.

7. Larsson, J. and Gustafsson, B. *Stability criteria for hybrid difference methods,* J. comp. phys. 227 (2008) 2886-2898.

8. LeVeque, R. J. *Wave propagation algorithms for multidimensional hyperbolic systems,* J. comp. phys. 131 (1997) 327-353.

9. LeVeque, R. J. *Finite Volume Methods for Hyperbolic Problems,* Cambridge University Press, Cambridge, 2004.

10. Li, Z. and Ito, K. *The immersed interface method: numerical solutions of PDEs involving interfaces and irregular domains,* SIAM, 2006.

11. Peskin, C. S. *Numerical analysis of blood flow in the heart,* J. Comput. Phys., 25 (1977) 220-252.

12. Piraux, J. and Lombard, B. *A new interface method for hyperbolic problems with discontinuous coefficients. one-dimensional acoustic example,* J. Comput. Phys., 168 (2001) 227-248.

13. Qiu, J. and Shu, C. W. *Finite difference WENO schemes with Lax-Wendroff type time discretizations,* SIAM J. Sci. Comput. 24 (2003) 2185-2198.

14. Sei, A. and Symes, W. W. *Error analysis of numerical schemes for the wave equation in heterogeneous media,* Appl. Numer. Math. 15 (1994) 465-480.

15. Symes, W. W. and Vdovina, T. *Interface error analysis for numerical wave propagation,* Comput. Geosci. 13 (2009) 363-371.

16. Trefethen, L. N. *Group velocity in finite difference schemes,* SIAM. Rev. 24 (1982) 113-136.

17. Wiegmann, A. and Bube, K. P. *The explicit-jump immersed interface method: finite difference methods for PDE with piecewise smooth solutions,* SIAM J. Numer. Anal., 37 (2000) 827-862.

18. Zhang, C. and LeVeque, R. J. *Immersed interface methods for wave equations with discontinuous coefficients,* Wave Motion, 25 (1997) 237-263.

19. Zhao, S. and Wei, G. W. *High-order FDTD methods via derivative matching for Maxwell's equations with material interfaces,* J. Comput. Phys., 200 (2004) 60-103.

Iranian Journal of Numerical Analysis and Optimization
Vol 4, No. 1, (2014), pp 25-39

Numerical solution of stiff systems of differential equations arising from chemical reactions

G. Hojjati*, A. Abdi, F. Mirzaee and S. Bimesl

Abstract

Long time integration of large stiff systems of initial value problems, arising from chemical reactions, demands efficient methods with good accuracy and extensive absolute stability region. In this paper, we apply second derivative general linear methods to solve some stiff chemical problems such as chemical Akzo Nobel problem, HIRES problem and OREGO problem.

Keywords: General linear methods; Ordinary differential equation; Chemical reactions; Stiff systems.

1 Introduction

Chemical reaction mechanisms often include individual steps with very different reaction rates. Mathematically, this means that the corresponding ordinary differential equations (ODEs) are likely to be stiff, since the different components of the system have dramatically different time constants. Moreover, these systems are often nonlinear [4].

In the last 40 years or so, numerous works have been focusing on the development of more advanced and efficient methods for stiff problems. A potentially good numerical method for the solution of stiff systems of ODEs must have good accuracy and some reasonably wide region of absolute stabil-

*Corresponding authour
Received 3 September 2013; revised 11 December 2013; accepted 25 December 2013
G. Hojjati
Faculty of Mathematical Sciences, University of Tabriz, Tabriz, Iran.

A. Abdi
Faculty of Mathematical Sciences, University of Tabriz, Tabriz, Iran.

F. Mirzaee
Department of Mathematics, Faculty of Science, Malayer University, Malayer, Iran

S. Bimesl
Department of Mathematics, Faculty of Science, Malayer University, Malayer, Iran

ity. A-stability requirement puts a severe limitation on the choice of suitable methods for stiff problems.

Traditional numerical methods for solving an initial value problem generally fall into two main classes: linear multistep (multivalue) and Runge–Kutta (multistage) methods. In 1966, Butcher [5] introduced general linear methods (GLMs) as a unifying framework for the traditional methods to study the properties of consistency, stability and convergence, and to formulate new methods with clear advantages over these classes.

On the other hand, one of the main directions to construct methods with higher order and extensive stability region, is using higher derivatives of the solutions, and some methods have been introduced that have good properties, especially for stiff problems. See [7, 8, 9]. Although GLMs include linear multistep methods, Runge–Kutta and many other standard methods, but they were extended to second derivative general linear methods (SGLMs) to cover second derivative methods, too. These methods were introduced by Butcher and Hojjati in [6] and were studied more by Abdi and Hojjati in [1, 2, 3]. There are several interrelated aims in the use of such methods, such as high orders and stage orders, high accuracy, low error constants, satisfactory stability properties, such as A-stability or L-stability and low implementation costs. In [3], the efficiency of SGLMs are shown by comparing the accuracy versus stepsize and the number of function evaluations of SGLMs with those of SDIRK methods. These advantages of SGLMs motivate us to apply them for solving large stiff systems of initial value problems arising from chemical reactions.

The rest of the paper is organized as follows. In Section 2, we recall the basic concepts and theory of SGLMs. In Section 3, we introduce types of SGLMs and give an SGLM of order 3. In Section 4, we apply the method to solve some important initial value problems that arise from mathematical modeling of chemical reaction and give numerical results, and the paper is closed in Section 5 by concluding and giving ideas for future work.

2 A review on the SGLMs

In this section, we give a brief review of SGLMs for the numerical solution of an autonomous system of ordinary differential equation

$$y' = f(y(x)), \qquad y : \mathbb{R} \to \mathbb{R}^m, \qquad f : \mathbb{R}^m \to \mathbb{R}^m. \tag{1}$$

These methods are characterized by four integers: (p, q, r, s) where p and q are respectively order and stage order of the method, r is the number of input and output approximations, and s is the number of internal stages. Let $Y^{[n]} = [Y_i^{[n]}]_{i=1}^s$ be an approximation of stage order q to the vector $y(x_{n-1} + ch) = [y(x_{n-1}+c_ih)]_{i=1}^s$ and the vectors $f(Y^{[n]}) = [f(Y_i^{[n]})]_{i=1}^s$ and $g(Y^{[n]}) =$

$[g(Y_i^{[n]})]_{i=1}^s$ denote the stage first and second derivative values, where $g(\cdot) = f'(\cdot)f(\cdot)$. The c_i's represent position of the internal stages within one step. The vector $c = [c_1 \;\; c_2 \;\; \cdots \;\; c_s]^T$ is called the abscissa vector. Also, let denote by $y^{[n-1]} = [y_i^{[n-1]}]_{i=1}^r$ and $y^{[n]} = [y_i^{[n]}]_{i=1}^r$ the input and output vectors at step number n, respectively. An SGLM used for the numerical solution of (2) is given by

$$\begin{aligned} Y_i^{[n]} &= h\sum_{j=1}^{s} a_{ij} f(Y_j^{[n]}) + h^2 \sum_{j=1}^{s} \overline{a}_{ij} g(Y_j^{[n]}) + \sum_{j=1}^{r} u_{ij} y_j^{[n-1]}, \quad i = 1, 2, \cdots, s, \\ y_i^{[n]} &= h\sum_{j=1}^{s} b_{ij} f(Y_j^{[n]}) + h^2 \sum_{j=1}^{s} \overline{b}_{ij} g(Y_j^{[n]}) + \sum_{j=1}^{r} v_{ij} y_j^{[n-1]}, \quad i = 1, 2, \cdots, r, \end{aligned} \tag{2}$$

where $n = 1, 2, \cdots, N$, $Nh = \overline{x} - x_0$ and h is the stepsize. We denote $A = [a_{ij}], \overline{A} = [\overline{a}_{ij}], U = [u_{ij}], B = [b_{ij}], \overline{B} = [\overline{b}_{ij}]$ and $V = [v_{ij}]$.

We now state the fundamental theorem on SGLMs.

Theorem 2.1 [1] *The necessary and sufficient conditions for an SGLM to be convergent are that it be consistent and zero-stable.*

The derivation of order and stage order conditions for general p and q is quite complicated. However, this analysis is quite simple for methods of stage order $q = p$. In this case, the order and stage order conditions can be expressed conveniently using the theory of functions of a complex variable. We have the following theorem on order conditions.

Theorem 2.2 [2] *The SGLM (2) with*

$$y_i^{[n-t]} = \sum_{k=0}^{p} h^k \alpha_{ik} y^{(k)}(x_{n-t}) + O(h^{p+1}), \quad i = 1, 2, \cdots, r, \quad t = 0, 1,$$

has order p and stage order $q = p$ if and only if

$$\exp(cz) = zA\exp(cz) + z^2\overline{A}\exp(cz) + Uw + O(z^{p+1}), \tag{3}$$

$$\exp(z)w = zB\exp(cz) + z^2\overline{B}\exp(cz) + Vw + O(z^{p+1}), \tag{4}$$

where $e^{cz} = [e^{c_1 z}, \;\; e^{c_2 z}, \;\; \cdots \;\; e^{c_s z}]^T$ and $w = w(z) = [\sum_{k=0}^{p} \alpha_{ik} z^k]_{i=1}^r$.

The stability behavior of SGLMs is defined using the standard test problem of Dahlquist $y'(x) = \xi y(x)$, where ξ is a (possibly complex) number. If method (2) is applied to this problem, then the stability matrix is

$$M(z) = V + \left(zB + z^2\overline{B}\right)\left(I - zA - z^2\overline{A}\right)^{-1}U, \tag{5}$$

where $z = h\xi$. If $M(z)$ has only a single non-zero eigenvalue, $R(z)$, then the method is said to possess Runge–Kutta stability (RKS).

3 Types of SGLMs and an example

It is convenient to write coefficients of the method, that is elements of A, $\overline{A}$, U, B, $\overline{B}$ and V as a partitioned $(s+r) \times (2s+r)$ matrix

$$\left[\begin{array}{c|c|c} A & \overline{A} & U \\ \hline B & \overline{B} & V \end{array}\right].$$

It is desirable to impose some restrictions on the matrices A and $\overline{A}$ to ensure that the stages of the method can be evaluated independently and sequentially [1]. Thus these two matrices will be chosen to be of lower triangular form. Furthermore, to lower implementation costs we will assume that each of A and $\overline{A}$ have constant diagonal elements. In [1] the authors by considering SGLMs in diagonally implicit multi-stage form, which the matrices A and $\overline{A}$ have the lower triangular form

$$A = \begin{bmatrix} \lambda & & & \\ a_{21} & \lambda & & \\ \vdots & \vdots & \ddots & \\ a_{s1} & a_{s2} & \cdots & \lambda \end{bmatrix}, \quad \overline{A} = \begin{bmatrix} \mu & & & \\ \overline{a}_{21} & \mu & & \\ \vdots & \vdots & \ddots & \\ \overline{a}_{s1} & \overline{a}_{s2} & \cdots & \mu \end{bmatrix},$$

have divided SGLMs into four types, depending on the nature of the differential system to be solved and the computer architecture that is used to implement these methods. Types 1 and 2 are those with arbitrary a_{ij} and $\overline{a}_{ij}$ where $\lambda = \mu = 0$ and $\lambda > 0$, $\mu < 0$, respectively. Such methods are appropriate respectively for nonstiff and stiff differential systems in a sequential computing environment. For type 3 or 4 methods, $A = \lambda I$ and $\overline{A} = \mu I$, where $\lambda = \mu = 0$ or $\lambda > 0$, $\mu < 0$, respectively. Such methods are appropriate for nonstiff or stiff differential systems in a parallel computing environment.

Second derivative diagonally implicit multistage integration methods (SDIMSIMs) as a subclass of SGLMs have been introduced in [2]. They are characterized by the following properties:

- Coefficients matrices A and $\overline{A}$ are lower triangular with the same parameters λ and μ on the diagonal respectively.
- Coefficients matrix V is a rank 1 matrix with nonzero eigenvalue equal to 1 to guarantee preconsistency.
- Order p, stage order q, number of external stages r, and the number of internal stages s are all approximately equal.

SDIMSIMs can be divided into four types according to the above classification of SGLMs [1]. These four types, together with their intended applications and architectures, are shown in Table 1.

Table 1: Types of SDIMSIMs with their intended applications and architectures

Type 1	A strictly lower triangular	$\overline{A}$ strictly lower triangular	nonstiff	sequential
Type 2	$A-\lambda I$ strictly lower triangular	$\overline{A}-\mu I$ strictly lower triangular	stiff	sequential
Type 3	$A=\mathbf{0}$	$\overline{A}=\mathbf{0}$	nonstiff	parallel
Type 4	$A=\lambda I$	$\overline{A}=\mu I$	stiff	parallel

An SDIMSIM with $p=q=3$ and $r=s=2$

We consider an SDIMSIM with $p=q=3$, $r=s=2$, $U=I$ and $V=ev^T$ for which $ve^T=1$. This method which has been introduced in [2], is A- and L-stable. The abscissa vector of the method is $c=[0 \quad 1]^T$ and its coefficients are given by the partitioned matrix

$$\left[\begin{array}{cc|cc|cc} \frac{2}{5} & 0 & -\frac{1}{12} & 0 & 1 & 0 \\ \frac{55}{27} & \frac{2}{5} & -\frac{7}{27} & -\frac{1}{12} & 0 & 1 \\ \hline \frac{2737}{2700} & \frac{9}{100} & -\frac{7}{270} & 0 & \frac{9}{10} & \frac{1}{10} \\ \frac{217}{2700} & -\frac{37}{2700} & -\frac{293}{540} & -\frac{31}{540} & \frac{9}{10} & \frac{1}{10} \end{array}\right]. \tag{6}$$

We apply this method to solve some important initial value problems which exhibit stiffness and arise from mathematical modeling of chemical reactions. Other efficient methods in this class can be found in [1, 2, 3].

4 Numerical solution of stiff chemical problems

In this section, we apply the method (6) on some famous chemical problems to show its efficiency.

4.1 Chemical Akzo Nobel problem

General information

This initial value problem is a stiff system of 6 non-linear differential equations. It has been taken from [10].

Mathematical description of the problem

The problem is of the form

$$\frac{dy}{dt} = f(y), \quad y(0) = y_0, \tag{7}$$

with

$$y \in \mathbb{R}^6, \quad 0 \leq t \leq 180. \tag{8}$$

The function f is defined by

$$f(y) = \begin{pmatrix} -2r_1 + r_2 - r_3 - r_4 \\ -\frac{1}{2}r_1 - r_4 - \frac{1}{2}r_5 + F_{in} \\ r_1 - r_2 + r_3 \\ -r_2 + r_3 - 2r_4 \\ r_2 - r_3 + r_5 \\ -r_5 \end{pmatrix},$$

where the r_i and F_{in} are auxiliary variables, given by

$$\begin{aligned} r_1 &= k_1 \cdot y_1^4 \cdot y_2^{\frac{1}{2}}, \quad k_1 = 18.7, \\ r_2 &= k_2 \cdot y_3 \cdot y_4, \quad k_2 = 0.58, \\ r_3 &= \frac{k_2}{K} \cdot y_1 \cdot y_5, \quad K = 34.4, \\ r_4 &= k_3 \cdot y_1 \cdot y_4^2, \quad k_3 = 0.09, \\ r_5 &= k_4 \cdot y_6^2 \cdot y_2^{\frac{1}{2}}, \quad k_4 = 0.42, \\ F_{in} &= klA \cdot \big(\frac{p(O_2)}{H} - y_2\big), \quad klA = 3.3, \\ p(O_2) &= 0.9, \ H = 737. \end{aligned} \tag{9}$$

Finally, the initial vector y_0 is given by

$$y_0 = (0.437, 0.00123, 0, 0, 0, 0.367)^T.$$

Origin of the problem

The problem originates from Akzo Nobel Central Research in Arnhem, The Netherlands. It describes a chemical process, in which 2 species, MBT and CHA, are mixed, while oxygen is continuously added. The resulting species of importance is CBS. The reaction equations, as given by Akzo Nobel, are

$$
\begin{aligned}
&2MBT + \tfrac{1}{2}O_2 \xrightarrow{k_1} MBTS + H_2O \\
&CBS + MBT \underset{k_2}{\overset{k_2/K}{\rightleftarrows}} MBTS + CHA \\
&MBT + 2CHA + O_2 \xrightarrow{k_3} BT + sulfate \\
&MBT + CHA + \tfrac{1}{2}O_2 \xrightarrow{k_4} CBS + H_2O \\
&MBT + CHA \rightleftarrows MBT.CHA.
\end{aligned}
$$

The last equation describes an equilibrium

$$Ks^1 = \frac{[MBT.CHA]}{[MBT] \cdot [CHA]},$$

while the others describe reactions, whose velocities are given by

$$
\begin{aligned}
r_1 &= k_1 \cdot [MBT]^4 \cdot [O_2]^{\frac{1}{2}}, \\
r_2 &= k_2 \cdot [MBTS] \cdot [CHA], \\
r_3 &= \frac{k_2}{K} \cdot [MBT] \cdot [CBS], \\
r_4 &= k_3 \cdot [MBT] \cdot [CHA]^2, \\
r_5 &= k_4 \cdot [MBT.CHA]^2 \cdot [O_2]^{\frac{1}{2}},
\end{aligned}
$$

respectively. Here the square brackets '[ ]' denote concentrations. The inflow of oxygen per volume unit is denoted by F_{in}, and satisfies

$$F_{in} = klA \cdot \big(\frac{p(O_2)}{H} - [O_2]\big),$$

where klA is the mass transfer coefficient, H is the Henry constant and $p(O_2)$ is the partial oxygen pressure. $p(O_2)$ is assumed to be independent of $[O_2]$. The parameters k_1, k_2, k_3, k_4, K, klA, H and $p(O_2)$ are given constants. The process is started by mixing 0.437 mol/liter $[MBT]$ with 0.367 mol/liter $[MBT.CHA]$. The concentration of oxygen at the beginning

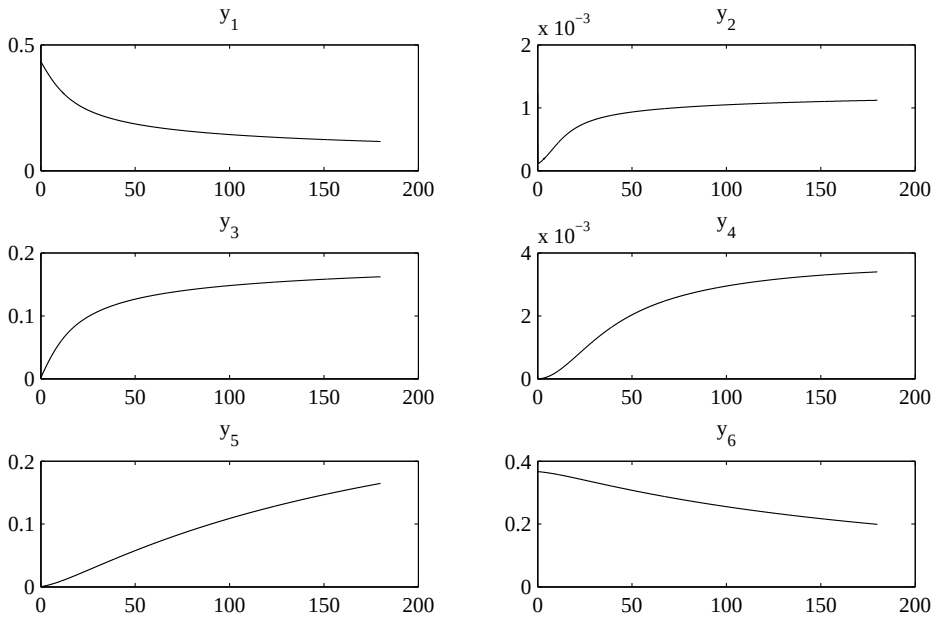

Figure 1: Chemical Akzo Nobel problem: numerical solution obtained by SDIMSIM of order $p = q = 3$ and $r = s = 2$

is 0.00123 mol/liter. Initially, no other species are present. The simulation is performed on the time interval [0 180$minutes$].

Identifying the concentrations $[MBT]$, $[O_2]$, $[MBTS]$, $[CHA]$, $[CBS]$, $[MBT.CHA]$ with $y_1, \ldots, y_6$ respectively, one easily arrives at the mathematical formulation of the preceding subsection. Solution of this problem at $t = 180$ using method (6) is reported in Table 2. Behavior of the solution components is shown in Figure 1.

Table 2: Results of the Chemical Akzo Nobel problem at $t = 180$

y_i	Solution at $t = 180$
y_1	0.116160227121356
y_2	0.001119418167053
y_3	0.162126172160781
y_4	0.003396981306527
y_5	0.164618511821187
y_6	0.198953326600100

4.2 Problem HIRES

General information

This initial value problem is a stiff system of 8 non-linear differential equations. It was proposed by Schäfar in 1975. The name HIRES was given by Hairer and Wanner [13]. It refers to "High Irradiance Response", which is described by this IVP ODE.

Mathematical description of the problem

The problem is of the form

$$\frac{dy}{dt} = f(y), \quad y(0) = y_0,$$

with

$$y \in \mathbb{R}^8, \quad 0 \leq t \leq 321.8122.$$

The function f is defined by

$$f(y) = \begin{pmatrix} -1.71y_1 + 0.43y_2 + 8.32y_3 + 0.0007 \\ 1.71y_1 - 8.75y_2 \\ -10.03y_3 + 0.43y_4 + 0.035y_5 \\ 8.32y_2 + 1.71y_3 - 1.12y_4 \\ -1.745y_5 + 0.43y_6 + 0.43y_7 \\ -280y_6y_8 + 0.69y_4 + 1.71y_5 - 0.43y_6 + 0.69y_7 \\ 280y_6y_8 - 1.81y_7 \\ -280y_6y_8 + 1.81y_7 \end{pmatrix}. \tag{10}$$

The initial vector y_0 is given by

$$y_0 = (1, 0, 0, 0, 0, 0, 0, 0.0057)^T.$$

Origin of the problem

The problem originates from plant physiology and is described in [14]. It explains the 'High Irradiance Response' (HIRES) of Photomorphogenesis on the basis of Phytochrome, by means of a chemical reaction involving 8 reactants. The reaction scheme is given below.

$$\begin{array}{ccc} \xrightarrow{o_{k_s}} & P_r & \underset{\xleftarrow{k_2}}{\xrightarrow{k_1}} \quad P_{fr}, \\ & k_6 \uparrow & \qquad \downarrow k_3 \\ & P_rX & \underset{\xleftarrow{k_2}}{\xrightarrow{k_1}} \quad P_{fr}X, \\ & k_5 \uparrow & \qquad \downarrow k_4 \\ & P_rX' & \underset{\xleftarrow{k_2}}{\xrightarrow{k_1}} \quad P_{fr}X', \end{array}$$

$$\begin{array}{ccccc} E + P_rX' & \xleftarrow{k_2} & P_{fr}X'E & \underset{\xleftarrow{k_+}}{\xrightarrow{k_-}} & P_{fr}X' + E, \\ & & \downarrow k^* & & \\ & & P_{fr} + X' + E. & & \end{array}$$

The values of the parameters were taken from [13].

$$\begin{array}{l} k_1 = 1.71,\ k_2 = 0.43,\ k_3 = 8.32,\ \ k_4 = 0.69,\ k_5 = 0.035, \\ k_6 = 8.32,\ k_+ = 280,\ k_- = 0.69,\ k^* = 0.69,\ o_{k_s} = 0.0007. \end{array}$$

Identifying $P_r, P_{fr}, P_rX, P_{fr}X, P_rX', P_{fr}X', P_{fr}X'E$ and E with y_i, $i = 1, 2, \cdots 8$, respectively, the differential equations mentioned in (10) easily follow. The obtained solution of this problem at the end of time interval is reported in Table 3. Plots in the Figure 2 show the behavior of P_r, P_{fr}, P_rX, $P_{fr}X$, P_rX', and $P_{fr}X'$, computed using the method (6).

Table 3: Results of the problem HIRES at $t = 321.8122$

y_i	Solution at $t = 321.8122$
y_1	$0.73714105836 \times 10^{-3}$
y_2	$0.14425050468 \times 10^{-3}$
y_3	$0.58889121959 \times 10^{-4}$
y_4	$0.11756696043 \times 10^{-2}$
y_5	$0.23866504368 \times 10^{-2}$
y_6	$0.62398915376 \times 10^{-2}$
y_7	$0.28502050925 \times 10^{-2}$
y_8	$0.28497949075 \times 10^{-2}$

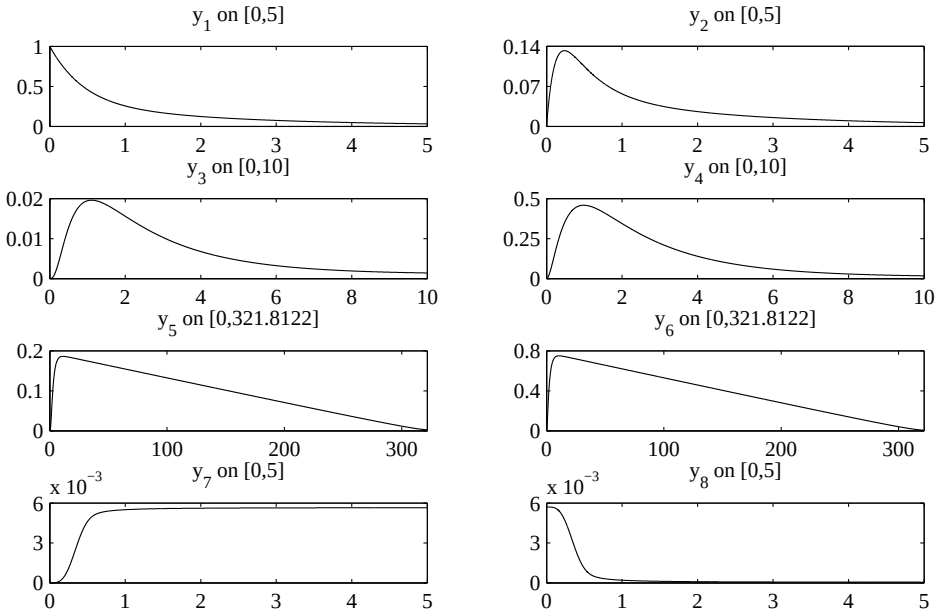

Figure 2: Problem HIRES: numerical solution obtained by SDIMSIM of order $p = q = 3$ and $r = s = 2$

4.3 Problem OREGO

General information

The problem consists of a stiff system of 3 non-linear ordinary differential equations. The name Orego was given by Hairer and Wanner [13] and refers to the Oregonator model which is described by this ODE. The Oregonator model takes its name from the University of Oregon where in the 1972 Field, Körös and Noyes [11] proposed this model for the Belousov–Zhabotinskii reaction.

Mathematical description of the problem

The problem is of the form

$$\frac{dy}{dt} = f(y), \quad y(0) = y_0,$$

with

$$y \in \mathbb{R}^3, \quad 0 \leq t \leq 360.$$

The function f is defined by

$$f(y) = \begin{pmatrix} s(y_2 - y_1 y_2 + y_1 - q y_1^2) \\ \frac{1}{s}(-y_2 - y_1 y_2 + y_3) \\ w(y_1 - y_3) \end{pmatrix}.$$

The values of the parameters s, q and w are

$$s = 77.27, \quad w = 0.161, \quad q = 8.375 \times 10^{-6}.$$

The initial vector y_0 is given by $(1, 2, 3)^T$.

Origin of the problem

The OREGO problem originates from the celebrated Belousov–Zhabotinskii (BZ) reaction. When certain reactions, like bromous acid, bromide ion and cerium ion, are combined, they exhibit a chemical reaction which, after an induction period of inactivity, oscillates with change in structure and in color, from red to blue and viceversa.

The color changes are caused by alternating oxidation–reductions in which the cerium switches its oxidation state from $Ce(III)$ to $Ce(IV)$.

Field, Körös and Noyes formulated the following model for the most important parts of the kinetic mechanism that gives rice to oscillation in the BZ reaction. This mechanism can be summarized as three concurrent processes [12]:

- the reduction of Bromate (BrO_3^-) to Bromine (Br) via the reducing agent bromide (Br^-). Bromomalonic acid ($BrMA$) is produced;
- the increase of hypobromous acid ($HBrO_2$) at an accelerating rate and the production of $Ce(IV)$. Here we have a sudden change in color from red to blue;
- the reduction of Cerium catalyst $Ce(IV)$ to $Ce(III)$. Here we have a gradual change in color from blue to red.

Then, from this mechanism the following Oregonator scheme is obtained

$$\begin{array}{ll} A+Y \to X+P & r = k_3 AY \\ X+Y \to 2P & r = k_2 XY \\ A+X \to 2X+2Z & r = k_5 AX \\ 2X \to A+P & r = k_4 X^2 \\ B+Z \to \frac{1}{2} fY & r = k_c BZ \end{array}$$

Here, using the conventional notation the assignments and the effective concentration are

$$\begin{array}{rll} \text{hypobromous acid} & [HBrO2] = X & 5.025 \times 10^{-11} \\ \text{Bromide} & [Br^-] = Y & 3.0 \times 10^{-7} \\ \text{Cerium} - 4 & [CE(IV)] = Z & 2.412 \times 10^{-8} \\ \text{Bromate} & [BrO_3^-] = A & \\ \text{all oxidizable organic species} & [Org] = B & \\ & [HOBr] = P & \end{array}$$

The reaction rate equations for the intermediate species X, Y , and Z are

$$\begin{aligned} \frac{dX}{dt} &= s(Y - XY + X - qX^2), \\ \frac{dY}{dt} &= \frac{1}{s}(-Y - XY + fZ), \\ \frac{dZ}{dt} &= w(X - Z), \end{aligned}$$

with $f = 1$, and s, w, and q as in the previous subsection.

Solution of this problem at $t = 360$ using method (6) is reported in Table 4. Behavior of the solution components is shown in Figure 3.

Table 4: Results of the OREGO problem at $t = 360$

y_i	Solution at $t = 360$
y_1	$0.1000814868842 \times 10^1$
y_2	$0.1228180744895 \times 10^4$
y_3	$0.1320568339839 \times 10^3$

5 Conclusion

For stiff systems, because of the stability condition, the time step restriction becomes severe, specially when they have to be integrated over long periods of time. High order accuracy, good stability properties and low implementation

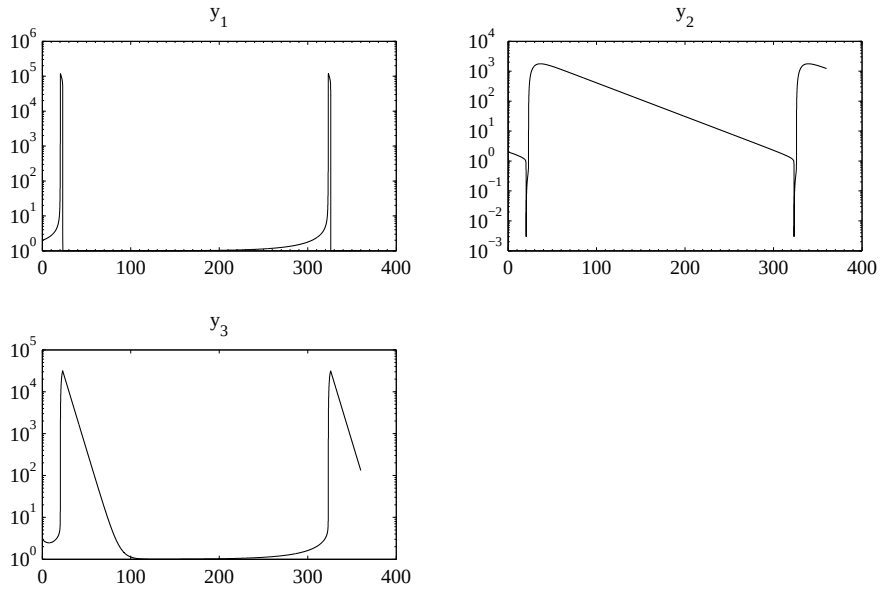

Figure 3: Chemical OREGO problem: numerical solution obtained by SDIMSIM of order $p = q = 3$ and $r = s = 2$

cost of the SGLMs make them to be successful in applying on large stiff systems of initial value problems arising from chemical reactions. Although the SGLMs are capable in giving accurate and stable results, as reported in the numerical experiments, but in can be equipped by a strategy for adjusting stepsize when the integration proceeds. It is the subject of our future works.

References

1. Abdi, A. and Hojjati, G. *An extension of general linear methods*, Numer. Algor., 57 (2011), 149–167.

2. Abdi, A. and Hojjati, G. *Maximal order for second derivative general linear methods with Runge-Kutta stability*, Appl. Numer. Math., 61 (2011), 1046–1058.

3. Abdi, A., Braś, M. and Hojjati, G. *On the construction of second derivative diagonally implicit multistage integration methods*, Appl. Numer. Math., 76 (2014), 1–18.

4. Burg, K.V. *Statistical Models in Applied Science*, J. Wiley, New York, 1975.

5. Butcher, J. C. *On the convergence of numerical solutions to ordinary differential equations*, Math. Comp., 20 (1966), 1–10.

6. Butcher, J. C. and Hojjati, G. *Second derivative methods with RK stability*, Numer. Algor., 40 (2005), 415–429.

7. Cash, J. R. *Second derivative extended backward differentiation formula for the numerical integration of stiff systems*, SIAM J. Numer. Anal., 18 (1981), 21–36.

8. Enright, W. H. *Second derivative multistep methods for stiff ordinary differential equations*, SIAM J. Numer. Anal., 11 (1974), 321–331.

9. Hojjati, G., Rahimi Ardabili, M.Y. and Hosseini, S.M. *New second derivative multistep methods for stiff systems*, Appl. Math. Model., 30 (2006), 466–476.

10. Eriksson, K., Johnson, C. and Logg, A. *Explicit time-stepping for stiff ODEs*, SIAM J. Sci. Comput., 25 (2003), 11–42.

11. Field, R. J., Körös, E. and Noyes, R. M. *Oscillation in chemical systems, part. 2. thorough analysis of temporal oscillations in the bromate–cerium–malonic acid system. Journal of the American Society*, 94 (1972), 8649–8664.

12. Gray, C. *An analysis of the Belousov–Zhabotinskii reaction. Rose-Hulman Undergraduate Mathematics Journal*, 3(1), 2002. http://www.rose-hulman.edu/mathjournal/.

13. Hairer, E. and Wanner, G. *Solving Ordinary Differential Equations II: Stiff and Differential-algebraic Problems*, Springer-Verlag, 1991.

14. Schäfer, E. *A new approach to explain the 'high irradiance responses' of photomorphogenesis on the bais of phytochrome*, J. of Math. Biology, 2 (1975), 41–56.

Iranian Journal of Numerical Analysis and Optimization
Vol 4, No. 1, (2014), pp 41-56

A numerical technique based on operational matrices for solving nonlinear integro-differential equations

A. Golbabai

Abstract

This paper presents a computational method for solving two types of integro-differential equations, system of nonlinear high order Volterra-Fredholm integro-differential equation(VFIDEs) and nonlinear fractional order integro-differential equations. Our tools for this aims is operational matrices of integration and fractional integration. By this method the given problems reduce to solve a system of algebraic equations. Illustrative examples are included to demonstrate the efficiency and high accuracy of the method.

Keywords: Operational matrix of integration; Volterra-Fredholm; Nonlinear system of integro-differential equations; Fractional order; Legendre wavelet.

1 Introduction

Integro-differential equations frequently appear in all fields of sciences such as physics, chemistry and engineering problems [11, 20, 23, 24]. In last few decades fractional calculus and fractional differential equations have found application in several different disciplines, many important phenomena in electromagnetic, acoustics, viscolasticity, electrochemistry and material science are well described by differentiable and integro differentiable equation of fractional order[3, 22]. There are various numerical and analytical methods to solve such problems, for example, the homotopy perturbation method [4, 7, 8, 9], the Adomian decomposition method [5], fractional differential transform method [21] and Gronwald–Letnikov discretization method [6].

In recent years the approximation of orthogonal functions has been playing role in the solution of different kinds of mathematical and engineering problems such as identification, analysis and optimal control[15, 16, 18]. The main feature of this technique is to reduce the integro-differential equations

Received 9 September 2013; revised 11 December 2013; accepted 8 January 2014
A. Golbabai
Islamic Azad university, Karaj Branch, Karaj, Iran. e-mail: golbabai@iust.ac.ir

to a nonlinear algebraic equation by introducing integration matrix of basis functions. In present article, we are concerned with the application of Legendre wavelet to the numerical solution of:
(I). Nonlinear fractional order integro-differential equations

$$D^{\alpha}_{*t}u(t) = f(t) + \int_0^x K(t, u(t), D^{\alpha}_{*t}u(t))dt, \qquad 0 \leq \alpha < 1. \tag{1}$$

(II). Nonlinear system of high order (VFIDe) of the form

$$\begin{aligned}\sum_{j=0}^{n} p_{ij}(x){u_l}^{(j)}(x) = f_i(x) + \lambda_{i1}\int_0^x K_{i1}(x,t,u(t),u'(t),\ldots,u^{(n)}(t))dt \\ +\lambda_{i2}\int_0^1 K_{i2}(x,t,u(t),u'(t),\ldots,u^{(n)}(t))dt, \quad i=1,\ldots,s,\end{aligned} \tag{2}$$

where $u^{(j)}(x) = \left(u_1^{(j)},\ldots,u_s^{(j)}\right)$ for $j = 0,\ldots,n$ and initial conditions are

$$u_i^{(j)}(0) = a_j, \quad j = 0, 1\ldots, n-1, \tag{3}$$

where $f(x)$,K, K_{i1} and K_{i2} are known functions assumed to be in $L^2(\mathbb{R})$ on the interval $0 \leq x, t \leq 1$, u(t) is unknown, K_{i1} and K_{i2} are nonlinear in $x, t, u(t), \ldots, u^{(n)}(t)$. This type of equations whose integrand contain high order derivatives arise in many fields such as theory of elasticity .

The article is organized as follows: in Section 2 we define the Legendre wavelets and operational matrix of integration. Section 3 is devoted to the solution of Eq. (1). In Section 4, we obtain an error bound for our method. Section 5, include our numerical findings and demonstrate the accuracy of the proposed scheme.

2 Preliminaries and notation

This section gives some necessary definition and mathematical preliminaries of the fractional calculus theory which are used further in this paper. The Riemann-Lioville fractional integration of order $\alpha > 0$ is defined as [14]

$$\begin{aligned} &I_t^{\alpha} f(t) = \tfrac{1}{\Gamma(\alpha)}\int_0^t \tfrac{f(\tau)}{(t-\tau)^{(1-\alpha)}}d\tau, \\ &I_t^0 f(t) = f(\tau), \end{aligned} \tag{4}$$

and its fractional derivative of order $\alpha > 0$ is normally used:

$$D_t^{\alpha} f(t) = (\frac{d}{dt})^n I_t^{n-\alpha} f(t) \quad (n-1 < \alpha \leq n), \tag{5}$$

where n is an integer. For Riemann-Lioville definition, one has

$$I_t^{\alpha} t^{\upsilon} = \frac{\Gamma(\upsilon+1)}{\Gamma(\alpha+\upsilon+1)} t^{\upsilon+\alpha}. \tag{6}$$

The modified fractional differential operator D_{*t}^{α} proposed by Caputo is

$$D_{*t}^{\alpha} f(t) = \begin{cases} \frac{1}{\Gamma(n-\alpha)} \int_0^t (t-\tau)^{n-\alpha-1} f^{(n)}(\tau) \;\; (n-1 < \alpha \leq n), \\ \\ \frac{d^n}{dt^n} f(t) \;\; \alpha = n \in \mathbb{N}, \end{cases} \tag{7}$$

where n is an integer. Caputos integral operator has an useful property:

$$I_t^{\alpha} D_{*t}^{\alpha} f(t) = f(t) - \sum_{k=0}^{n-1} f^{(k)}(0^+) \frac{t^k}{k!}, \qquad (n-1 < \alpha \leq n), \tag{8}$$

where n is an integer.

3 Properties of Legendre wavelet

3.1 Wavelets and Legendre wavelet

Wavelet constitute a family of functions constructed by a single function called the mother wavelet. When the dilation parameter a and translation parameter b vary continuously, we have the following family of continuous wavelet as [10]

$$\psi_{(a,b)} = |a|^{-1/2} \psi(\frac{t-b}{a}), \;\; a, b \in R, a \neq 0.$$

If we restrict the parameters a and b to discrete values as $a = a_0^{-m}, b = kb_0 a_0^{-m}, a_0 > 1, b_0 > 0$ and $m, k \in$ Z.We have the following family of discrete wavelets

$$\psi_{m.k}(t) = |a_0|^{m/2} \psi(a_0^m t - kb_0),$$

where $\psi_{m.k}(t)$ forms a wavelet basis for $L^2(R)$. In particular, when $a_0 = 2$, $b_0 = 1$, $\psi_{m.k}(t)$ forms an orthonormal basis.

The Legendre wavelets are defined on interval [0,1) see [16, 17].

$$\psi_{nm=} \begin{cases} \sqrt{m+\frac{1}{2}} 2^{k/2} L_m(2^k t - \hat{n}), for \frac{\hat{n}-1}{2^k} \leq t < \frac{\hat{n}+1}{2^k}, \\ \\ 0 \quad otherwise, \end{cases}$$

where $m = 0, 1, \ldots M-1$ and $n = 1, 2, 3, \ldots, 2^{k-1}$. The coefficient $\sqrt{m+\frac{1}{2}}$ is for orthogonality. Here, $L_m(t)$ are the well-known Legendre polynomials

of order m which are defined on the interval [- 1,1] and can be determined with the aid of the following recurrence formulae:

$$L_0(t) = 1, \;\; L_1(t) = t,$$

$$L_{m+1}(t) = (\frac{2m+1}{m+1})tL_m(t) - (\frac{m}{m+1})L_{m-1}(t), \; m = 1, 2, 3, \ldots$$

3.2 Function approximation

Theorem. *A function $f(t)$ defined on [0,1) can be expanded as infinite sum of Legendre wavelets, and the series converges uniformly to the function $f(x)$, that is*

$$f(t) = \sum_{n=1}^{\infty} \sum_{m=0}^{\infty} c_{nm}\psi_{nm}(t), \tag{9}$$

where, $c_{nm} = (f(t), \psi_{nm}(t))$, in which $(.,.)$ denote the inner product.
Proof. see[13].

If the infinite series in Eq. (9) is truncated, then it can be written as

$$f(t) \simeq \sum_{n=1}^{2^{k-1}} \sum_{m=1}^{M-1} c_{nm}\psi_{nm}(t) = C^T\Psi(t), \tag{10}$$

where C and $\Psi(t)$ are $2^M \times 1$ matrices given by

$$C = [c_{10}, c_{11}, \ldots, c_{1M-1}, c_{20}, \ldots, c_{2M-1}, \ldots, c_{2^{k-1}0}, \ldots, c_{2^{k-1}M}]^T, \tag{11}$$

$$\Psi(t) = [\psi_{10}, \psi_{11}, \ldots, \psi_{1M-1}, \psi_{20}, \ldots, \psi_{2M-1}, \ldots, \psi_{2^{k-1}0}, \ldots, \psi_{2^{k-1}M}]^T. \tag{12}$$

Now we want to find an upper bound to the estimate error . Suppose that $f(x)$ is a $(m+1)-$times differentiable function on $\Omega = [0, 1)$. An error function between $f(x)$ and its Legendre-wavelet approximation $f_{nm}(x)$ is defined on every subinterval $\Omega_n = [\frac{\hat{n}-1}{2^k} \leq t < \frac{\hat{n}+1}{2^k}]$ as

$$e_{nm}(x) = f(x) - f_{nm}(x) = f(x) - c_{nm}\psi_{nm}(x). \tag{13}$$

Then we can write

$$\| e_{nm}(x)\|^2 = \int_{\frac{\hat{n}-1}{2^k}}^{\frac{\hat{n}+1}{2^k}} |f(x) - c_{nm}\psi_{nm}(x)|^2. \tag{14}$$

Since $\psi_{nm}(x)$ is a polynomial of degree m,we can use the error bound for interpolation of degree m on Ω_n that is

$$|f(x)-p_n(x)| \leq \frac{h^{(m+1)}}{4(m+1)} \max_{\xi\in[\frac{\hat{n}-1}{2^k},\frac{\hat{n}+1}{2^k}]} \left|f^{(m+1)}(\xi)\right|, \tag{15}$$

where $h=\frac{1}{2^k m}$.By Eq. (14)and Eq. (15)

$$\begin{aligned} \|e_{nm}(x)\|^2 &\leq \int_{\frac{\hat{n}-1}{2^k}}^{\frac{\hat{n}+1}{2^k}} \left|\frac{h^{(m+1)}}{4(m+1)} \max_{\xi\in[\frac{\hat{n}-1}{2^k},\frac{\hat{n}+1}{2^k}]} \left|f^{(m+1)}(\xi)\right|\right|^2 \\ &\leq \frac{1}{2^k}\left|\frac{h^{(m+1)}}{4(m+1)} \max_{\xi\in[\frac{\hat{n}-1}{2^k},\frac{\hat{n}+1}{2^k}]} \left|f^{(m+1)}(\xi)\right|\right|^2 . \end{aligned} \tag{16}$$

According to above equation we find an error bound for each subinterval as

$$\|e_{nm}(x)\| \leq \frac{1}{2^{k/2}} \frac{h^{(m+1)}}{4(m+1)} \max_{\xi\in[\frac{\hat{n}-1}{2^k},\frac{\hat{n}+1}{2^k}]} \left|f^{(m+1)}(\xi)\right|. \tag{17}$$

Then for error on Ω we get

$$\|e(x)\| \leq \frac{1}{2^{k/2}} \frac{h^{(m+1)}}{4(m+1)} \max_{\xi\in[0,1]} \left|f^{(m+1)}(\xi)\right|. \tag{18}$$

3.3 The Legendre wavelets operational matrix of integration

The integration of the Vector defined in Eq.(12) can be obtained as

$$\int_0^t \Psi(t')dt' = P\Psi(t), \tag{19}$$

where P is the $2^{k-1}M \times 2^{k-1}M$ operational matrix for integration [18]

$$P=\frac{1}{2^k}\begin{bmatrix} L & H & H & H & \cdots & H \\ 0 & L & H & H & \cdots & H \\ 0 & 0 & L & H & \cdots & H \\ \vdots & \vdots & \vdots & \ddots & \ddots & \cdots \\ 0 & 0 & 0 & \cdots & L & H \\ 0 & 0 & 0 & 0 & \cdots & L \end{bmatrix}.$$

H and L are $M \times M$ matrices given by :

$$H = \begin{bmatrix} 2 & 0 & \cdots & 0 \\ 0 & 0 & \cdots & 0 \\ \cdots & \cdots & \ddots & \vdots \\ 0 & 0 & \cdots & 0 \end{bmatrix},$$

and

$$L = \begin{bmatrix} 1 & \frac{1}{3^{1/2}} & 0 & 0 & \cdots & 0 & 0 & 0 \\ -\frac{3^{1/2}}{3} & 0 & \frac{3^{1/2}}{3\times 5^{1/2}} & 0 & \cdots & 0 & 0 & 0 \\ 0 & -\frac{5^{1/2}}{5\times 3^{1/2}} & 0 & \frac{5^{1/2}}{5\times 7^{1/2}} & & 0 & 0 & 0 \\ 0 & 0 & -\frac{7^{1/2}}{7\times 5^{1/2}} & 0 & \ddots & 0 & 0 & 0 \\ \vdots & \vdots & \vdots & \vdots & \ddots & \ddots & \ddots & \vdots \\ 0 & 0 & 0 & 0 & \cdots & -\frac{(2M-3)^{1/2}}{(2M-3)(2M-5)^{1/2}} & 0 & \frac{(2M-3)^{1/2}}{(2M-3)(2M-1)^{1/2}} \\ 0 & 0 & 0 & 0 & \cdots & 0 & -\frac{(2M-1)^{1/2}}{(2M-1)(2M-3)^{1/2}} & 0 \end{bmatrix}.$$

3.4 Operational matrix of fractional integration

We defined a m-set of Block Pulse function (BPF)as:

$$b_i(t) = \begin{cases} 1, & i/m \le t < (i+1)/m \\ 0, & otherwise, \end{cases} \tag{20}$$

where $i = 0, 1, 2, \ldots (m-1)$.

The function $b_i(t)$ are disjoint and orthogonal. That is

$$b_i(t)b_j(t) = \begin{cases} 0, & i \neq j \\ b_i(t), & i = l. \end{cases} \tag{21}$$

The Legendre wavelet may be expanded into m-terms of block pulse function (BPF) as

$$\Psi_m(t) = \Phi_{m\times m} B_m(t), \tag{22}$$

where

$$B_m(t) \triangleq [\, b_0(t)\ b_1(t)\ \ldots\ b_i(t)\ \ldots\ b_{(m-1)}(t)\,]^T. \tag{23}$$

The Block Pulse operational matrix of the fractional integration give in [12] F^α as following:

$$(I_t^\alpha B_m)(t) \approx F^\alpha B_m(t), \tag{24}$$

where

$$F^{\alpha}=\frac{1}{m^{\alpha}}\frac{1}{\Gamma(\alpha+2)}\begin{bmatrix}1 & \xi_1 & \xi_2 & \cdots & \xi_{(m-1)}\\ 0 & 1 & \xi_1 & \cdots & \xi_{(m-2)}\\ 0 & 0 & 1 & \cdots & \xi_{(m-3)}\\ & & & \ddots & \vdots\\ 0 & 0 & 0 & 0 & 1\end{bmatrix}.$$

with $\xi_k=(k+1)^{\alpha+1}-2k^{\alpha+1}+(k-1)^{\alpha+1}$. The Legendre wavelet operational matrix of of fractional integration is defined in [19] as

$$P^{\alpha}_{m\times m}=\Phi_{m\times m}F^{\alpha}\Phi^{-1}_{m\times m}, \tag{25}$$

so the fractional integration of vector in Eq. (12) is defined as

$$(I^{\alpha}_{t}\Psi)(t)\approx P^{\alpha}\Psi_m(t). \tag{26}$$

4 Application to nonlinear system of VFIDEs

Here, before presenting our method, we prove the next lemma. By this lemma we can approximate the high order derivative of a function by Legendre wavelet.

Lemma. *Suppose that $u(x)=C^T\Psi(x)$ where C and $\Psi(x)$ are defined in Eq. (11) and Eq. (12), then*

$$u^{(k)}(x)=(C^TP^{-k}-\sum_{i=0}^{k-1}u_0^{(i)}E^TP^{i-k})\Psi(x), \tag{27}$$

where P is operational matrix of integration, $u^{(i)}(0)=u_0^{(i)}$ and E is defined as $E^T\Psi(t)=1$.

Proof. suppose that $f(x)=u^k(x)$ and we approximate $u(x)$ and $f(x)$ by Legender wavelet as

$$\begin{cases}u(x)=C^T\Psi(x),\\ f(x)=F^T\Psi(x),\end{cases} \tag{28}$$

by integrating $f(t)$ on $[0,t]$

$$\begin{aligned}\int_0^t\int_0^t\cdots\int_0^t f(t')\underbrace{dt'\ldots dt'}_{k-times}&=\int_0^t\int_0^t\cdots\int_0^t F^TP\Psi(t')\underbrace{dt'\ldots dt'}_{(k-1)times}\\ &=\int_0^t\int_0^t\cdots\int_0^t F^TP^2\Psi(t')\underbrace{dt'\ldots dt'}_{(k-2)times}\\ &\vdots\\ &=F^TP^k\Psi(t),\end{aligned} \tag{29}$$

Since $f(x) = u^k(x)$, then

$$\begin{aligned}\int_0^t \int_0^t \cdots \int_0^t f(t') \underbrace{dt' \cdots dt'}_{k-times} &= \int_0^t \int_0^t \cdots \int_0^t (u^{(k-1)}(t) - u^{(k-1)}(0)) \underbrace{d(t') \cdots dt'}_{(k-1)-times} \\ &= \int_0^t \int_0^t \cdots \int_0^t u^{(k-1)}(t) \underbrace{dt' \cdots dt'}_{(k-1)-times} - u^{(k-1)}(0) \int_0^t \int_0^t \cdots \int_0^t \underbrace{dt' \cdots dt'}_{(k-1)-times} \\ &\vdots \\ &= u(t) - u^{(0)}(0) - u^{(1)}(0) - \cdots - u^{(k-1)}(0) \int_0^t \int_0^t \cdots \int_0^t \underbrace{dt' \cdots dt'}_{(k-1)-times},\end{aligned} \tag{30}$$

by $u^{(i)}(0) = u_0^{(i)}$ we get

$$u_0^{(i)} \int_0^t \int_0^t \cdots \int_0^t \underbrace{dt' \cdots dt'}_{k-times} = u_0^{(i)} E^T P^i \Psi(t), \tag{31}$$

Eq. (29)-(31) result

$$\begin{aligned}F^T P^k \Psi(t) &= C\Psi(t) - u_0^{(0)} E^T \Psi(t) - u_0^{(1)} E^T P \Psi(t) - \cdots - u_0^{(k-1)} E^T P^{k-1} \Psi(t) \\ &= C^T \Psi(t) - \sum_{i=0}^{k-1} u_0^{(i)} E^T P^i \Psi(t),\end{aligned} \tag{32}$$

Since the basis functions are linear independent, we omit $\Psi(t)$ from both sides of Eq. (32), then this equation can be written as

$$F^T P^k = C^T - \sum_{i=0}^{k-1} u_0^{(i)} E^T P^i, \tag{33}$$

and then

$$F^T = C^T P^{-k} - \sum_{i=0}^{k-1} u_0^{(i)} E^T P^{i-k}, \tag{34}$$

according to Eq. (28)

$$u^{(k)}(x) = (C^T P^{-k} - \sum_{i=0}^{k-1} u_0^{(i)} E^T P^{i-k}) \Psi(x). \tag{35}$$

This ends the proof of lemma. □

To solve Eq. (2) by Legendre wavelets, we assume that each $u_\ell(x)$ has the expansion as

$$u_\ell(x) = C_\ell^T \Psi(x), \qquad \ell = 1, \ldots, s, \tag{36}$$

by Eq. (35) the derivative expansion is given by

$$y_\ell^{(k)}(x) = (C_\ell^T P^{-k} - \sum_{i=0}^{k-1} y_{\ell 0}^{(i)} E^T P^{i-k})\Psi(x), \qquad \ell = 1, \ldots, s, \tag{37}$$

substituting Eq. (36) and Eq. (37) in Eq. (2) results for $\ell = 1, \ldots, s$

$$\begin{aligned} p_{\ell 0} C_\ell^T \Psi(x) + \sum_{i=1}^{n} p_{\ell i}(x)(C_\ell^T P^{-i} - \sum_{m=0}^{i-1} u_{\ell 0}^{(m)} E^T P^{m-i})\Psi(x) = f_\ell(x) \\ +\lambda_{\ell 1} \int_0^1 K_{\ell 1}(x, t, C_1^T \Psi(t), \ldots, (C^T P^{-n} - \sum_{i=0}^{n-1} u_0^{(i)} E^T P^{i-n})\Psi(x))dt \\ +\lambda_{\ell 2} \int_0^x K_{\ell 2}(x, t, C_1^T \Psi(t), \ldots, (C^T P^{-n} - \sum_{i=0}^{n-1} u_0^{(i)} E^T P^{i-n})\Psi(x))dt. \end{aligned} \tag{38}$$

by suitable collocation points, the zeros of Chebyshve polynomials [16]

$$x_i = \cos(\frac{(2i-1)\pi}{2^k M}), \quad i = 1, \ldots, 2^{k-1} M, \tag{39}$$

we collocate the Eq. (38). In order to use the Gaussian integration formula for Eq. (38), we transfer the t-intervals $[0, x_i]$ and [0,1] into ζ_1 and ζ_2 intervals [-1,1] by

$$\zeta_1 = \frac{2}{x_i} t - 1, \qquad \zeta_2 = 2t - 1. \tag{40}$$

Let

$$\begin{cases} H_{\ell 1}(x_j, t) = K_{\ell 1}(x_j, t, C_1^T \Psi(t), \ldots, (C^T P^{-n} - \sum_{i=0}^{n-1} y_0^{(i)} E^T P^{i-n})\Psi(x)), \\ \\ H_{\ell 2}(x_j, t) = K_{\ell 2}(x_j, t, C_1^T \Psi(t), \ldots, (C^T P^{-n} - \sum_{i=0}^{n-1} u_0^{(i)} E^T P^{i-n})\Psi(x)), \end{cases} \quad \ell = 1, \ldots, s. \tag{41}$$

We rewrite Eq. (38) as

$$\begin{aligned} p_{\ell 0} C_\ell^T \Psi(x_j) + \sum_{i=1}^{n} p_{\ell i}(x_j)(C_\ell^T P^{-i} - \sum_{m=0}^{i-1} u_{\ell 0}^{(m)} E^T P^{m-i})\Psi(x_j) = f_\ell(x_j) \\ +\lambda_{l1} \tfrac{x_j}{2} \int_{-1}^1 H_{\ell 1}(x_j, \tfrac{x_j}{2}(\zeta_1 + 1))d\zeta_1 \\ +\tfrac{\lambda_{\ell 2}}{2} \int_{-1}^1 H_{\ell 2}(x_j, \tfrac{1}{2}(\zeta_2 + 1))d\zeta_2, \qquad \ell = 1, \ldots, s, \end{aligned} \tag{42}$$

and with the Gaussian integration

$$\begin{aligned} p_{\ell 0} C_\ell^T \Psi(x_j) + \sum_{i=1}^{n} p_{\ell i}(x_j)(C_\ell^T P^{-i} - \sum_{m=0}^{i-1} u_{\ell 0}^{(m)} E^T P^{m-i})\Psi(x_j) \approx f_\ell(x_j) \\ +\lambda_{\ell 1} \tfrac{x_j}{2} \sum_{h=1}^{s_1} \omega_{1h} H_{\ell 1}(x_j, \tfrac{x_j}{2}(\zeta_{1h} + 1)) \\ +\tfrac{\lambda_{\ell 2}}{2} \sum_{h=1}^{s_2} \omega_{2h} H_{\ell 2}(x_j, \tfrac{1}{2}(\zeta_{2h} + 1)), \qquad \ell = 1, \ldots, s, \end{aligned} \tag{43}$$

where ζ_{1h} and ζ_{2h} are s_1 and s_2 zeros of Legendre polynomials L_{s_1+1} and L_{s_2+1} respectively, and ω_{1h}, ω_{2l} are the corresponding weights. If we assume that

$$\begin{cases} A_\ell(x) = p_{\ell 0} C_\ell^T \Psi(x_j) + \sum_{i=1}^{n} p_{\ell i}(x_j)(C_\ell^T P^{-i} - \sum_{m=0}^{i-1}) u_{\ell 0}^{(m)} E^T P^{m-i}) \Psi(x_j) \\ \quad -\lambda_{\ell 1} \frac{x_j}{2} \sum_{h=1}^{s_1} \omega_{1h} H_{\ell 1}(x_j, \frac{x_j}{2}(\zeta_{1h}+1)) - \frac{\lambda_{\ell 2}}{2} \sum_{h=1}^{s_2} \omega_{2h} H_{\ell 2}(x_j, \frac{1}{2}(\zeta_{2h}+1)), \\ B_\ell(x) = f_\ell(x), \qquad \ell = 1, \ldots, s, \end{cases} \tag{44}$$

Then our problem has the next matrix representation form

$$\begin{pmatrix} A_1(x_1) \\ \vdots \\ A_1(x_{2^{k-1}M}) \\ - - - - - \\ \vdots \\ - - - - - \\ A_s(x_1) \\ \vdots \\ A_s(x_{2^{k-1}M}) \end{pmatrix} = \begin{pmatrix} B_1(x_1) \\ \vdots \\ B_1(x_{2^{k-1}M}) \\ - - - - - \\ \vdots \\ - - - - - \\ B_s(x_1) \\ \vdots \\ B_s(x_{2^{k-1}M}) \end{pmatrix}$$

This $2^{k-1}Ms \times 2^{k-1}Ms$ nonlinear system of equations which can be solved using Newton iterative method for the elements of C.

5 Application to nonlinear fractional order integro-differential equations

In this section we want to apply the operational matrix of fractional integration to fractional order integro-differential equation. Assume that we approximate $D_{*t}^{\alpha} u(x)$ by Legndre wavelet as

$$D_{*t}^{\alpha} u(x) = K^T \Psi(x), \tag{45}$$

then Eq. (8)and Eq. (26) result

$$u(x) = K^T P_{m\times m}^{\alpha} \Psi(x) + u(0). \tag{46}$$

By Eq. (45)and Eq. (46) we rewrite Eq. (1) as

$$K^T \Psi(x) = f(x) + \int_0^x k(t, K^T P_{m\times m}^{\alpha} \Psi(t) + u(0), K^T \Psi(t)) dt \tag{47}$$

Assume that

$$H(t) = k(t, K^T P^{\alpha}_{m\times m}\Psi(t) + u(0), K^T\Psi(t)), \tag{48}$$

and like the last chapter, we collocated this equation by Eq. (39)in $2^{k-1}M$ points and then use the Gaussian integration. Finally, we can write Eq. (39) as

$$K^T\Psi(x_i) = f(x_i) + \sum_{h=1}^{s_1} \frac{x_i}{2}\omega_{1h} H(\frac{x_i}{2}(\zeta_h + 1)) \quad i = 1, \ldots, 2^{k-1}M \tag{49}$$

which is the $2^{k-1}M \times 2^{k-1}M$ nonlinear of system equation which can be solved using Newton iterative method for the elements of C.

6 Numerical examples

In this section we consider some examples which show that operational matrices are powerful and demonstrate the accuracy of our method.

Example 5.1. Consider the nonlinear system of integro-differential equation

$$\begin{cases} 3xu_1(x) + u_1''(x) = 5x^3 + 2u_2'(x) - \int_0^x (u_2'(t) + u_1(t)u_3''(t))dt, + \int_0^1 xu_1'(t)u_2'(t)dt, \\ 2u_2'(x) + u_2''(x) = -4x^2 - xu_1(x) + \int_0^x (txu_2'(t)u_1''(t) + u_3'(t))dt + \int_0^1 x^2u_3(t) + u_2'(t)u_1''(t)dt \\ x/3y_3(x) + u_3''(x) = 2 - \frac{4}{3}x^3 + u_1''^2(x) - 2u_1^2(x) + \int_0^x (x^2u_2(t) + u'^2(t) + t^3u_3''(t))dt + \int_0^1 x^2u_1'(t)dt \\ u_1(0) = u_1'(0) = 0, u_2(0) = 0, u_2'(0) = 1, u_3(0) = u_3(0) = 0, \end{cases} \tag{50}$$

which has the exact solution $u_1(x) = x^2$, $u_2(x) = x$ and $u_3(x) = 3x^2$. Figure.1 show the absolute error when we apply our method for $M = 3$ and $k = 1$.

It is clear form figures that our approximate solution is in good agreement with exact one.

Example 5.2. As a second example, consider the nonlinear system given in [2, 1]

$$\begin{cases} u_1'(x) = 1 - \frac{1}{2}u_2'(x) + \int_0^x ((x-t)u_2(t) + u_1(t)u_2(t))dt, \\ u_2'(x) = 2x + \int_0^x ((x-t)u_1(t) - u_2^2(t) + u_1^2(t))dt, \\ u_1(0) = 0, u_2(0) = 1, \end{cases} \tag{51}$$

which has the exact solution $u_1(x) = sinh(x)$ and $u_2(x) = cosh(x)$ for $M = 6$ and $k = 1$.

Results for Example 5.2 are reported in Table 1 for $u_1(x_i)$ and $u_2(x_i)$.

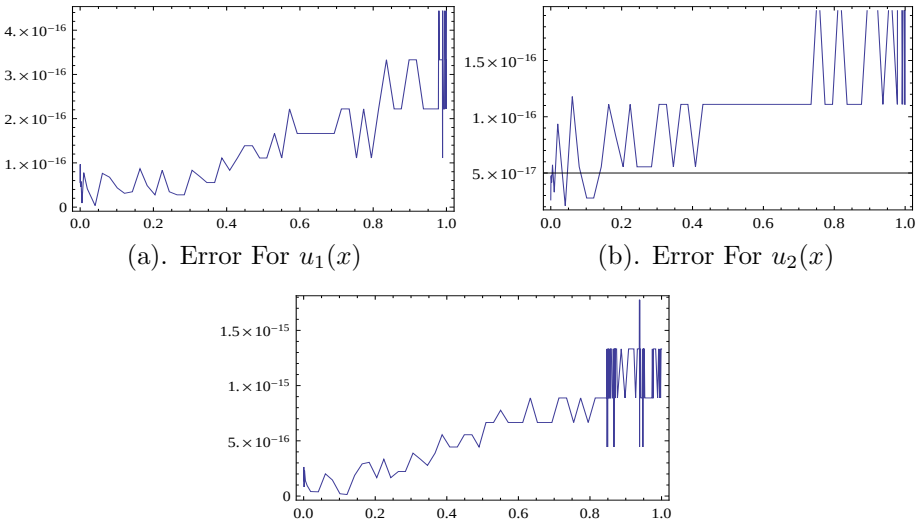

(a). Error For $u_1(x)$ (b). Error For $u_2(x)$

(c). Error For $u_3(x)$

Figure 1: Absolute error for Example 5.1 for M=3 And k=1

Example 5.3. Consider the nonlinear fractional order integro differential equation given in[7]

$$D^{\alpha}_{*t}u(t) = 1 + \int_0^x u(t)D^{\alpha}_{*t}u(t)dt \qquad 0 \leq x < 10 \leq \alpha < 1 \tag{52}$$

The exact solution of this problem for $\alpha = 1$ is $\sqrt{2}Tan(\frac{\sqrt{2}}{2}t)$ we solve this equation for $m = 20$ and different α numerical results are shown in Figure 2.

Example 5.4. Finally Consider the nonlinear fractional order integro differential equations in[7]

$$D^{\alpha}_{*t}u(t) = -1 + \int_0^x u^2(t)dt 0 \leq x < 1 \;\; 0 \leq \alpha < 1 \tag{53}$$

subject to the initial conditions $y(0) = 0$. Table 2 shows the numerical results for $\alpha = 0.8, 0.9, 1$ when $m = 20$. From Table 2 we can see that the approximate solutions obtained by our method are in good agreement with the exact solution for $\alpha = 1$, and with the approximate solutions for $\alpha = 0.8, 0.9$ in [7].

Table 1: Numerical result of Example 5.2

	Error for $M=6, k=1$		Error for Method of [2] $N=5$		Error for Method of [1] $N=6$	
x_i	$u_2(x)$	$u_1(x)$	$u_2(x)$	$u_1(x)$	$u_2(x)$	$u_1(x)$
0	1.70×10^{-6}	7.66×10^{-7}	0	0	0	0
0.1	6.82×10^{-7}	3.42×10^{-7}	1.3×10^{-8}	1×10^{-8}	1.41×10^{-9}	1.41×10^{-9}
0.2	2.85×10^{-7}	8.94×10^{-8}	7.98×10^{-7}	1.33×10^{-7}	9.15×10^{-8}	9.15×10^{-8}
0.3	5.17×10^{-7}	2.50×10^{-7}	9.06×10^{-6}	2.17×10^{-6}	1.06×10^{-6}	1.06×10^{-6}
0.4	1.17×10^{-7}	1.22×10^{-8}	5.06×10^{-5}	1.53×10^{-5}	6.03×10^{-6}	6.03×10^{-6}
0.5	5.43×10^{-7}	2.40×10^{-7}	1.90×10^{-4}	6.64×10^{-5}	2.34×10^{-5}	2.34×10^{-5}
0.6	1.75×10^{-7}	1.08×10^{-7}	5.05×10^{-4}	2.12×10^{-4}	7.08×10^{-5}	7.08×10^{-5}
0.7	4.65×10^{-7}	2.43×10^{-7}	1.36×10^{-3}	5.27×10^{-4}	1.81×10^{-5}	1.81×10^{-5}
0.8	2.68×10^{-7}	4.02×10^{-7}	2.87×10^{-3}	1.05×10^{-3}	4.10×10^{-4}	4.10×10^{-4}
0.9	7.65×10^{-7}	5.10×10^{-7}	5.34×10^{-3}	1.66×10^{-3}	8.45×10^{-4}	8.45×10^{-4}
1	2.85×10^{-6}	1.44×10^{-6}	8.71×10^{-3}	1.17×10^{-3}	1.62×10^{-3}	1.62×10^{-3}

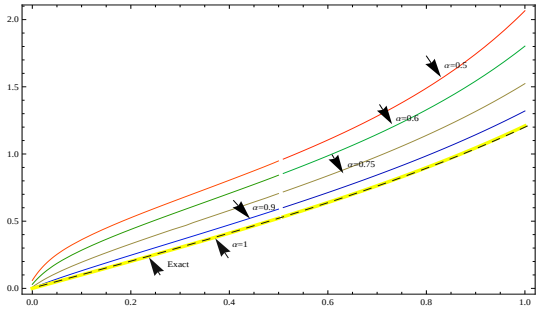

Figure 2: Numerical result for Example 5.3 for different α and m=20

7 Conclusion

Most nonlinear integro-differential equation with nonlinear differential part are usually difficult to solve analytically. In many cases it is required to obtain the approximate solution. We have shown that the properties of operational of matrix of integration and operational matrix of fractional integration together with Legendre wavelet can reduce the system of nonlinear integro-differential equation and nonlinear fractional order integro differential equation to a system of algebraic equations. The advantage of this method is that it can solve high and fractional order integro-differential equation easier and more time efficient. Also we found an error bound. Although we solved our problem by Legender wavelet, other orthogonal basis also can be used. Illustrative examples show the high accuracy of the method in compar-

Table 2: Numerical result of Example 5.4

x_i	Exact solution $\alpha = 1$	Our method			Method of [7]		
		$\alpha = 1$	$\alpha = 0.9$	$\alpha = 0.8$	$\alpha = 1$	$\alpha = 0.9$	$\alpha = 0.8$
0	0	0	-0.00013	-0.00046	0	0	0
0.0625	-0.06250	-0.06249	-0.08574	-0.11683	-0.06250	-0.08574	-0.11682
0.125	-0.12498	-0.124977	-0.15995	-0.20327	-0.12498	-0.15997	-0.20328
0.1875	-0.18740	-0.18749	-0.23023	-0.28080	-0.18740	-0.23024	-0.28082
0.2500	-0.24968	-0.24966	-0.29788	-0.35269	-0.24968	-0.29790	-0.35272
0.3125	-0.31171	-0.31172	-0.36339	-0.42026	-0.31171	-0.36342	-0.42039
0.3750	-0.37336	-0.37333	-0.42695	-0.48409	-0.37336	-0.42689	-0.48413
0.4375	-0.43446	-0.43443	-0.48858	-0.54446	-0.43446	-0.48861	-0.54451
0.5000	-0.49482	-0.49478	-0.54818	-0.60140	-0.49482	-0.54824	-0.60150
0.5625	-0.55423	-0.55418	-0.60565	-0.65501	-0.55423	-0.60571	-0.65510
0.6250	-0.61243	-0.61237	-0.66078	-0.70511	-0.61243	-0.66086	-0.70521
0.6875	-0.66917	-0.66910	-0.71337	-0.75162	-0.66917	-0.71345	-0.75172
0.7500	-0.72415	-0.72418	-0.76318	-0.79440	-0.72415	-0.76327	-0.79451
0.8125	-0.77710	-0.77710	-0.80997	-0.83330	-0.77710	-0.81006	-0.83341
0.8750	-0.82767	-0.82771	-0.85348	-0.86820	-0.82767	-0.85395	-0.86831
0.9375	-0.87557	-0.87564	-0.89349	-0.89896	-0.87557	-0.89361	-0.89908

ison with other methods. This procedure can also be used for solving other functional equations such as ordinary and partial differential equations.

References

1. Abbasbandy, S. and Taati, A. *Numerical solution of the system of nonlinear Volterra integro-differential equations with nonlinear differential part by the operational Tau method and error estimation*, journal of computational and Applied Mathematics, 231(2009)106-113.

2. Biazar, J., Ghazvini, H. and Eslami, M. *He's homotopy perturbation method for systems of integro-differential equations*, Chaos Solition and Fractals, doi:10.1016/j.chaos.2007.06.001.

3. Caputo, M. *Linear modles of dissipation whose Q is almost frequenty independent*, Part II, J.Roy. Astr. Soc.,13:529-539.

4. El-shahed, M. *Application of He*'s *homotopy perturbation method to Volterra*'s *intgro-differential equation*, International Journal of Nonlinear sciences and Numerical Simulation 8 (2) (2007) 223-228.

5. Elsayed, S. M., Kaya, D. and Zarea, S. *The decomposition method applied to solve high order linear Volterra-Fredholm integro-differential equations*, International Journal of Nonlinear sciences and Numerical Simulation 8 (2) (2007) 211-222.

6. Erjaee, G. H., Taghvafard, H. and Alnasr, M. *Numerical solution of the high thermal loss problem presented by a fractional differential equa-*

tion, Communication in Nonlinear sciences and Numerical Simulation 16 (2011) 1356–1362.

7. Gazanfari, B., Ghazanfari, A. G. and Veisif, F. *Homotopy perturbation Method for the nonlinear fractional integro differentioal equations*, Australian Journal of Basic an Applied Sciencec 4 (12) (2010) 5823-5829.

8. Golbabai, A. and Javidi, M. *Application of He's homotopy perturbation method for n-th order integro differential equations*, Applied Mathematics and Computation, 190 (2007) 1409-1416.

9. Golbabai, A. and Javidi, M. *A numerical solution for solving system of Fredholm integral equation by using perturbation method*, Applied Mathematics and Computation, 189 (2007) 1921-1928.

10. Guf, J. S. and Jiang, W. S. *The Haar wavelet operational m atrix of integration*, International Journal of Systems Science, 27 (1996) 623-628.

11. Hu, X. B. and Wu, Y. T. *Application of the Hirota bilinear formalism to a new integrable differential-difference equation*, Physics Letters A, 246 (1998) 523-529.

12. Kilicman, A. and Al Zhour, Z. A. A.*Kronecker operational matrices for fractional calculus and some application*, Applied Mathematic and Computation 187(2007)250-265.

13. Liu, N. and Ling, E. B. *Legendre wavelets method for numerical solutions of partial differential equations*, Numerical Methods for partial Differential Equations. 26 (2009) 81-94.

14. Podlubny, I. *Fractional differential equations:an introduction to fractional derivatives, fractional differentional equations, to methods of their solution and some their application*. New York: Academic Press; 1999.

15. Razzaghi, M. and Yousefi, S. *Legendre wavelets method for constrained optimal control problems*, Mathematical method in Applied Sciences. 25 (2002)529-539.

16. Razzaghi, M. and Yousefi, S. *Legendre wavelet method for the nonlinear Volterra-Fredholm integral equations*, Mathematics and Computer in Simulation. 70 (2005) 1-8.

17. Razzaghi, M. and Yousefi, S. *Legendre wavelets direct method for variational problems*, Mathematics and Computer in Simulation. 53 (2000) 185-192.

18. Razzaghi, M. and Yousefi, S. *The Legendre wavelet operational matrix of integration*, International Journal of Systems Science, 32 (2001) 495-502.

19. Rehman, M. and Ali Khan, R. *The Legendre wavelet methosd for solving fractional differentional equations*, Communication in Nonlinear sciences and Numerical Simulation 16 (2011) 4163-4173.

20. Sun, F. Z., Gao, M., Lei, S. H., Zaho, Y. B., Wang, K., Shi, Y. T. and Wang, N. H. *The fractal dimension of the fractal model of dropwise condensation and its experimental study*, International Journal of Nonlinear sciences and Numerical Simulation 8 (2) (2007) 211-222.

21. Taghvafard, H. and Erjaee, G. H. *On solving a system of singular Volterra integral equations of convolution type*, Communication in Nonlinear sciences and Numerical Simulation 16 (2011) 3486–3492.

22. Tarasov, V. E. *Fractional integro diffe rentional equations for electromagnetic waves in dielectric media*, Theoritical and Mathematical Physics, 153 (3) (2009) 355-359.

23. Wang, H., Fu, H. M. , Zhang, H. F. and Hu, Z. Q. *A practical thermodynamic method to calculate the best glass-forming composition for bulk metallic glasses*, International Journal of Nonlinear sciences and Numerical Simulation 8 (2) (2007) 171-178.

24. Xu, L., He, J. H. and Liu, Y. *Electrospun nanoporous spheres whit Chinese drug*, International Journal of Nonlinear sciences and Numerical Simulation 8 (2) (2007) 199-202.

Iranian Journal of Numerical Analysis and Optimization
Vol 4, No. 1, (2014), pp 57-76

Solving an inverse problem for a parabolic equation with a nonlocal boundary condition in the reproducing kernel space

M. Mohammadi, R. Mokhtari* and F. T. Isfahani

Abstract

On the basis of a reproducing kernel space, an iterative algorithm for solving the inverse problem for heat equation with a nonlocal boundary condition is presented. The analytical solution in the reproducing kernel space is shown in a series form and the approximate solution v_n is constructed by truncating the series to n terms. The convergence of v_n to the analytical solution is also proved. Results obtained by the proposed method imply that it can be considered as a simple and accurate method for solving such inverse problems.

Keywords: Inverse problem; Parabolic equation; Nonlocal boundary conditions; Reproducing kernel space.

1 Introduction

The problem of finding the solution of partial differential equations with source control parameter has appeared increasingly in physical phenomena such as heat transfer, thermoelasticity, control theory, population dynamics, nuclear reactor dynamics, medical sciences, biochemistry, etc. [1, 2, 3]. The

∗Corresponding authour
Received 1 July 2013; revised 25 December 2013; accepted 22 January 2014
M. Mohammadi
Department of Mathematical Sciences, Isfahan University of Technology, Isfahan 84156-83111, Iran. e-mail: m_mohammadi@math.iut.ac.ir

R. Mokhtari
Department of Mathematical Sciences, Isfahan University of Technology, Isfahan 84156-83111, Iran.
e-mail: mokhtari@cc.iut.ac.ir

F. T. Isfahani
Department of Mathematical Sciences, Isfahan University of Technology, Isfahan 84156-83111, Iran.
e-mail: f.toutianesfahani@math.iut.ac.ir

parameter determination in a parabolic partial differential equation from the over-specified data plays a crucial role in applied mathematics and physics. This technique has been widely used to determine the unknown properties of a region by measuring a specified location in the domain. These unknown properties such as the conductivity medium are important to the physical process but usually can not be measured directly, or very expensive to be measured [2, 3]. In general, these problems are ill-posed. Therefore a variety of numerical techniques based on regularization, finite differences, finite element and finite volume methods are given to approximate solutions of such problems [2, 3, 4].

In recent years all kinds of boundary conditions and over-specified conditions arise in the inverse problems which make them more and more difficult to solve. The integral over-specified condition arises from many important applications in heat transfer, termoelasticity, control theory, life sciences, etc. Some different partial differential equations with nonlocal boundary and over specified conditions can be found in [5, 6, 7, 8, 9, 10].

The theory of reproducing kernels [11], was used for the first time at the beginning of the 20th century by S. Zaremba in his work on boundary value problems for harmonic and biharmonic functions. This theory has been successfully applied for solving a bunch of problems, see e.g. [12, 13, 14, 15, 16, 17, 18] and references cited therein. The book [19] provides excellent overviews of the existing reproducing kernel methods.
In this paper, a new algorithm for determining unknown solution and unknown control parameter of the parabolic inverse problem with nonlocal boundary and integral over-specified conditions based on the reproducing kernel space, is presented. The advantages of the approach must lie in the following facts. The approximate solution converges uniformly to the analytical solution. The method is mesh free, easily implemented and it needs no time discretization. Also we can evaluate the approximate solution $v_n(x,t)$ for fixed n once, and use it over and over.

The rest of the paper is organized as follows. In section 2 we describe the governing equation. Several reproducing kernel spaces are defined in Section 3. The method implementation and convergence analysis are prepared in Section 4. Numerical results are presented in section 5. The last section is a brief conclusion.

2 Governing equation

Consider the inverse problem of determination a pair of functions $\{v, p\}$ in the following parabolic equation

$$\frac{\partial v}{\partial t} - \frac{\partial^2 v}{\partial x^2} = p(t)v + f(x,t) \qquad (x,t) \in \Omega = (0,1) \times (0,T] \qquad (1)$$

with the initial condition

$$v(x,0)=\varphi(x), \qquad x\in[0,1] \tag{2}$$

nonlocal boundary conditions

$$v(0,t)=v(1,t), \qquad v_x(1,t)=0, \qquad 0\le t\le T \tag{3}$$

and the integral over-specified condition

$$\int_0^1 v(x,t)dx=E(t), \qquad t\in[0,T] \tag{4}$$

where $f(x,t)$, $\varphi(x)$, and $E(t)$ are known functions.

The existence, uniqueness, and continuous dependence of the solution upon the data for this problem are demonstrated in [20].

After taking integration from both sides of the equation (1) and using integral over-specified condition, we obtain

$$p(t)=\frac{E'(t)+v_x(0,t)-\int_0^1 f(x,t)dx}{E(t)}. \tag{5}$$

Then we have the following model problem

$$\begin{cases} \frac{\partial v}{\partial t}-\frac{\partial^2 v}{\partial x^2}=\frac{E'(t)+v_x(0,t)-\int_0^1 f(x,t)dx}{E(t)}v+f(x,t), \quad (x,t)\in\Omega=(0,1)\times(0,T] \\ v(x,0)=\varphi(x), \quad v(0,t)=v(1,t), \quad v_x(1,t)=0. \end{cases}$$

After homogenizing the initial condition, we have

$$\begin{cases} \frac{\partial u}{\partial t}-\frac{\partial^2 u}{\partial x^2}+\frac{\int_0^1 f(x,t)dx-E'(t)}{E(t)}u=F(x,t,u,u_x) \quad (x,t)\in\Omega=(0,1)\times(0,T] \\ u(x,0)=0, \quad u(0,t)=u(1,t), \quad u_x(1,t)=0, \end{cases} \tag{6}$$

where

$$F(x,t,u,u_x)=\frac{(u(x,t)+\varphi(x))\,(u_x(0,t)+\varphi'(0))}{E(t)} + \frac{E'(t)-\int_0^1 f(x,t)dx}{E(t)}\varphi(x)+\varphi''(x)+f(x,t).$$

3 Reproducing kernel spaces

Definition 1. *Let H be a real Hilbert space of functions $f : \Omega \to \mathbb{R}$. Denote by $\langle \cdot, \cdot \rangle$ the inner product and let $\| \cdot \| = \sqrt{\langle \cdot, \cdot \rangle}$ be the induced norm in H. A real valued function $K(x, y) : \Omega \times \Omega \to \mathbb{R}$ is called a reproducing kernel of H if the followings are satisfied:*

$$\begin{aligned} &(i)\ K_y(x) = K(x, y) \in H \qquad \text{for all } y \in \Omega, \\ &(ii)\ f(y) = \langle f(x), K_y(x) \rangle \qquad \text{for all } f \in H \text{ and for all } y \in \Omega. \end{aligned}$$

Definition 2. *A Hilbert space H of functions on a set Ω is called a reproducing kernel Hilbert space if there exists a reproducing kernel K of H.*

Remark 1. *The existence of the reproducing kernel of a Hilbert space H is due to the Riesz Representation Theorem. It is known that the reproducing kernel is unique.*

Now, we define some useful reproducing kernel spaces. The corresponding reproducing kernels can be found by the usual technique in many articles in literature (see [13]).

Definition 3. *$W_0[0, 1] = \{u(x) | u(x), u'(x), u''(x)$ are absolutely continuous in $[0, 1], u^{(3)}(x) \in L^2[0, 1], u(0) = u(1), u'(1) = 0\}$. The inner product and the norm in $W_0[0, 1]$ are defined respectively by*

$$\langle u, v \rangle_{W_0} = \sum_{i=0}^{2} u^{(i)}(0) v^{(i)}(0) + \int_0^1 u^{(3)}(x) v^{(3)}(x) dx, \quad u, v \in W_0[0, 1], \quad (7)$$

and

$$\|u\|_{W_0} = \sqrt{\langle u, u \rangle_{W_0}}, \quad u \in W_0[0, 1].$$

The space $W_0[0, 1]$ is a reproducing kernel space and its reproducing kernel function is called $R_y(x)$.

Definition 4. *$W_1[0, T] = \{u(t) | u(t), u'(t)$ are absolutely continuous in $[0, T], u''(t) \in L^2[0, T]$, $u(0) = 0\}$. The inner product and the norm in $W_1[0, T]$ are defined respectively by*

$$\langle u, v \rangle_{W_1} = \sum_{i=0}^{1} u^{(i)}(0) v^{(i)}(0) + \int_0^T u''(t) v''(t) dt, \quad u, v \in W_1[0, T],$$

and

$$\|u\|_{W_1} = \sqrt{\langle u, u \rangle_{W_1}}, \quad u \in W_1[0, T].$$

The space $W_1[0, T]$ is a reproducing kernel space and its reproducing kernel function $r_s(t)$ is given by

$$r_s(t) = \begin{cases} st + \frac{s}{2}t^2 - \frac{1}{6}t^3 & t \le s, \\ st + \frac{s^2}{2}t - \frac{1}{6}s^3 & t > s. \end{cases}$$

Definition 5. *$W_2[0,1] = \{u(x) | u(x), u'(x)$ are absolutely continuous in $[0,1], u''(x) \in L^2[0,1]\}$. The inner product and the norm in $W_2[0,1]$ are defined respectively by*

$$\langle u, v \rangle_{W_2} = \sum_{i=0}^{1} u^{(i)}(0) v^{(i)}(0) + \int_0^1 u''(x) v''(x) dx, \quad u, v \in W_2[0,1],$$

and

$$\|u\|_{W_2} = \sqrt{\langle u, u \rangle_{W_2}}, \quad u \in W_2[0,1].$$

The space $W_2[0,1]$ is a reproducing kernel space and its reproducing kernel function $Q_y(x)$ is given by

$$Q_y(x) = \begin{cases} 1 + yx + \frac{y}{2}x^2 - \frac{1}{6}x^3 & x \le y, \\ 1 + yx + \frac{y^2}{2}x - \frac{1}{6}y^3 & x > y. \end{cases}$$

Definition 6. *$W_3[0,T] = \{u(t) | u(t)$ is absolutely continuous in $[0,T], u'(t) \in L^2[0,T]\}$. The inner product and the norm in $W_3[0,T]$ are defined respectively by*

$$\langle u, v \rangle_{W_3} = u(0)v(0) + \int_0^T u'(t) v'(t) dt, \quad u, v \in W_3[0,T],$$

and

$$\|u\|_{W_3} = \sqrt{\langle u, u \rangle_{W_3}}, \quad u \in W_3[0,T].$$

The space $W_3[0,T]$ is a reproducing kernel space and its reproducing kernel function $q_s(t)$ is given by

$$q_s(t) = \begin{cases} 1 + t & t \le s, \\ 1 + s & t > s. \end{cases}$$

Definition 7. *$W(\overline{\Omega}) = \{u(x,t) | \frac{\partial^3 u}{\partial x^2 \partial t}$ is completely continuous in $\overline{\Omega}$, $\frac{\partial^5 u}{\partial x^3 \partial t^2} \in L^2(\Omega), u(x,0) = 0, u(0,t) = u(1,t), u_x(1,t) = 0\}$. The inner product and the norm in $W(\overline{\Omega})$ are defined respectively by*

$$\begin{aligned}\langle u,v\rangle_W = & \sum_{i=0}^{2}\int_0^T\left[\frac{\partial^2}{\partial t^2}\frac{\partial^i}{\partial x^i}u(0,t)\frac{\partial^2}{\partial t^2}\frac{\partial^i}{\partial x^i}v(0,t)\right]dt\\ &+\sum_{j=0}^{1}\langle\frac{\partial^j}{\partial t^j}u(x,0),\frac{\partial^j}{\partial t^j}v(x,0)\rangle_{W_0}\\ &+\int_0^T\int_0^1\left[\frac{\partial^3}{\partial x^3}\frac{\partial^2}{\partial t^2}u(x,t)\frac{\partial^3}{\partial x^3}\frac{\partial^2}{\partial t^2}v(x,t)\right]dxdt,\quad u,v\in W(\overline{\Omega}),\end{aligned}$$

and

$$\|u\|_W=\sqrt{\langle u,u\rangle_W},\quad u\in W(\overline{\Omega}).$$

Theorem 1. *$W(\overline{\Omega})$ is a reproducing kernel space and its reproducing kernel function is*

$$K_{(y,s)}(x,t)=R_y(x)r_s(t),$$

such that for any $u(x,t)\in W(\overline{\Omega})$,

$$u(y,s)=\langle u(x,t),K_{(y,s)}(x,t)\rangle_W,$$

where $R_y(x)$, $r_s(t)$ are the reproducing kernel functions of $W_0[0,1]$ and $W_1[0,T]$, respectively.

Proof. see [19]. □

Definition 8. *$\widetilde{W}(\overline{\Omega})=\{u(x,t)|\frac{\partial u}{\partial x}$ is completely continuous in $\overline{\Omega}$, $\frac{\partial^3 u}{\partial x^2\partial t}\in L^2(\Omega)\}$. The inner product and the norm in $\widetilde{W}(\overline{\Omega})$ are defined respectively by*

$$\begin{aligned}\langle u(x,t),v(x,t)\rangle_{\widetilde{W}}= & \sum_{i=0}^{1}\int_0^T\left[\frac{\partial}{\partial t}\frac{\partial^i}{\partial x^i}u(0,t)\frac{\partial}{\partial t}\frac{\partial^i}{\partial x^i}v(0,t)\right]dt\\ &+\langle u(x,0),v(x,0)\rangle_{W_2}\\ &+\int_0^T\int_0^1\left[\frac{\partial^2}{\partial x^2}\frac{\partial}{\partial t}u(x,t)\frac{\partial^2}{\partial x^2}\frac{\partial}{\partial t}v(x,t)\right]dxdt,\quad u,v\in\widetilde{W}(\overline{\Omega}),\end{aligned}$$

and

$$\|u\|_{\widetilde{W}}=\sqrt{\langle u,u\rangle_{\widetilde{W}}},\quad u\in\widetilde{W}(\overline{\Omega}).$$

$\widetilde{W}(\overline{\Omega})$ is a reproducing kernel space and its reproducing kernel function is

$$G_{(y,s)}(x,t)=Q_y(x)q_s(t).$$

4 The method implementation

By defining the linear operator $L : W(\overline{\Omega}) \to \widetilde{W}(\overline{\Omega})$ as

$$Lu = \frac{\partial u}{\partial t} - \frac{\partial^2 u}{\partial x^2} + \frac{\int_0^1 f(x,t)dx - E'(t)}{E(t)}\ u,$$

model problem (6) changes to the following problem

$$\begin{cases} Lu(x,t) = F(x,t,u,u_x), \quad (x,t) \in \Omega, \\ \\ u(x,0) = 0, \qquad u(0,t) = u(1,t), \qquad u_x(1,t) = 0. \end{cases} \tag{8}$$

Lemma 1. *L is a bounded linear operator.*

Proof. see [13]. □

Now, we choose a countable dense subset $\{(x_1,t_1),(x_2,t_2),\dots,\}$ in $\overline{\Omega}$, and define

$$\phi_i(x,t) = G_{(x_i,t_i)}(x,t), \qquad \psi_i(x,t) = L^*\phi_i(x,t),$$

where L^* is the adjoint operator of L. The orthonormal system $\{\bar{\psi}_i(x,t)\}_{i=1}^{\infty}$ of $W(\overline{\Omega})$ can be derived from Gram-Schmidt orthogonalization process of $\{\psi_i(x,t)\}_{i=1}^{\infty}$ as

$$\bar{\psi}_i(x,t) = \sum_{k=1}^{i} \beta_{ik}\psi_k(x,t),$$

where the orthogonal coefficients β_{ik} are given by

$$\beta_{ik} = \begin{cases} \frac{1}{\|\psi_1\|}, & i = k = 1, \\ \\ \dfrac{1}{\sqrt{\|\psi_i\|^2 - \sum_{j=1}^{i-1} c_{ij}^2}}, & i = k \neq 1, \\ \\ -\dfrac{\sum_{j=k}^{i-1} c_{ij}\beta_{jk}}{\sqrt{\|\psi_i\|^2 - \sum_{j=1}^{i-1} c_{ij}^2}}, & i \neq k, \end{cases}$$

where

$$\begin{aligned} c_{ij} &= \langle \psi_i(x,t), \bar{\psi}_j(x,t) \rangle_W \\ &= \langle L^* \phi_i(x,t), \bar{\psi}_j(x,t) \rangle_W \\ &= \langle \phi_i(x,t), L_{(x,t)} \bar{\psi}_j(x,t) \rangle_W \\ &= \left(L_{(x,t)} \bar{\psi}_j(x,t) \right)_{(x,t)=(x_i,t_i)} \\ &= \left(\sum_{m=1}^{j} \beta_{jm} L_{(x,t)} \psi_m(x,t) \right)_{(x,t)=(x_i,t_i)} . \end{aligned}$$

Like in [13], we get the following theorems.

Theorem 2. *Suppose that* $\{(x_i,t_i)\}_{i=1}^{\infty}$ *is dense in* $\overline{\Omega}$*, then* $\{\psi_i(x,t)\}_{i=1}^{\infty}$ *is a complete system in* $W(\overline{\Omega})$ *and* $\psi_i(x,t) = L_{(y,s)} K_{(y,s)}(x,t)|_{(y,s)=(x_i,t_i)}$.

Theorem 3. *If* $\{(x_i,t_i)\}_{i=1}^{\infty}$ *is dense in* $\overline{\Omega}$*, then the analytical solution of (8) is*

$$u(x,t) = \sum_{i=1}^{\infty} \sum_{k=1}^{i} \beta_{ik} \left[F(x_k, t_k, u(x_k,t_k), \partial_x u(0,t_k)) \right] \bar{\psi}_i(x,t). \tag{9}$$

By truncating the series in (9), we can obtain the approximate solution of (8). But, since the the series terms are not known, we need to construct an iterative method for obtaining the approximate solution. For this purpose, we choose nonnegative integer n and put the initial function $u_0(x,t) = 0$. Then the approximate solution is defined by

$$u_n(x,t) = \sum_{i=1}^{n} B_i \bar{\psi}_i(x,t), \tag{10}$$

where

$$B_i = \sum_{k=1}^{i} \beta_{ik} F(x_k, t_k, u_{k-1}(x_k,t_k), \partial_x u_{k-1}(0,t_k)). \tag{11}$$

On account of (26), the approximate solution $p_n(t)$ can also be obtained by

$$p_n(t) = \frac{E'(t) + \partial_x u_n(0,t) + \varphi'(0) - \int_0^1 f(x,t)dx}{E(t)}. \tag{12}$$

4.1 Convergence analysis

The convergence of $u_n(x,t)$ can lead to that of $p_n(t)$, due to (26). So we only need to show that the approximate solution $u_n(x,t)$ converges to the analytical solution $u(x,t)$. At first, the following lemma is given.

Lemma 2. *Assume that u_n is a bounded sequence in $W(\overline{\Omega})$, $u_n \xrightarrow{\|\cdot\|} \bar{u}$, $(x_n, t_n) \to (y, s)$, as $n \to \infty$. If $F(x, t, u(x,t), u_x(0,t))$ is continuous, then $F(x_n, t_n, u_{n-1}(x_n, t_n), \partial_x u_{n-1}(0, t_n)) \to F(y, s, \bar{u}(y,s), \partial_x \bar{u}(0,s))$.*

Proof. Similar to proof of Lemma 2 in [13], we have

$$|u_{n-1}(x_n, t_n) - \bar{u}(y, s)| \to 0, \quad \text{as} \quad n \to \infty.$$

Since

$$|t_n - s| \leq \sqrt{|x_n - y|^2 + |t_n - s|^2},$$

if follows that

$$(0, t_n) \longrightarrow (0, s).$$

Thus in a same manner

$$|\partial_x u_{n-1}(0, t_n) - \partial_x \bar{u}(0, s)| \to 0, \quad \text{as} \quad n \to \infty.$$

The continuation of $F(x, t, u(x), v(x))$ implies that

$$F(x_n, t_n, u_{n-1}(x_n, t_n), \partial_x u_{n-1}(0, t_n)) \to F(y, s, \bar{u}(y, s), \partial_x \bar{u}(0, s)), \quad \text{as} \quad n \to \infty.$$

□

Theorem 4. *Suppose that u_n is a bounded sequence in $W(\overline{\Omega})$ and (8) has a unique solution. If $\{(x_i, t_i)\}_{i=1}^{\infty}$ is dense in $\overline{\Omega}$, then the n-term approximate solution $u_n(x,t)$ derived from the above method converges to the analytical solution $u(x,t)$ of (8) in $W(\overline{\Omega})$, such that*

$$u(x,t) = \sum_{i=1}^{\infty} B_i \bar{\psi}_i(x,t),$$

where B_i is given by (11).

Proof. Similar to proof of Theorem 4 in [13], $u_n(x,t)$ converges to $\bar{u}(x,t)$ of the form

$$\bar{u}(x,t) = \sum_{i=1}^{\infty} B_i \bar{\psi}_i(x,t),$$

such that

$$L\bar{u}(x_l, t_l) = F(x_l, t_l, u_{l-1}(x_l, t_l), \partial_x u_{l-1}(0, t_l)).$$

Since $\{(x_i, t_i)\}_{i=1}^{\infty}$ is dense in $\overline{\Omega}$, for each $(y, s) \in \Omega$, there exist a subsequence $\{x_{n_j}, t_{n_j}\}_{j=1}^{\infty}$ such that

$$(x_{n_j}, t_{n_j}) \to (y, s) \quad (j \to \infty).$$

We know that $L\bar{u}(x_{n_j}, t_{n_j}) = F(x_{n_j}, t_{n_j}, u_{n_j-1}(x_{n_j}, t_{n_j}), \partial_x u_{n_j-1}(0, t_{n_j}))$. Let $j \to \infty$, by Lemma (2) and the continuity of F, we have

$$(L\bar{u})(y, s) = F(y, s, \bar{u}(y, s), \partial_x \bar{u}(0, s),$$

which indicates that $\bar{u}(x, t)$ satisfies (8). □

Theorem 5. *Under the conditions of Theorem 4, the approximate solution $u_n(x, t)$ and its derivatives $\partial_{xt}^{i+j} u_n(x, t)$, $i = 0, 1, 2$, $j = 0, 1$, converge uniformly to exact solution $u(x, t)$ and its derivatives $\partial_{xt}^{i+j} u(x, t)$, $i = 0, 1, 2$, $j = 0, 1$, respectively.*

Proof.

$$\begin{aligned} |\partial_{xt}^{i+j} u_n(x, t) - \partial_{xt}^{i+j} u(x, t)| &= |\partial_{xt}^{i+j} \langle u_n(y, s) - u(y, s), K_{(x,t)}(y, s)\rangle_W| \\ &= |\langle u_n(y, s) - u(y, s), \partial_{xt}^{i+j} K_{(x,t)}(y, s)\rangle_W| \\ &\leq \|\partial_{xt}^{i+j} K_{(x,t)}(y, s)\|_W \|u_n(y, s) - u(y, s)\|_W \\ &\leq C_{i+j} \|u_n - u\|_W, \quad n \to \infty. \end{aligned}$$

□

5 Numerical experiments

To test the accuracy of the proposed method, two examples are treated in this section. The results are compared with the exact solutions.

Example 1. *Consider problem (25)-(4) with*

$$\begin{aligned} &\varphi(x) = 2 + \cos(2\pi x), \\ &E(t) = 1 + e^{-t}, \\ &f(x, t) = 1 + 4\pi^2 e^{-t} \cos(2\pi x). \end{aligned}$$

It is easy to check that the exact solution is

$$\{v(x, t), p(t)\} = \{\mathrm{e}^{-t}(1 + \cos(2\pi x)), -1\}.$$

Using our method, we choose 81 points in the region $\overline{\Omega}$, and obtain the approximate solution $v_{81}(x, t)$. We have listed approximate versus exact solutions, along with the relative errors at some nodal points at time $T = \frac{1}{4}$ in Tables 1-2 and at time $T = \frac{1}{2}$ in Tables 3-4. Numerical results are in good agreement with the exact solutions. In Figs. 1-2, we display the exact and approximate solutions of v at times $T = \frac{1}{4}$, and $T = \frac{1}{2}$, respectively. In order to verify the convergence of the exact solution and its partial derivatives to the approximate solution and its partial derivatives, we depicted the relative

errors graphs of v, v_{xt} and v_{xxt} at time $T = \frac{1}{4}$ for different values of n in Figs. 3-5, respectively. The results show that the errors becomes smaller as n increases.

Example 2. *Consider problem (25)-(4) with*

$$\varphi(x) = 1 + \cos^2(2\pi x),$$
$$E(t) = \frac{1}{2}e^t + 1,$$
$$f(x,t) = -8\pi^2 e^t + 16\pi^2 e^t \cos^2(2\pi x) - t - te^t \cos^2(2\pi x) - 1.$$

The exact solution is

$$\{v(x,t), p(t)\} = \{1 + \mathrm{e}^t \cos^2(2\pi x), 1 + t\}.$$

Taking $T = \frac{1}{4}$ and choosing 81 and 144 points in the region $\overline{\Omega}$, we have listed approximate versus exact solutions, along with the relative errors at some nodal points in Tables 5-6 and 7-8, respectively. Numerical results are in good agreement with the exact solutions and the accuracy of approximate solution is getting better as n increases. In Fig. 6, we display the exact and approximate solutions of v at time $T = \frac{1}{4}$. Relative error distribution of v at time $T = \frac{1}{2}$ is also given in Fig. 7a. It is clear that the numerical results are in good agreement with the exact solutions. Artificial errors 10^{-2} were introduced into the right end and conditional condition. It can be seen from Fig. 7b that the error never affects the results of the method.

Example 3. *Consider problem (25)-(4) with*

$$\varphi(x) = 1 + \cos(2\pi x),$$
$$E(t) = \exp(-(2\pi)^2 t),$$
$$f(x,t) = (2\pi)^2 \cos(2\pi x)\exp(-(2\pi)^2 t) + 2t(1 + \cos(2\pi x)\exp(-(2\pi)^2 t + 10t^2).$$

The exact solution is given by

$$\{v(x,t),\ p(t)\} = \{(1 + \cos(2\pi x)\exp(-(2\pi)^2 t), (2\pi)^2 + 2t\exp(10t^2)\}.$$

Relative error distribution of v at time $T = \frac{1}{2}$ is given in Fig. 8a. It can be noted from Fig. 8a that our results are in better accuracy than the results in [20]. In order to demonstrate the stability of our algorithm, we shall give a perturbation $\epsilon = 10^{-2}$ to the right side function $f(x,t)$ and over-specified condition $E(t)$. The relative error distribution of v at time $T = \frac{1}{2}$ depicted in Fig. 8b shows that the method is stable and gives excellent approximation to the solution.

6 Conclusion

In this paper, the reproducing kernel Hilbert space method was applied successfully for solving an inverse problem for a parabolic equation with nonlocal boundary condition. Proposed method is shown to be of good convergence, simple in principle, easy to program and easy to treat the boundary conditions. It seems that the method can also be applied to higher dimensional inverse problems. We leave this to our further works.

References

1. Cannon J.R. and Van de Hoek J. *The one phase stefan problem subject to energy*, J. Math. Anal. Appl. 86 (1982) 281-292.
2. Dehghan M. *An inverse problem of finding a source parameter in a semilinear parabolic equation*, Appl. Math. Model. 25 (2001) 743-754.
3. Dehghan M. *Numerical solution of one-dimensional parabolic inverse problem*, Appl. Math. Comput. 136 (2003) 333-344.
4. Fatullayev A. and Can E. procedures for determining unknown source parameter in parabolic equations, Math. Comput. Simulat. 54 (2000) 159-167.
5. Cannon JR., Lin Y. and Wang S. *Determination of a control parameter in a parabolic partial differential equation*, J. Aust. Math. Soc. B. 33 (1991) 149-163.
6. Ivanchov MI. and Pabyrivska NV. *Simultaneous determination of two coefficients of a parabolic equation in the case of nonlocal and integral conditions*, Ukr. Math. J. 53 (2001) 674-684.
7. Ivanchov MI. *Inverse Problems for Equations of Parabolic Type*, VNTL Publishers: Lviv, Ukraine. 2003.
8. Namazov GK. *Definition of the unknown coefficient of a parabolic equation with nonlocal boundary and complementary-conditions*, Transactions of Academy of Sciences of Azerbaijan, Series of Physical-Technicaland Mathematical Sciences. 19 (1999) 113-117.
9. Sapagovas M. and Jakubėlienė K. *Alternating direction method for two-dimensional parabolic equation with nonlocal integral condition*, Nonlinear Anal. Modelling Control. 17(1) (2012) 91-98.
10. Sapagovas M. and Štikonienė O. *Alternating-direction method for a mildly nonlinear elliptic equation with nonlocal integral conditions*, Nonlinear Anal Modelling Control. 16(2) (2011) 220-230.

11. Aronszajn N. *Theory of reproducing kernels*, Trans. Amer. Math. Soc. 68 (1950) 337-404.

12. Geng F. *Solving singular second order three-point boundary value problems using reproducing kernel Hilbert space method*, Appl. Math. Comput. 215 (2009) 2095-2102.

13. Mohammadi M. and Mokhtari R. *Solving the generalized regularized long wave equation on the basis of a reproducing kernel space*, J. Comput. Appl. Math. 235 (2011) 4003-4011.

14. Geng F.and Cui M. *A reproducing kernel method for solving nonlocal fractional boundary value problems*, Appl. Math. Lett. 25 (2012) 818-823.

15. Mokhtari R., Toutian Isfahani F. and Mohammadi M. *Solving a class of nonlinear differential-difference equations in the reproducing kernel space*, Abstr. Appl. Anal. 2012 (2012) Articel ID 514103.

16. Mohammadi M. and Mokhtari R. *A new algorithm for solving nonlinear Shrödinger equation in the reproducing kernel space*, to appear in IJS & T-Transaction A.

17. Mohammadi M. and Mokhtari R. *A reproducing kernel method for solving a class of nonlinear systems of PDEs*, to appear in Math. Model. Anal.

18. Mohammadi M., Mokhtari R. and Panahipour H. *A Galerkin-reproducing kernel method: application to the 2D nonlinear coupled Burgers' equations*, Eng. Anal. Bound. Elem. 37 (2013) 1642-1652.

19. Cui M. and Lin Y. *Nonlinear Numerical Analysis in the Reproducing Kernel Space*. Nova Science Publisher: New York. 2008.

20. Ismailova M. and Kancab F. *An inverse coefficient problem for a parabolic equation in the case of nonlocal boundary and overdetermination conditions*, Math. Meth. Appl. Sci. 34 (2011) 692-702.

Table 1: Relative errors of $v(x,t)$ for Example 1; $n = 81$, $T = \frac{1}{4}$

(x,t)	v_{exact}	v_{app}	Relative errors	(x,t)	v_{exact}	v_{app}	Relative errors
$(1, \frac{1}{1000})$	2.998001	2.998100	3.315676E-05	$(\frac{7}{8}, \frac{1}{6})$	2.445035	2.443523	6.182374E-04
$(\frac{1}{2}, \frac{12}{1000})$	1	1.000715	7.151300E-04	$(1, \frac{1}{6})$	2.692963	2.691261	6.321103E-04
$(1, \frac{1}{100})$	2.980099	2.980922	2.758099E-04	$(\frac{3}{4}, \frac{1}{5})$	1.818731	1.8169752	9.652627E-04
$(\frac{1}{10}, \frac{1}{10})$	2.636866	2.637919	3.995758E-03	$(\frac{1}{10}, \frac{1}{5})$	2.481098	2.479660	5.795225E-04
$(\frac{1}{4}, \frac{1}{10})$	1.904837	1.909188	2.283755E-03	$(\frac{2}{3}, \frac{1}{5})$	1.409365	1.408556	5.742847E-04
$(1, \frac{1}{10})$	2.809675	2.810196	1.853823E-04	$(\frac{1}{2}, \frac{2}{9})$	1	1.002348	2.347800E-03
$(\frac{1}{2}, \frac{1}{9})$	1	1.002317	2.317300E-03	$(\frac{3}{5}, \frac{2}{9})$	1.152927	1.152638	2.505188E-04
$(\frac{2}{3}, \frac{1}{9})$	1.447420	1.448317	6.202361E-04	$(\frac{1}{3}, \frac{2}{9})$	1.400369	1.399123	8.895521E-04
$(1, \frac{1}{8})$	2.764994	2.764715	1.009424E-04	$(\frac{3}{5}, \frac{1}{4})$	1.148738	1.148205	4.639945E-04
$(\frac{2}{3}, \frac{1}{8})$	1.441248	1.441835	4.073198E-04	$(\frac{1}{2}, \frac{1}{4})$	1	1.002458	2.458400E-03
$(\frac{3}{4}, \frac{1}{6})$	1.846482	1.845673	4.378733E-04	$(1, \frac{1}{4})$	2.557601	2.552739	1.901260E-03

Table 2: Relative errors of $p(t)$ for Example 1; $n = 81$, $T = \frac{1}{4}$

t	p_{exact}	p_{app}	Relative errors	t	p_{exact}	p_{app}	Relative errors
$\frac{1}{1000}$	-1	-1.000064	6.453900E-05	$\frac{1}{8}$	-1	-1.000684	6.838260E-04
$\frac{12}{1000}$	-1	-1.000669	6.689750E-04	$\frac{1}{6}$	-1	-0.999358	6.414128E-04
$\frac{1}{100}$	-1	-1.000585	5.854630E-04	$\frac{1}{5}$	-1	-0.9984953	1.504941E-03
$\frac{1}{10}$	-1	-1.000343	3.435430E-04	$\frac{2}{9}$	-1	-0.997999	2.000439E-03
$\frac{1}{9}$	-1	-1.000717	7.166060E-04	$\frac{1}{4}$	-1	-0.997132	2.868264E-03

Table 3: Relative errors of $v(x,t)$ for Example 1; $n = 81$, $T = \frac{1}{2}$

(x,t)	v_{exact}	v_{app}	Relative errors	(x,t)	v_{exact}	v_{app}	Relative errors
$(1, \frac{1}{1000})$	2.998001	2.998135	4.480185E-05	$(\frac{7}{8}, \frac{1}{6})$	2.445035	2.445058	9.422361E-06
$(\frac{1}{2}, \frac{12}{1000})$	1	1.000089	8.926900E-05	$(1, \frac{1}{6})$	2.692963	2.693930	3.587980E-04
$(1, \frac{1}{100})$	2.980099	2.981268	3.922174E-04	$(\frac{3}{4}, \frac{1}{5})$	1.818731	1.816356	1.305423E-03
$(\frac{1}{10}, \frac{1}{10})$	2.636866	2.640780	1.484401E-03	$(\frac{1}{10}, \frac{1}{5})$	2.481098	2.485261	1.677789E-03
$(\frac{1}{4}, \frac{1}{10})$	1.904837	1.912180	3.854839E-03	$(\frac{2}{3}, \frac{1}{5})$	1.409365	1.407343	1.434693E-03
$(1, \frac{1}{10})$	2.809675	2.809855	6.428644E-05	$(\frac{1}{2}, \frac{2}{9})$	1	1.002219	2.219280E-03
$(\frac{1}{2}, \frac{1}{9})$	1	1.004321	4.321410E-03	$(\frac{3}{5}, \frac{2}{9})$	1.152927	1.151739	1.030525E-03
$(\frac{2}{3}, \frac{1}{9})$	1.447420	1.447886	3.219329E-04	$(\frac{1}{3}, \frac{2}{9})$	1.400369	1.407778	5.291163E-03
$(1, \frac{1}{8})$	2.764994	2.765560	2.047726E-04	$(\frac{3}{5}, \frac{1}{4})$	1.148738	1.146675	1.795169E-03
$(\frac{2}{3}, \frac{1}{8})$	1.441248	1.441568	2.220845E-04	$(\frac{1}{2}, \frac{1}{4})$	1	1.001966	1.966360E-03
$(\frac{3}{4}, \frac{1}{6})$	1.846482	1.845236	6.746695E-04	$(1, \frac{1}{4})$	2.557601	2.556291	5.124707E-04

Table 4: Relative errors of $p(t)$ for Example 1; $n = 81$, $T = \frac{1}{2}$

t	p_{exact}	p_{app}	Relative errors	t	p_{exact}	p_{app}	Relative errors
$\frac{1}{1000}$	-1	-0.999794	2.063958E-04	$\frac{1}{8}$	-1	-0.977383	2.261733E-02
$\frac{12}{1000}$	-1	-0.997471	2.528598E-03	$\frac{1}{6}$	-1	-0.979758	2.024151E-02
$\frac{1}{100}$	-1	-0.997903	2.096714E-03	$\frac{1}{5}$	-1	-0.975690	2.430969E-02
$\frac{1}{10}$	-1	-0.976715	2.328518E-02	$\frac{2}{9}$	-1	-0.971106	2.889415E-02
$\frac{1}{9}$	-1	-0.976639	2.336095E-02	$\frac{1}{4}$	-1	-0.964804	3.519553E-02

Table 5: Relative errors of $v(x,t)$ for Example 2; $n = 81$, $T = \frac{1}{4}$

(x,t)	v_{exact}	v_{app}	Relative errors	(x,t)	v_{exact}	v_{app}	Relative errors
$(1, \frac{1}{1000})$	2.001000	2.000890	5.523337E-05	$(\frac{7}{8}, \frac{1}{6})$	1.590680	1.591406	4.562790E-04
$(\frac{1}{2}, \frac{12}{1000})$	2.012072	2.001377	5.315484E-03	$(1, \frac{1}{6})$	2.181360	2.164421	7.765664E-03
$(1, \frac{1}{100})$	2.010050	2.008924	5.601139E-04	$(\frac{3}{4}, \frac{1}{5})$	1	1.002636	2.636500E-03
$(\frac{1}{10}, \frac{1}{10})$	1.723344	1.715849	4.348790E-03	$(\frac{1}{10}, \frac{1}{5})$	1.799418	1.801355	1.076466E-03
$(\frac{1}{4}, \frac{1}{10})$	1	0.996456	3.544300E-03	$(\frac{2}{3}, \frac{1}{5})$	1.305351	1.276493	2.210723E-02
$(1, \frac{1}{10})$	2.105171	2.089205	7.583953E-03	$(\frac{1}{2}, \frac{2}{9})$	2.248849	2.171894	3.421967E-02
$(\frac{1}{2}, \frac{1}{9})$	2.117519	2.073065	2.099328E-02	$(\frac{3}{5}, \frac{2}{9})$	1.817382	1.751413	3.629875E-02
$(\frac{2}{3}, \frac{1}{9})$	1.279380	1.256824	1.762984E-02	$(\frac{1}{3}, \frac{2}{9})$	1.312212	1.303871	6.356607E-03
$(1, \frac{1}{8})$	2.133148	2.116888	7.622889E-03	$(\frac{3}{5}, \frac{1}{4})$	1.840405	1.768371	3.914031E-02
$(\frac{2}{3}, \frac{1}{8})$	1.283287	1.260171	1.801297E-02	$(\frac{1}{2}, \frac{1}{4})$	2.284025	2.199602	3.696255E-02
$(\frac{3}{4}, \frac{1}{6})$	1	0.999525	4.751000E-04	$(1, \frac{1}{4})$	2.284025	2.266547	7.652462E-03

Table 6: Relative errors of $p(t)$ for Example 2; $n = 81$, $T = \frac{1}{4}$

t	p_{exact}	p_{app}	Relative errors	t	p_{exact}	p_{app}	Relative errors
$\frac{1}{1000}$	1.001000	1.000778	2.216753E-04	$\frac{1}{8}$	1.125000	1.177465	4.663580E-02
$\frac{12}{1000}$	1.012000	1.009609	2.363016E-03	$\frac{1}{6}$	1.166667	1.138380330	2.424571E-02
$\frac{1}{100}$	1.010000	1.007937	2.042468E-03	$\frac{1}{5}$	1.200000	1.157718084	3.523493E-02
$\frac{1}{10}$	1.100000	1.141458	3.768888E-02	$\frac{2}{9}$	1.222222	1.170887564	4.200091E-02
$\frac{1}{9}$	1.111111	1.156422	4.077993E-02	$\frac{1}{4}$	1.250000	1.211209275	3.103258E-02

Table 7: Relative errors of $v(x,t)$ for Example 2; $n = 144$, $T = \frac{1}{4}$

(x,t)	v_{exact}	v_{app}	Relative errors	(x,t)	v_{exact}	v_{app}	Relative errors
$(1, \frac{1}{1000})$	2.001000	2.000941	2.983507E-05	$(\frac{7}{8}, \frac{1}{6})$	1.590680	1.595549	3.060781E-03
$(\frac{1}{2}, \frac{12}{1000})$	2.012072	2.008807	1.622859E-03	$(1, \frac{1}{6})$	2.181360	2.180958	1.846293E-04
$(1, \frac{1}{100})$	2.010050	2.009449	2.992512E-04	$(\frac{3}{4}, \frac{1}{5})$	1	1.013353	1.335274E-02
$(\frac{1}{10}, \frac{1}{10})$	1.723344	1.722972	2.159116E-04	$(\frac{1}{10}, \frac{1}{5})$	1.799418	1.810589	6.207763E-03
$(\frac{1}{4}, \frac{1}{10})$	1	1.001805	1.805350E-03	$(\frac{2}{3}, \frac{1}{5})$	1.305351	1.309086	2.861377E-03
$(1, \frac{1}{10})$	2.105171	2.101083	1.941670E-03	$(\frac{1}{2}, \frac{2}{9})$	2.248849	2.230536	8.143059E-03
$(\frac{1}{2}, \frac{1}{9})$	2.117519	2.102535	7.076129E-03	$(\frac{3}{5}, \frac{2}{9})$	1.817382	1.808653	4.803084E-03
$(\frac{2}{3}, \frac{1}{9})$	1.279380	1.276005	2.637737E-03	$(\frac{1}{3}, \frac{2}{9})$	1.312212	1.325054	9.786674E-03
$(1, \frac{1}{8})$	2.133148	2.129999	1.476139E-03	$(\frac{3}{5}, \frac{1}{4})$	1.840405	1.833820	3.578477E-03
$(\frac{2}{3}, \frac{1}{8})$	1.283287	1.280545	2.136414E-03	$(\frac{1}{2}, \frac{1}{4})$	2.284025	2.266462	7.689720E-03
$(\frac{3}{4}, \frac{1}{6})$	1	1.008052	8.052170E-03	$(1, \frac{1}{4})$	2.284025	2.293042	3.947540E-03

Table 8: Relative errors of $p(t)$ for Example 2; $n = 144$, $T = \frac{1}{4}$

t	p_{exact}	p_{app}	Relative errors	t	p_{exact}	p_{app}	Relative errors
$\frac{1}{1000}$	1.001000	1.000929	7.116752E-05	$\frac{1}{8}$	1.125000	1.148678	2.104750E-02
$\frac{12}{1000}$	1.012000	1.010731951	1.253013E-03	$\frac{1}{6}$	1.166667	1.145867427	1.782820E-02
$\frac{1}{100}$	1.010000	1.008977553	1.012324E-03	$\frac{1}{5}$	1.200000	1.196111194	3.240672E-03
$\frac{1}{10}$	1.100000	1.118037	1.639767E-02	$\frac{2}{9}$	1.222222	1.264996	3.499686E-02
$\frac{1}{9}$	1.111111	1.131717	1.854514E-02	$\frac{1}{4}$	1.250000	1.245162209	3.870233E-03

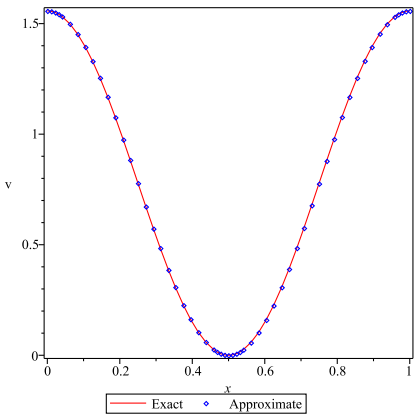

Figure 1: Exact and approximate solution of v for Example 1 at $T = \frac{1}{4}$

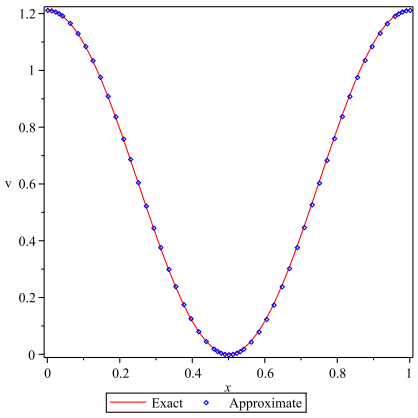

Figure 2: Exact and approximate solution of v for Example 1 at $T = \frac{1}{2}$

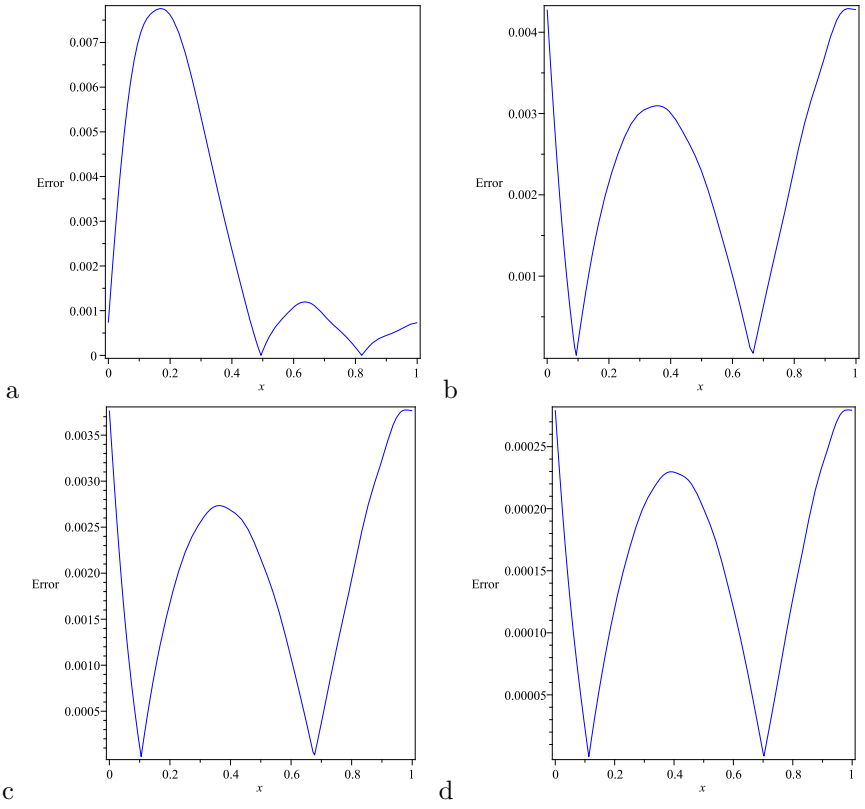

Figure 3: Relative errors graphs of v for Example 1 at time $T = \frac{1}{4}$; a($n = 36$), b($n = 64$), c($n = 81$), d($n = 100$)

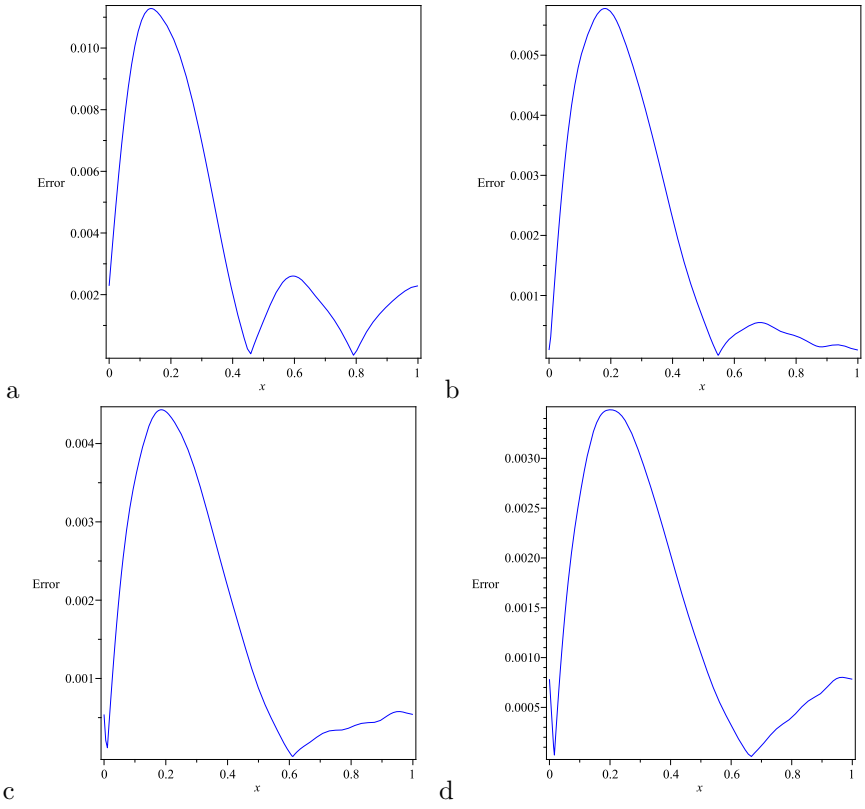

Figure 4: Relative errors graphs of v_{xt} for Example 1 at time $T = \frac{1}{4}$; a($n = 36$), b($n = 64$), c($n = 81$), d($n = 100$)

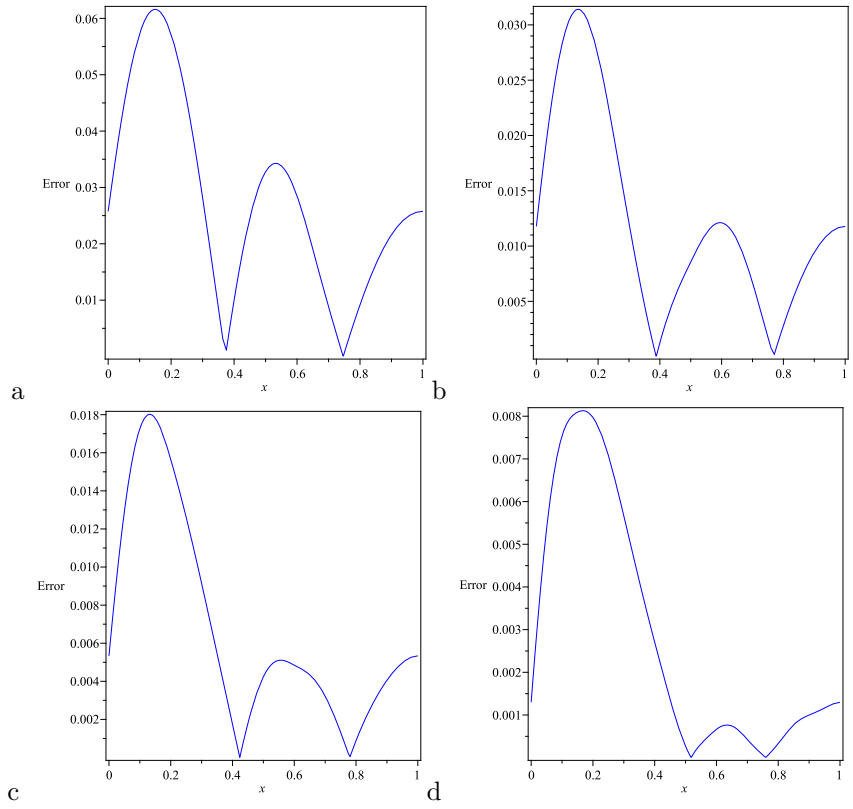

Figure 5: Relative errors graphs of v_{xxt} for Example 1 at time $T = \frac{1}{4}$; a($n = 36$), b($n = 64$), c($n = 81$), d($n = 100$)

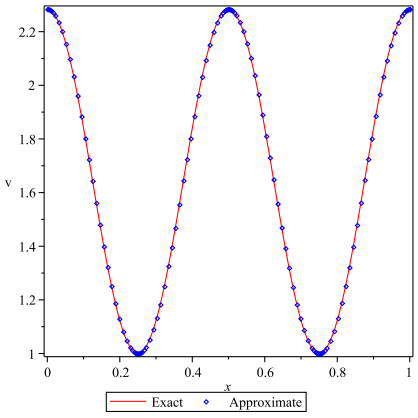

Figure 6: Exact and approximate solution of v for Example 2 at $T = \frac{1}{4}$

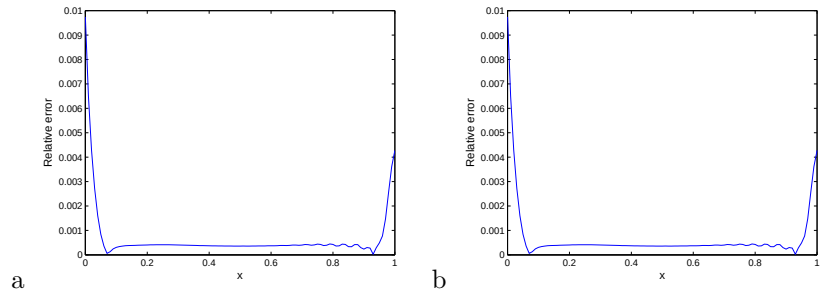

a b

Figure 7: Relative error graphs of v for Example 2 at time $T = \frac{1}{2}$; a(without noise), b(with noise)

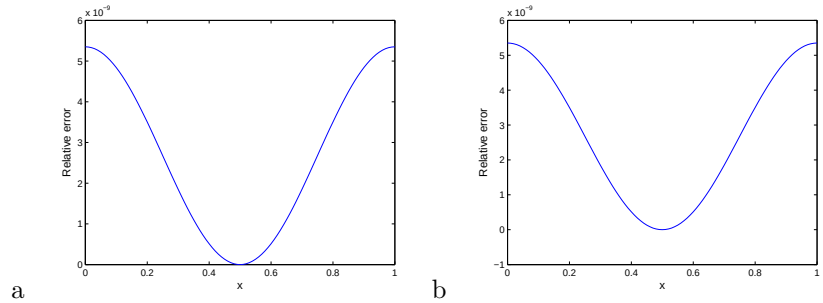

a b

Figure 8: Relative error graphs of v for Example 3 at time $T = \frac{1}{2}$; a(without noise), b(with noise)

Iranian Journal of Numerical Analysis and Optimization
Vol 4, No. 1, (2014), pp 77-94

An approximation method for numerical solution of multi-dimensional feedback delay fractional optimal control problems by Bernstein polynomials

E. Safaie* and M. H. Farahi

Abstract

In this paper, we present a new method for solving fractional optimal control problems with delays in state and control. This method is based upon Bernstein polynomials basis and feedback control. The main advantage of feedback or closed-loop control is that one can monitor the effect of such control on the system and modify the output accordingly. In this work, we use Bernstein polynomials to transform the fractional time-varying multi-dimensional optimal control system with both state and control delays, into an algabric system in terms of the Bernstein coefficients approximating state and control functions. We use Caputo derivative of degree $0 < \alpha \leq 1$ as the fractional derivative in our work. Finally, some numerical examples are given to illustrate the effectiveness of this method.

Keywords: Delay fractional optimal control problem; Caputo fractional derivative; Bernstein polynomial.

1 Introduction

The general definition of an optimal control problem requires the minimization of a functional over an admissible set of control and state functions sub-

*Corresponding authour
Received 25 November 2013; revised 29 January 2014; accepted 5 March 2014
E. Safaie
Department of Applied Mathematics, Faculty of Mathematical Sciences, Ferdowsi university of Mashhad, Mashhad, Iran. e-mail: elahe.safaie@stu.um.ac.ir

M. H. Farahi
Department of Applied Mathematics, Faculty of Mathematical Sciences, Ferdowsi university of Mashhad, Mashhad, Iran,
and
The center of Excellence on Modelling and Control Systems (CEMCS), Mashhad, Iran.
e-mail: farahi@math.um.ac.ir

ject to dynamic constraints on the states and controls. A Fractional Optimal Control Problem (FOCP) is an optimal control problem in which either the performance index or the differential equations governing the dynamic of the system or both contain at least one fractional order derivative term [1, 2, 17].

Fractional Differential Equations (FDEs) have been the focus of many studies due to their appearance in various applications in real-world physical systems. For example, it has been illustrated that materials with memory and hereditary effects and dynamical processes including gas diffusion and heat conduction can be more adequately modeled by FDEs than integer-order differential equations [13, 18, 20]. Some other applications of FDEs are in behaviors of viscoelastic materials, biomechanics and electrochemical processes (see [3, 5] for more details).

Most FOCPs do not have exact solutions, so in these cases approximation methods and numerical techniques must be used. Recently, several approximation methods to solve FOCPs have been introduced [4, 14, 18].

Real life phenomena have been described more precisely by Delay Differential Equations, so Delay Fractional Optimal Control Problem (DFOCP) has become the focus of many researchers in the last decade. Baleanu in [6] and Jarad in [11] analyzed the fractional variational principles for some kinds of DFOCPs within Riemann-Liouville and Caputo fractional derivatives respectively and made their corresponding Euler-Lagrange equations. In this paper, we present a novel strategy based on Bernstein polynomials (BPs) to solve DFOCPs. Consider the following DFOCP

$$Min \;\; J = \tfrac{1}{2}\int_0^1 [x^T(t)Q(t)x(t) + u^T(t)R(t)u(t)]dt, \tag{1}$$

$s.t$

$$\begin{aligned} &{}_0^cD_t^\alpha x_i(t) = \Sigma_{j=1}^r a_{i,j}(t)x_j(t) + \Sigma_{k=1}^s b_{i,k}(t)u_k(t) \\ &+\Sigma_{j=1}^r (a_d)_{i,j}(t)x_j(t-\eta_1) + \Sigma_{k=1}^s (b_d)_{i,k}(t)u_k(t-\eta_2), \;\; 1 \le i \le r, \end{aligned} \tag{2}$$

$$\begin{aligned} x_j(t) &= x_{j,0}, \; t \in [-\eta_1, 0], && 1 \le j \le r, \\ u_k(t) &= u_{k,0}, \; t \in [-\eta_2, 0], && 1 \le k \le s, \end{aligned} \tag{3}$$

where $x(t) = [x_1(t) \cdots x_r(t)]^T$ and $u(t) = [u_1(t) \cdots u_s(t)]^T$ are respectively the state and control functions. Also, $Q(t)$ and $R(t)$ are respectively, $r \times r$ and $s \times s$ semi-positive and positive definite time-varying matrices of the state and control's coefficients in the cost function with continuous functions as their entries. Furthermore, $a_{i,j}(t)$, $(a_d)_{i,j}(t)$, $b_{i,k}(t)$ and $(b_d)_{i,k}(t)$ are continuous functions which are respectively the coefficients of $x_j(t)$, $x_j(t-\eta_1)$ for $(1 \le j \le r)$ and $u_k(t)$, $u_k(t-\eta_2)$ for $(1 \le k \le s)$ in the i-th fractional differential equation (2) and $\eta_1, \eta_2 > 0$ are given constant delays. The fractional derivative is defined in Caputo sense, i.e.

$${}_0^cD_t^\alpha x_i(t) = \begin{cases} \frac{1}{\Gamma(1-\alpha)} \int_0^t (t-\tau)^{-\alpha} \frac{d}{d\tau} x_i(\tau) d\tau, & 0 < \alpha < 1, \\ \dot{x_i}, & \alpha = 1. \end{cases} \tag{4}$$

In the numerical solution of dynamical systems, polynomials or piecewise polynomial functions are often used to present the approximate solutions [9, 10, 21]. The effectiveness of using Bernstein polynomials for solving FOCPs have been demonstrated before [4, 14]. In the present paper, we seek an optimal feedback control function to find the approximate solution of DFOCP (1) - (3) by using Bernstein polynomials.

This paper is organized as follows. In Section 2 we give some preliminiaries in fractional calculus. In Section 3 Bernstein polynomials are introduced and their properties are shown in several lemmas. In Section 4, a FOCP with time delay will be solved using BPs. Section 5 contains some numerical examples. Finally Section 6 consists of a brief conclusion.

2 Some preliminaries in fractional calculus

Definition 2.1. *A real function $f(t)$, $t > 0$, is said to be in the space C_μ, $\mu \in \mathbb{R}$, if there exists a real number $p > \mu$ such that $f(t) = t^p f_1(t)$, where $f_1(t) \in C[0, +\infty)$ and it is said to be in the space C_μ^m iff $f^{(m)} \in C_\mu$ for $m \in \mathbb{N}$.*

Definition 2.2. *The Riemann-Liouville fractional integral operator of order $\alpha > 0$ of a function $f \in C_\mu$, $\mu > 1$, is defined as:*

$$\begin{array}{l} {}_0I_t^\alpha f(t) = \frac{1}{\Gamma(\alpha)} \int_0^t (t-\tau)^{\alpha-1} f(\tau) d\tau, \\ {}_0I_t^0 f(t) = f(t). \end{array} \tag{5}$$

Definition 2.3. *The fractional derivative of $f(t)$ in the Caputo sense is defined as follows:*

$${}_0^cD_t^\alpha f(t) = \frac{1}{\Gamma(1-\alpha)} \int_0^t (t-\tau)^{-\alpha} \frac{d^n}{d\tau^n} f(\tau), \quad n-1 < \alpha < n,\ n \in \mathbb{N},\ \ f \in C_{-1}^m. \tag{6}$$

In [15], the following properties for $f \in C_\mu$ and $\mu \geq -1$ have been proved

1. ${}_0I_t^\alpha t^k = \frac{\Gamma(k+1)}{\Gamma(k+1+\alpha)} t^{\alpha+k}, \qquad k \in \mathbb{N} \cup \{0\}, \qquad t > 0,$

2. ${}_0^cD_t^\alpha {}_0I_t^\alpha f(t) = f(t),$

3. ${}_0I_t^\alpha {}_0^cD_t^\alpha f(t) = f(t) - \sum_{k=0}^{n-1} f(0^+) \frac{t^k}{k!}, \qquad t > 0,$

4. ${}_0^cD_t^\beta f(t) = {}_0I_t^{\alpha-\beta} {}_0^cD_t^\alpha f(t), \qquad \alpha, \beta > 0.$

3 Properties of Bernstein polynomials

The Bernstein polynomial of degree n over the interval $[a, b]$ is defined as follows:

$$B_{i,n}\left(\frac{t-a}{b-a}\right) = \binom{n}{i}\left(\frac{t-a}{b-a}\right)^{i}\left(\frac{b-t}{b-a}\right)^{n-i},$$

so, within the interval $[0, 1]$ we have

$$B_{i,n}(t) = \binom{n}{i} t^{i}(1-t)^{n-i}.$$

Define $\Phi_m(t) = [B_{0,m}(t)\ B_{1,m}(t)\ \cdots\ B_{m,m}(t)]^T$. To consider the vector $\Phi_m(t-\eta)$ (η is the given delay) in terms of $\Phi_m(t)$, we state the following lemmas.

Lemma 3.1. *We can write $\Phi_m(t) = \Lambda T_m(t)$, where $\Lambda = (\Upsilon_{i,j})_{i,j=1}^{m+1}$ is an upper triangular $(m+1)\times(m+1)$ matrix with entry*

$$\Upsilon_{i+1,j+1} = \begin{cases} (-1)^{j-i}\binom{m}{i}\binom{m-i}{j-i}, & i \le j, \\ 0, & i > j, \end{cases} \qquad i, j = 0, 1, \cdots, m,$$

and $T_m(t) = [1\ t\ \cdots\ t^m]^T$.

Proof. [4].

Lemma 3.2. *For each given constant delay $\eta > 0$, $\Phi_m(t-\eta) = \Omega\Phi_m(t)$, where Ω is an $(m+1)\times(m+1)$ matrix in terms of η.*

Proof. According to Lemma 3.1 we have

$$\Phi_m(t-\eta) = \Lambda T_m(t-\eta).$$

But, the right hand side of the above equation can be written as

$$\Lambda T_m(t-\eta) = \Lambda \begin{bmatrix} 1 \\ t-\eta \\ (t-\eta)^2 \\ \vdots \\ (t-\eta)^m \end{bmatrix} = \Lambda\Psi \begin{bmatrix} 1 \\ t \\ t^2 \\ \vdots \\ t^m \end{bmatrix} = \Lambda\Psi T_m(t),$$

where

$$\Psi = \begin{bmatrix} 1 & 0 & 0 & \cdots & 0 \\ -\eta & 1 & 0 & \cdots & 0 \\ \eta^2 & -2\eta & 1 & \cdots & 0 \\ \vdots & \vdots & \ddots & & \vdots \\ (-\eta)^m & \binom{m}{m-1}(-\eta)^{m-1} & \cdots & & 1 \end{bmatrix}.$$

By Lemma 3.1, $T_m(t) = \Lambda^{-1}\Phi_m(t)$, thus

$$\Phi(t-\eta) = \Lambda\Psi\Lambda^{-1}\Phi_m(t) = \Omega\Phi_m(t). \quad \square \tag{7}$$

Lemma 3.3. *Let $L^2[0,1]$ be a Hilbert space with inner product $\langle f, g\rangle = \int_0^1 f(t)g(t)dt$ and $y \in L^2[0,1]$. Then one can find the unique vector $C = [c_0\ c_1\ \cdots\ c_m]^T$ such that*

$$y(t) \approx \sum_{i=0}^{m} c_i B_{i,m}(t) = C^T\Phi_m(t). \tag{8}$$

Proof. [12].

In Lemma 3.3 we have $C^T = Q^{-1}\langle y, \Phi_m\rangle$ such that

$$\langle y, \Phi_m\rangle = \int_0^1 y(t)\Phi_m(t)dx = [\langle y, B_{0,m}\rangle\ \langle y, B_{1,m}\rangle\ \cdots\ \langle y, B_{m,m}\rangle]^T,$$

and each entry of the matrix $Q = (Q_{i+1,j+1})_{i,j=0}^{m}$ is defined as follows:

$$Q_{i+1,j+1} = \int_0^1 B_{i,m}(t)B_{j,m}(t)dx = \frac{\binom{m}{i}\binom{m}{j}}{(2m+1)\binom{2m}{i+j}}.$$

Since the set $\{B_{0,m}(t), B_{1,m}(t), \cdots, B_{m,m}(t)\}$ forms a basis for the vector space of polynomials of real coefficients and degree no more than m [7, 16], a polynomial of degree m can be expanded in terms of a linear combination of $B_{i,m}(t), (i = 0, 1, \cdots, m)$ as follows

$$P(t) = \sum_{i=0}^{m} c_i B_{i,m}(t),$$

moreover we have

$$t^k = \sum_{i=k-1}^{m-1} \frac{\binom{i}{k}}{\binom{m}{k}} B_{i,m}(t).$$

Lemma 3.4. *Derivatives of $P_n(f) = \sum_{j=0}^{n} f(\frac{j}{n})B_{j,n}(t)$ of any order converge*

to corresponding derivatives of f. So if $f \in C^k[0,1]$ then

$$lim_{n\to\infty}(P_n(f))^{(k)} = f^{(k)},$$

uniformly on [0, 1].

Proof. [8].

4 Fractional optimal control problem with delays in control and state

Consider fractional delay control system (2). For each $0 \le i \le r$, one can apply the Riemann-Liouville fractional integral ${}_0I_t^\alpha$ to both sides of that equation

$$\begin{aligned} x_i(t) - x_i(0) = {} & \Sigma_{j=1}^{r}{}_0I_t^\alpha\{a_{i,j}(t)x_j(t)\} + \Sigma_{k=1}^{s}{}_0I_t^\alpha\{b_{i,k}(t)u_k(t)\}+ \\ & \Sigma_{j=1}^{r}{}_0I_t^\alpha\{(a_d)_{i,j}(t)x_j(t-\eta_1)\} + \Sigma_{k=1}^{s}{}_0I_t^\alpha\{(b_d)_{i,k}(t)u_k(t-\eta_2)\}. \end{aligned} \tag{9}$$

Assume that $x_i(t) \approx X_i^T\Phi_m(t)$ $(1 \le i \le r)$ and $u_k(t) \approx U_k^T\Phi_m(t)$ $(1 \le k \le s)$ where the entries $X_i = [X_i(0)\cdots X_i(m)]^T$ and $U_k = [U_k(0)\cdots U_k(m)]^T$ are respectively the coeffitients of $x_i(t)$ and $u_k(t)$ in approximating them by Bernstein polynomials of degree m just like (8). Moreover, the Bernstein approximated coefficients vectors of functions $a_{i,j}(t)$, $b_{i,k}(t)$, $(a_d)_{i,j}(t)$ and $(b_d)_{i,k}(t)$ can be achieved by using equation (8). We denote the approximated vector coefficients of these functions respectively by $(A^{i,j})_{(m+1)\times 1}$, $(B^{i,k})_{(m+1)\times 1}$, $(A_d^{i,j})_{(m+1)\times 1}$ and $(B_d^{i,k})_{(m+1)\times 1}$.
By substituting the so called approximated vectors and matrices in (1), one can find the following equations:

$$\begin{aligned} X_i^T\Phi_m(t) - x_{i,0} = {} & \Sigma_{j=1}^{r}{}_0I_t^\alpha\{((A^{i,j})^T\Phi_m(t))(X_j^T\Phi_m(t))^T\} \\ & +\Sigma_{k=1}^{s}{}_0I_t^\alpha\{((B^{i,k})^T\Phi_m(t))(U_k^T\Phi_m(t))^T\} \\ & +\Sigma_{j=1}^{r}{}_0I_t^\alpha\{((A_d^{i,j})^T\Phi_m(t))(X_j^T\Phi_m(t-\eta_1))^T\} \\ & +\Sigma_{k=1}^{s}{}_0I_t^\alpha\{((B_d^{i,k})^T\Phi_m(t))(U_k^T\Phi_m(t-\eta_2))^T\}. \end{aligned} \tag{10}$$

Moreover, from Lemma 3.2 there exist $(m+1)\times(m+1)$ matrices Ω_1, Ω_2 where $\Phi_m(t-\eta_1) = \Omega_1\Phi_m(t)$ and $\Phi_m(t-\eta_2) = \Omega_2\Phi_m(t)$, while

$$\Omega_1 = \Lambda\Psi\Lambda^{-1},$$

$$\Omega_2 = \Lambda\Psi^{'}\Lambda^{-1},$$

and $\Psi, \Psi^{'}$ are obtained respectively in terms of η_1 and η_2.
As it was shown in [4], for each $1 \le i,j \le r$ and $1 \le k \le s$, the $(m+1)\times(m+1)$

matrices $A^{\tilde{i,j}}$, $B^{\tilde{i,k}}$, $A_d^{\tilde{i,j}}$ and $B_d^{\tilde{i,k}}$ can be calculated such that:

$$(A^{i,j})^T\Phi_m(t)\Phi_m^T(t) = \Phi_m^T(t)A^{\tilde{i,j}},$$

$$(B^{i,k})^T\Phi_m(t)\Phi_m^T(t) = \Phi_m^T(t)B^{\tilde{i,k}},$$

$$(A_d^{i,j})^T\Phi_m(t)\Phi_m^T(t) = \Phi_m^T(t)A_d^{\tilde{i,j}},$$

$$(B_d^{i,k})^T\Phi_m(t)\Phi_m^T(t) = \Phi_m^T(t)B_d^{\tilde{i,k}}.$$

Therefore, by replacing the above equalities, (2) can be rewritten as follows:

$$X_i^T\Phi_m(t) - x_{i,0} = \Sigma_{j=1}^r({}_0I_t^\alpha\Phi_m^T(t))(A^{\tilde{i,j}}X_j) + \Sigma_{k=1}^s({}_0I_t^\alpha\Phi_m^T(t))(B^{\tilde{i,k}}U_k)+ \Sigma_{j=1}^r({}_0I_t^\alpha\Phi_m^T(t))(A_d^{\tilde{i,j}}\Omega_1^TX_j) + \Sigma_{k=1}^s({}_0I_t^\alpha\Phi_m^T(t))(B_d^{\tilde{i,j}}\Omega_2^TU_k),$$

or

$$X_i^T\Phi_m(t) - x_{i,0} = \Sigma_{j=1}^r(A^{\tilde{i,j}}X_j)^T({}_0I_t^\alpha\Phi_m(t)) + \Sigma_{k=1}^s(B^{\tilde{i,k}}U_k)^T({}_0I_t^\alpha\Phi_m(t))+ \Sigma_{j=1}^r(A_d^{\tilde{i,j}}\Omega_1^TX_j)^T({}_0I_t^\alpha\Phi_m(t)) + \Sigma_{k=1}^s(B_d^{\tilde{i,j}}\Omega_2^TU_k)^T({}_0I_t^\alpha\Phi_m(t)). \quad (11)$$

where $i = 1, \cdots, r$.

One can approximate ${}_0I_t^\alpha\Phi_m(t)$ by $I_\alpha \times \Phi_m(t)$, where I_α is an $(m+1)\times(m+1)$ matrix called the operational matrix of Riemann-Liouville fractional integral.
Infact, from Lemma 3.1, $\Phi_m(t) = \Lambda T_m(t)$, so

$${}_0I_t^\alpha\Phi_m(t) = \Lambda\ {}_0I_t^\alpha T_m(t) = \Lambda\ [{}_0I_t^\alpha 1\ \ {}_0I_t^\alpha t\ \ \cdots\ \ {}_0I_t^\alpha t^m]^T,$$

where ${}_0I_t^\alpha t^j = \frac{\Gamma(j+1)}{\Gamma(j+1+\alpha)}t^{j+\alpha}$. Therefore,

$${}_0I_t^\alpha T_m(t) = \tilde{\Sigma}\tilde{T}, \quad (12)$$

where $\tilde{\Sigma} = (\tilde{\Sigma}_{i+1,j+1})$ and $\tilde{T} = (\tilde{T}_{i+1})$ are respectively $(m+1)\times(m+1)$ and $(m+1)\times 1$ matrices, which are defined as follows:

$$\tilde{\Sigma}_{i+1,j+1} = \begin{cases} \frac{\Gamma(j+1)}{\Gamma(j+1+\alpha)}, & i = j, \\ 0, & o.w, \end{cases} \qquad i,j = 0,\cdots,m$$

and

$$(\tilde{T})_{i+1} = t^{i+\alpha}, \qquad i = 0,\cdots,m.$$

Also, from Lemma 3.3, since $t^{i+\alpha} \in L^2([0,1])$ for each integer i $(0 \le i \le m)$, one can find the $(m+1)\times 1$ vector P_i such that

$$t^{i+\alpha} \approx P_i^T\Phi_m(t), \quad (13)$$

where $P_i = Q^{-1}\langle t^{i+\alpha}, \Phi_m(t)\rangle$ and the entries of $\bar{P}_i = \langle t^{i+\alpha}, \Phi_m(t)\rangle = [\bar{P}_{i,0}\ \bar{P}_{i,1}\ \cdots\ \bar{P}_{i,m}]^T$ can be attained as

$$\bar{P}_{i,j} = \int_0^1 t^{i+\alpha} B_{j,m}(t)dt = \frac{m!\Gamma(i+j+\alpha+1)}{j!\Gamma(i+m+\alpha+2)}, \qquad i,j = 0,\cdots,m.$$

Now if P is an $(m+1)\times(m+1)$ matrix of the form $[P_0\ P_1\cdots P_m]$, then from (12) and (13) we have

$$ {}_0I_t^\alpha \Phi_m(t) \approx \Lambda\tilde{\Sigma}P^T\Phi_m(t), \tag{14}$$

therefore, $I_\alpha = \Lambda\tilde{\Sigma}P^T$ is the aforementioned operational matrix of Riemann-Liouville fractional integral ${}_0I_t^\alpha$.

Hence, by replacing ${}_0I_t^\alpha\Phi_m(t)$ from (14) into (4) and writing $x_{i,0}$ in terms of BPs of degree m, equation (4) can be written as the following

$$\begin{aligned} X_i^T\Phi_m(t) - X_{i,0}^T\Phi_m(t) = \Sigma_{j=1}^r(\tilde{A^{i,j}}X_j)^T\ I_\alpha\Phi_m(t) + \Sigma_{k=1}^s(\tilde{B^{i,k}}U_k)^T\ I_\alpha\Phi_m(t) \\ +\Sigma_{j=1}^r(\tilde{A_d^{i,j}}\Omega_1^TX_j)^T\ I_\alpha\Phi_m(t) + \Sigma_{k=1}^s(\tilde{B_d^{i,j}}\Omega_2^TU_k)^T\ I_\alpha\Phi_m(t), \end{aligned} \tag{15}$$

where

$$X_{i,0}^T = [X_{i,0}(0),\cdots,X_{i,0}(m)]^T$$

is the known Bernstein approximated coefficents vector of $x_{i,0}$ that can be computed using (8). By equalling the coefficents of $\Phi_m(t)$ from both sides of (5), we found that

$$\begin{aligned} X_i^T = X_{i,0}^T + \Sigma_{j=1}^r X_j^T(\tilde{A^{i,j}})^T\ I_\alpha + \Sigma_{k=1}^s U_k^T(\tilde{B^{i,k}})^T\ I_\alpha \\ +\Sigma_{j=1}^r X_j^T\Omega_1(\tilde{A_d^{i,j}})^T\ I_\alpha + \Sigma_{k=1}^s U_k^T\Omega_2(\tilde{B_d^{i,j}})^T\ I_\alpha, \end{aligned} \tag{16}$$

for $i = 1,\cdots,r$. Equations (8) can be written in compact form as follows:

$$X^T = \Pi + U^T\Gamma, \tag{17}$$

where Π and Γ are respectively $1\times(m+1)$ and $(m+1)\times(m+1)$ matrices that can be obtained by the following

$$\Pi = X_0^T(I_{m+1} - (\tilde{A}+\tilde{A}_d)I_\alpha)^{-1},$$

and

$$\Gamma = (\tilde{B}+\tilde{B}_d)I_\alpha(I_{m+1} - (\tilde{A}+\tilde{A}_d)I_\alpha)^{-1},$$

and I_{m+1} is the $(m+1)\times(m+1)$ identity matrix.

Moreover, by applying the approximations $x(t) \approx (X^T)_{1\times r(m+1)}\Phi_m(t)$ and $u(t) \approx (U^T)_{1\times s(m+1)}\Phi_m(t)$ where $X^T = [X_1^T,\cdots,X_r^T]$ and $U^T = [U_1^T,\cdots,U_s^T]$, the cost functional (1) can be approximated as bellow

$$J = \frac{1}{2}\int_0^1 \{x^T(t)Q(t)x(t) + u^T(t)R(t)u(t)\}dt$$
$$\approx \frac{1}{2}\int_0^1 \{X^T\Phi_m(t)(Q^T\Phi_m(t)\Phi_m^T(t)X)^T + U^T\Phi_m(t)(R^T\Phi_m(t)\Phi_m^T(t)U)^T\}dt, \quad (18)$$

where $Q = [Q_{i,j}]$ and $R = [R_{i,j}]$ that $Q_{i,j}, R_{i,j}$ are the $(m+1)\times 1$ vectors of Bernstein coefficents in approximating $Q_{i,j}(t)$ and $R_{i,j}(t)$ respectively. Therefore,

$$J \approx \frac{1}{2}\int_0^1 \{X^T\Phi_m(t)(\Phi_m^T(t)\tilde{Q}X)^T + U^T\Phi_m(t)(\Phi_m^T(t)\tilde{R}U)^T\}dt,$$

or

$$J \approx \frac{1}{2}\int_0^1 \{(X^T\Phi_m(t))(X^T\tilde{Q}^T\Phi_m(t)) + (U^T\Phi_m(t))(U^T\tilde{R}^T\Phi_m(t))\}dt, \quad (19)$$

where $\tilde{Q} = [\tilde{Q_{i,j}}]$ and $\tilde{R} = [\tilde{R_{i,j}}]$. Also $\tilde{Q_{i,j}}$ and $\tilde{R_{i,j}}$ are $(m+1)\times(m+1)$ matrices that can be calculated from

$$(Q^{i,j})^T\Phi_m(t)\Phi_m^T(t) = \Phi_m^T(t)\tilde{Q^{i,j}},$$

$$(R^{i,j})^T\Phi_m(t)\Phi_m^T(t) = \Phi_m^T(t)\tilde{R^{i,j}}.$$

Let $Z_{i,j} = H \bigotimes \tilde{Q}_{i,j}$ and $W_{i,j} = H \bigotimes \tilde{R}_{i,j}$, where $\bigotimes$ is the Kronecker product and $H = [H_{i,j}]_{(m+1)\times(m+1)}$ and each entry $H_{i,j}$ is defined by

$$H_{i,j} = \int_0^1 B_{i,m}(t)B_{j,m}(t)dt,$$

then (19) can be rewritten in compact form as:

$$J \approx \frac{1}{2}\{(X^TZX) + (U^TWU)\}, \quad (20)$$

where $Z = [z_{i,j}]$ and $W = [w_{i,j}]$.
From (17) we know that $X^T = \Pi + U^T\Gamma$, so the necessary condition that U minimizes (20) and satisfy (17) is that

$$\frac{\partial J}{\partial U} = X^TZ\Gamma^T + U^TW = 0,$$

so

$$U^{*T} = X^TZ\Gamma^TW^{-1}. \quad (21)$$

The above equation gives the optimal feedback control and by replacing (21) in (17), we can easily find the optimal state as well.

We need to mention that, since the Bernstein coefficients of positive functions in $L^2[0,1]$ are positive [7] and it was assumed that $R(t)$ is positive definite, then $R_{i,j}$ is a positive vector. Also because $B_{i,m}(t) > 0$ for $t \in (0,1)$, it's clear that

$$\Phi_m^T(t)\tilde{R}_{i,j} = R_{i,j}^T\Phi_m(t)\Phi_m^T(t) > 0, \qquad t \in [0,1],$$

therefore $\tilde{R}_{i,j}$ and as the result $W_{i,j} = H \bigotimes \tilde{R}_{i,j}$ are positive definite and consequently invertible matrices.

5 Convergence of the method

In this section, we show the convergence of the presented method discussed in this article. First we prove the following lemma.

Lemma 5.1. *Let $X^T\Phi_m(t) = \sum_{j=0}^m X_j B_{j,m}(t)$ be the Bernstein polynomial of order m that approximates the function $x(t) \in L^2[0,1]$. Then ${}_0I_t^\alpha(X^T\Phi_m(t))$, tends to ${}_0I_t^\alpha x(t)$ as m tends to infinity.*

Proof. By Lemma 3.3 we have

$$lim_{m\to\infty}\sum_{j=0}^m X_j B_{j,m}(t) = x(t). \tag{22}$$

Since $B_{j,m}(t)$ is a continuous function, we have

$$lim_{m\to\infty}\int_0^t \frac{\sum_{j=0}^m X_j B_{j,m}(\tau)}{(t-\tau)^{1-\alpha}}d\tau = lim_{m\to\infty}\sum_{j=0}^m X_j\int_0^t \frac{B_{j,m}(\tau)}{(t-\tau)^{1-\alpha}}d\tau.$$

By (22) and from Definition 2.2, we obtain

$$\int_0^t \frac{x(\tau)}{(t-\tau)^{1-\alpha}}d\tau = \Gamma(\alpha)\ lim_{m\to\infty}\sum_{j=0}^m X_j\ {}_0I_t^\alpha B_{j,m}(t),$$

or

$${}_0I_t^\alpha x(t) = lim_{m\to\infty}\sum_{j=0}^m X_j\ {}_0I_t^\alpha B_{j,m}(t) = lim_{m\to\infty}X^T\,{}_0I_t{}^\alpha\Phi_m(t). \tag{23}$$

In (14), $I_\alpha = \Lambda\tilde{\Sigma}P^T$ where the i-th column of P^T is the Bernstein approximated coefficients of $t^{i+\alpha}$ for $i = 0, \cdots, m$. Now, regarding the convergence of the Bernstein approximation of every functions in $L^2([0,1])$, one can write

$$lim_{n\to\infty}P^T\Phi_n(t) = lim_{n\to\infty}\begin{bmatrix}\sum_{j=0}^{n}P_{j,0}B_{j,n}(t)\\ \sum_{j=0}^{n}P_{j,1}B_{j,n}(t)\\ \vdots\\ \sum_{j=0}^{n}P_{j,m}B_{j,n}(t)\end{bmatrix} = \tilde{T} = \begin{bmatrix}t^{\alpha}\\ t^{1+\alpha}\\ t^{2+\alpha}\\ \vdots\\ t^{m+\alpha}\end{bmatrix},$$

therefore, $lim_{n\to\infty}\Lambda\tilde{\Sigma}P^T\Phi_n(t) = \Lambda\tilde{\Sigma}\ lim_{n\to\infty}P^T\Phi_n(t) = \Lambda\tilde{\Sigma}\tilde{T}$, or as explained in (12) and (13)

$$lim_{n\to\infty}I_{\alpha}\Phi_n(t) = {}_0I_t^{\alpha}\Phi_m(t). \tag{24}$$

From (23) and (24) we reach

$${}_0I_t^{\alpha}x(t) = lim_{m\to\infty}X^T\ lim_{n\to\infty}I_{\alpha}\Phi_n(t).$$

Given $n \geq m$ will complete the proof. □

Theorem 5.1. *The approximated solutions $\bar{x}(t) = \bar{X}^T\Phi_m(t)$ and $\bar{u}(t) = \bar{U}^T\Phi_m(t)$ in which $(\bar{X}, \bar{U})$ is achieved from* (17) *and* (21)*, converge to the optimal solutions $x^*(t)$ and $u^*(t)$ as the degree of the Bernstein polynomials tend to infinity.*

Proof. Suppose W_m is the set of all $(U^T, X^T)\Phi_m(\cdot)$ where $X, U \in \mathrm{R}^{m+1}$ and satisfy (17), also W is the set of all $(u(\cdot), x(\cdot))$ satisfy (2) and (3). Let $\bar{U}$ be the optimal solution of (20) where obtained from (21) and $\bar{X}$ be the solution of (17) obtained by replacing $\bar{U}$ in eqation (17). Therefore $(\bar{U}^T, \bar{X}^T)\Phi_m(\cdot) \in W_m$. By the convergence property of Bernstein polynomials, for $(\bar{U}^T, \bar{X}^T)\Phi_m(\cdot)$, there exists a unique pair of functions $(\bar{u}(\cdot), \bar{x}(\cdot))$ such that

$$(\bar{U}^T, \bar{X}^T)\Phi_m(\cdot) \longrightarrow (\bar{u}(\cdot), \bar{x}(\cdot)) \quad as \quad m \to \infty.$$

Now according to Lemma 5.1 it is clear that $(\bar{u}(\cdot), \bar{x}(\cdot)) \in W$. Moreover as $m \to \infty$, then $J(\bar{U}^T\Phi_m, \bar{X}^T\Phi_m) \longrightarrow \bar{J}$ where $\bar{J}$ is the value of cost function (1) corresponding to the feasible solution $(\bar{u}(\cdot), \bar{x}(\cdot))$. Now, since

$$W_1 \subseteq \cdots \subseteq W_m \subseteq W_{m+1} \subseteq \cdots \subseteq W,$$

consequently

$$Inf_{W_1}J_1 \geq \cdots \geq Inf_{W_m}J_m \geq Inf_{W_{m+1}}J_{m+1} \geq \cdots \geq Inf_W J.$$

Let $J_m^* = Inf_{W_m}J_m$, so $J_m^* = J(\bar{U}^T\Phi_m, \bar{X}^T\Phi_m)$. Furthermore, the sequence $\{J_m^*\}$ is nonincreasing and bounded bellow which converges to a number $\bar{J} \geq Inf_W J$. We want to show that $\bar{J} = lim_{m\to\infty}J_m^* = Inf_W J$. Given $\varepsilon > 0$, let $(u(\cdot), x(\cdot))$ be an element in W such that

$$J(u, x) < Inf_W J + \varepsilon, \tag{25}$$

by the definition of infimum, such $(u(\cdot), x(\cdot)) \in W$ exists.
Since $J(u, x)$ is continuous, for this value of ε, there exists $N(\varepsilon)$ so that if $m > N(\varepsilon)$,

$$|J(u, x) - J(U^T\Phi_m, X^T\Phi_m)| < \varepsilon, \tag{26}$$

Now if $m > N(\varepsilon)$, then using (25) and (26) gives

$$J(U^T\Phi_m, X^T\Phi_m) < J(u, x) + \varepsilon < Inf_W J + 2\varepsilon,$$

on the other hand

$$Inf_W J \leq J_m^* = Inf_{W_m} J_m \leq J(U^T\Phi_m, X^T\Phi_m),$$

so

$$Inf_W J \leq J_m^* < Inf_W J + 2\varepsilon,$$

or

$$0 \leq J_m^* - Inf_W J < 2\varepsilon,$$

where ε is chosen arbitrary. Thus

$$\bar{J} = lim_{m\to\infty} J_m^* = Inf_W J. \quad \square$$

6 Numerical examples

In this section we give some numerical examples and apply the method presented in Section 4 for solving them. Our examples are solved using $Matlab2011a$ on an Intel Core i5-430M processor with 4 GB of DDR3 Memory. These test problems demonstrate the validity and efficiency of this technique.

Example 6.1. Consider the following delay fractional optimal control problem in which $0 < \alpha \leq 1$,

$$\begin{array}{lll} min\ J = \frac{1}{2}\int_0^1 [x^2(t) + \frac{1}{2}u^2(t)]dt, & & \\ s.t \quad {}_0^cD_t^\alpha x(t) = -x(t) + x(t-\frac{1}{3}) + u(t) - \frac{1}{2}u(t-\frac{2}{3}), & 0 \leq t \leq 1, \\ \quad x(t) = 1, & -\frac{1}{3} \leq t \leq 0, \\ \quad u(t) = 0, & -\frac{2}{3} \leq t \leq 0. \end{array}$$

For $\alpha = 1$, this problem has been numerically solved by applying hybrid functions based on Legendre polynomials in [19] and the objective value $I = 0.3731$ has been achieved. Whilst, in the presented method the solution has the objective value $J^* = 0.3956$ for $\alpha = 1$ and $m = 6$. Thus, our results with $m = 6$ are in good agreement with the results demonstrated in [19] for $\alpha = 1$. In addition, by varying the value of α we can obtain the optimal control $u(\cdot)$ and trajectory function $x(\cdot)$ which are shown respectively

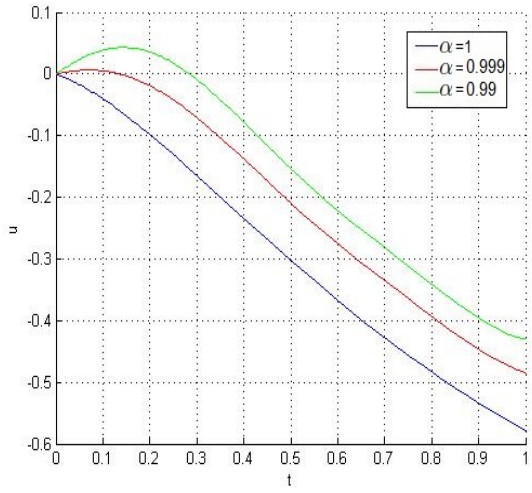

Figure 1: Approximate solution of $u(.)$ for $\alpha = 1, 0.999, 0.99$ in Example 6.1

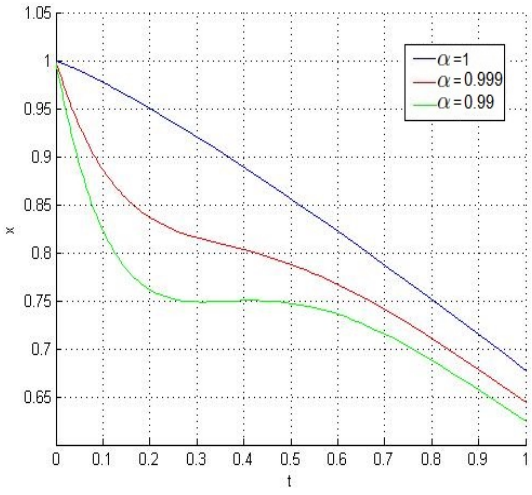

Figure 2: Approximate solution of $x(.)$ for $\alpha = 1, 0.999, 0.99$ in Example 6.1

Table 1: The objective value and the end point of trajectory for $\alpha = 1, 0.999, 0.99$ in Example 6.1

α	objective value	end-point
1	0.3956	0.6775
0.999	0.3283	0.6443
0.99	0.2907	0.6249

Table 2: The objective value and the end points of trajectories for $\alpha = 1, 0.9, 0.8$ in Example 6.2

α	objective value	end points
1	0.7245	$-0.4691\ ,\ -0.0113$
0.9	1.0291	$-0.6477\ ,\ 0.3202$
0.8	0.7299	$-0.4324\ ,\ 0.4674$

for some values of α in Fig.1 and Fig.2. Moreover, for these values of α the objective values and the end points of optimal trajectory are shown in Table 1.

Example 6.2. Consider the following two-dimensional DFOCP in which $0 < \alpha \leq 1$,

$$min\ J = \tfrac{1}{2}\int_0^1 \{[x_1(t)\ x_2(t)]\begin{bmatrix}1 & t\\ t & t^2\end{bmatrix}[x_1(t)\ x_2(t)]^T + (t^2+1)u^2(t)\}dt,$$

$$s.t\quad {}_0^cD_t^\alpha \begin{bmatrix}x_1(t)\\ x_2(t)\end{bmatrix} = \begin{bmatrix}t^2+1 & 1\\ 0 & 2\end{bmatrix}\begin{bmatrix}x_1(t-\frac{1}{2})\\ x_2(t-\frac{1}{2})\end{bmatrix} + \begin{bmatrix}1\\ t+1\end{bmatrix}u(t) + \begin{bmatrix}t+1\\ t^2+1\end{bmatrix}u(t-\frac{1}{4}),\ 0 \leq t \leq 1,$$

$$[x_1(t)\ x_2(t)] = [1,1],\ \ -\tfrac{1}{2} \leq t \leq 0,$$

$$u(t) = 1,\ \ -\tfrac{1}{4} \leq t \leq 0.$$

This problem for $\alpha = 1$ has been studied in [19], where the obtained approximated cost function is $I = 1.5622$. Using the presented method for $\alpha = 1$ and $m = 6$, gives the approximated cost function as $J^* = 0.7245$. So we achieved satisfactory numerical results in comparison with what have been obtained in [19] for $\alpha = 1$. Also by varying the value of α the obtained control and trajectories functions are shown respectively in Fig.3, Fig.4 and Fig.5. Moreover, for these values of α the objective values and the end points of optimal trajectories are shown in Table 2.

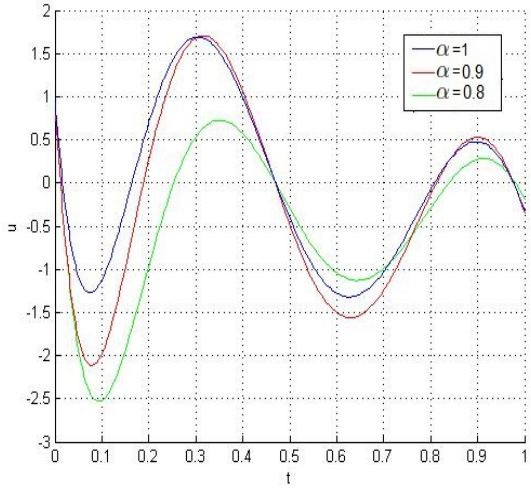

Figure 3: Approximate solution of $u(.)$ for $\alpha = 1, 0.9, 0.8$ in Example 6.2

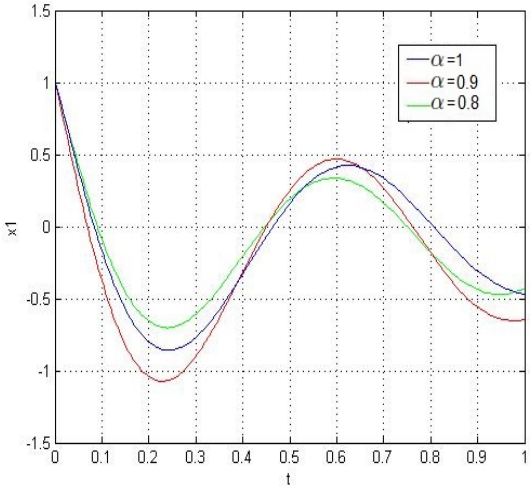

Figure 4: Approximate solution of $x_1(.)$ for $\alpha = 1, 0.9, 0.8$ in Example 6.2

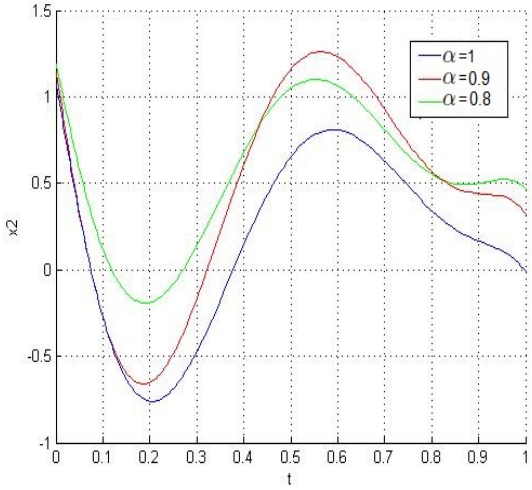

Figure 5: Approximate solution of $x_2(.)$ for $\alpha = 1, 0.9, 0.8$ in Example 6.2

7 Conclusion

In this paper, we peresent a new method of using Bernstein polynomials for solving DFOCP's. We approximate the objective function and find a feed back control which minimizes the cost function. Then by replacing the optimal control in the constraints, we get an algabric system which can be solved in terms of the approximate coefficents of trajectory. The convergence of the method is extensively discussed and some test problems are included to show the efficiency of this very easy to use and accurate method.

References

1. Agrawal, O. P. *A formulation and a numerical scheme for fractional optimal control problems*, Journal of Vibration and Control, 14, (2008), 1291-1299.

2. Agrawal, O. P. *A general formulation and solution scheme for fractional and optimal control problems*, Nonlinear Dynamics, 38, (2004), 323-337.

3. Agrawal, O. P. *A quadratic numerical scheme for fractional optimal control problems, Trans. ASME*, J. Dyn. Syst. Meas. Control, 130 (1), (2008), 0110101-0110-6.

4. Alipour, M., Rostamy, D. and Baleanu, D. *Solving multi-dimensional fractional optimal control problems with inequality constraint by Bernstein polynomials operational matrices*, Journal of Vibration and Control, (2012), DOI:10.1177/1077546312458308.

5. Bagley, R. L. and Torvik, P. J. *On the appearance of the fractional derivative in the behavior of real materials*, J. Appl. Mech., 51, (1984), 294-298.

6. Baleanu, D., Maaraba (Abdeljawad), T. and Jarad, F. *Fractional variational principles with delay*, J. Phys. A: Math. Theor, 41, (2008), Article Number: 315403.

7. Farouki, R. and Rajan, V. *On the numerical condition of polynomials in Bernstein form*, Computer Aided Geometric Design, 4 (3), (1987), 191-216.

8. Floater, M. S. *On the convergence of derivatives of Bernstein approximation*, Journal of Approximation Theory, 134, (2005), 130-135.

9. Ghomanjani, F., Farahi, M. H. and Gachpazan, M. *Bezier control points method to solve constrianed quadratic optimal control of time varying linear systems*, Computational and Applied Mathematics, 31, (2012), 34-42.

10. Ghomanjani, F. and Farahi, M. H. *The Bezier control points method for solving delay diffrential equations*, Intlligent Control and Automation, 3, (2012), 188-196.

11. Jarad, F, Abdeljawad (Maraaba), T. and Baleanu, D. *Fractional variational principles with delay within Caputo derivatives*, Reports on Mathematical Physics, 1, (2010), 17-28.

12. Kreyszig, E. *Introduction to Functional Analysis with applications*, John Wiley and Sons, New York, (1978).

13. Lopes, A. M., Tenreiro Machadob J. A, Pinto C. M. A. and Galhano A. M. S. F. *Fractional dynamics and MDS visualization of earthquake phenomena*, Computers and Mathematics with Applications, 66, (2013), 647-658.

14. Lotfi, A., Dehghan, M. and Yousefi, S. A. *A numerical technique for solving fractional optimal control problems*, Computers and Mathematics with Applications, 62, (2011), 1055-1067.

15. Oldham, K. B. and Spanier, J. *The fractional calculus*, New York: Academic Press, (1974).

16. Qian, W., Riedel, M. D. and Rosenberg, I. *Uniform approximation and Bernstein polynomials with coefficients in the unit interval*, European Journal of Combinatorics, 32, (2011), 448-463.

17. Tangprng, X. W. and Agrawal, O. P. *Fractional optimal control of a continum system*, ASME Journal of Vibration and Acoustic, 131, (2009), 232-245.

18. Tricaud, C. and Chen, Y. Q. *An approximate method for numerically solving fractional order optimal control problems of general form*, Computers and Mathematics with Applications, 59, (2010), 1644-1655.

19. Wang, X. T. *Numerical solutions of optimal control for linear time-varying systems with delays via hybrid functions*, Journal of the Franklin Institute, 344, (2007), 941-953.

20. Zamani, M., Karimi, G. and Sadati, N. *FOPID controller design for robust performance using particle swarm optimization*, J. Fract. Calc. Appl. Anal., 10, (2007), 169-188.

21. Zheng, J., Sederberg, T. W. and Johnson, R. W. *Least squares method for solving diffrential equations using Bezier control point methods*, Applied Numerical Mathematics, 48, (2004), 137-152.

Iranian Journal of Numerical Analysis and Optimization
Vol 4, No. 1, (2014), pp 95-104

A successive iterative approach for two dimensional nonlinear Volterra-Fredholm integral equations

A. H. Borzabadi* and M. Heidari

Abstract

In this paper, an iterative scheme for extracting approximate solutions of two dimensional Volterra-Fredholm integral equations is proposed. Considering some conditions on the kernel of the integral equation obtained by discretization of the integral equation, the convergence of the approximate solution to the exact solution is investigated. Several examples are provided to demonstrate the efficiency of the approach.

Keywords: Volterra-Fredholm integral equation; Iterative method; Discretization; Approximation.

1 Introduction

The integral equations provide important tools for modeling a wide range of phenomena and processes [14], and solving many problems in engineering and mechanics which are dependent on finding the solution of their integral equations. They are widely used in plasma physics [10], deblurring of two dimensional images [8, 20], solving applied boundary value problems [1] and Laplace's equations with boundary conditions [16]. Upon the importance of the integral equations, different numerical methods have been developed over the years to tackle them, such as time collocation and time discretization methods [6, 15], trapezoidal Nystrom method [11], Adomian decomposition method [9, 17] and successive iterative scheme [5] but few of them can be used for solving two dimensional integral equations such as two dimensional block pulse functions [3], finite difference inequalities [19], time-stepping methods [7] and block-by-block method [4].

*Corresponding authour
Received 2 October 2013; revised 14 December; accepted 24 january 2014
A. H. Borzabadi
School of Mathematics and Computer Science, Damghan University, Damghan, Iran. e-mail: borzabadi@du.ac.ir; akbar.h.borzabadi@gmail.com

M. Heidari
School of Mathematics and Computer Science, Damghan University, Damghan, Iran.

Studies on iterative approaches play an important role to accelerate convergence rate in solving any system of equations generated by discretizing mathematical models in science and engineering problems [5]. The objective of this study is to present an iterative approach for extracting approximate solutions of two dimensional Volterra-Fredholm integral equations as

$$u(x,t) = f(x,t) + \int_c^t \int_a^b k(x,t,y,z,u(y,z))dydz,\ (x,t) \in D := [a,b] \times [c,d], \tag{1}$$

where $f(x,t)$ (source function) and $k(x,t,y,z,u)$ (kernel function) are the given analytical functions defined on D and $D \times D \times \mathbb{R}$, respectively. The existence and uniqueness of the solution for equation (1) are discussed in [12, 15]. This work can be considered as an extension of the method proposed in [5]. Note that, the present approach is applicable to a wide class of integral equations. The structure of the report is as follows. In Section 2 we transform the integral equation into a discretized form. Then, in Section 3, we introduce an successful numerical approach which is used subsequently for making up the solution algorithm in Section 4. Section 5 demonstrates the efficiency and advantages of the proposed algorithm whilst Section 6 concludes the paper.

2 Integral equation transformation

Let $\triangle^{(1)} = \{a = x_0, x_1, \cdots, x_{n-1}, x_n = b\}, \triangle^{(2)} = \{c = t_0, t_1, \cdots, t_{m-1}, t_m = d\}$ be equidistance partitions of $[a,b]$ and $[c,d]$, respectively, where $h_x = x_{i+1} - x_i$, $i = 0, 1, \cdots, n-1$ and $h_t = t_{j+1} - t_j$, $j = 0, 1, \cdots, m-1$ are the discretization parameters of the partitions. Now, if $u^*(x,t)$ be an analytical solution of (1), then for the partitions $\triangle^{(1)}, \triangle^{(2)}$ on $[a,b]$ and $[c,d]$, we have

$$u^*(x_i,t_j) = f(x_i,t_j) + \int_c^{t_j} \int_a^b k(x_i,t_j,y,z,u^*(y,z))dydz, \tag{2}$$

where $i = 0, 1, \cdots, n$ and $j = 0, 1, \cdots, m$. In (2), the integral term can be estimated by a numerical method of integration, e.g. Newton-Cotes methods. Therefore, by taking equidistance partitions $\triangle^{(1)}, \triangle^{(2)}$, as above with $h_y = y_{i+1} - y_i,\ i = 0, 1, \cdots, n-1, h_z = z_{j+1} - z_j,\ j = 0, 1, \cdots, m-1$, and also the weights $w_i,\ i = 0, 1, \cdots, n$ and $w'_{j_r},\ r = 0, 1, \cdots, j$, equality (2) can be written as,

$$u^*_{i,j} = f_{i,j} + \sum_{r=0}^{j} \sum_{l=0}^{n} w'_{j_r} w_l k(x_i,t_j,y_l,z_r,u^*_{l,r}) + O(h_y^\nu) + O(h_z^\mu), \tag{3}$$

where $u^*_{i,j} = u^*(x_i, t_j),\ f_{i,j} = f(x_i, t_j),\ i = 0, 1, \cdots, n, j = 0, 1, \cdots, m$, and ν, μ depends upon the employed method of Newton-Cotes for estimating the integral in (2).

For partitions $\triangle^{(1)}, \triangle^{(2)}$, we consider a nonlinear equations system obtained by neglecting the truncation error of (2), as follows,

$$\xi_{i,j} = f_{i,j} + \sum_{r=0}^{j} \sum_{l=0}^{n} w'_{j_r} w_l k(x_i, t_j, y_l, z_r, \xi_{l,r}), i = 0, 1, \cdots, n, j = 0, 1, \cdots, m, \tag{4}$$

and suppose that the exact solution of nonlinear system (4) are $\xi^*_{i,j}, i = 0, 1, \cdots, n, j = 0, 1, \cdots, m$. In the following proposition, we seek the conditions of vanishing $|u^*_{i,j} - \xi^*_{i,j}|, i = 0, 1, \cdots, n, j = 0, 1, \cdots, m$.

proposition 2.1. *Suppose,*
(i) $|u^*_{p,q} - \xi^*_{p,q}| = \max_{\substack{0 \le i \le n \\ 0 \le j \le m}} |u^*_{i,j} - \xi^*_{i,j}|$,
(ii) $k(x, t, y, z, u(y, z)) \in C(D \times D \times \mathbb{R})$,
(iii) $k_u(x, t, y, z, u(y, z))$ *exists on* $D \times D \times \mathbb{R}$ *and* $\gamma < \frac{1}{(b-a)(d-c)}$, *where*

$$\gamma = \sup_{\substack{x,y \in [a,b] \\ t,z \in [c,d]}} |k_u(x, t, y, z, u(y, z))|.$$

Then

$$|u^*_{p,q} - \xi^*_{p,q}| \le \frac{|O(h^\nu_y)| + |O(h^\mu_z)|}{1 - \gamma(b-a)(d-c)}. \tag{5}$$

Proof. By (3) and (4), we have

$$u^*_{p,q} - \xi^*_{p,q} = \sum_{r=0}^{q} \sum_{l=0}^{n} w'_{q_r} w_l (k(x_p, t_q, y_l, z_r, u^*_{l,r}) - k(x_p, t_q, y_l, z_r, \xi^*_{l,r})) + O(h^\nu_y) + O(h^\mu_z).$$

According to *(iii)*

$$k(x_p, t_q, y_l, z_r, u^*_{l,r}) - k(x_p, t_q, y_l, z_r, \xi^*_{l,r}) = \frac{\partial k}{\partial u}(x_p, t_q, y_l, z_r, \eta^*_{l,r})(u^*_{l,r} - \xi^*_{l,r}), \tag{6}$$

where for each $l = 0, 1, \cdots, n, r = 0, 1, \cdots, m$, $\eta_{l,r}$ is a real number between $u^*_{l,r}$ and $\xi^*_{l,r}$. Again by *(iii)* and (6), we conclude that

$$\begin{aligned} |u^*_{p,q} - \xi^*_{p,q}| &\le \gamma \sum_{r=0}^{q} \sum_{l=0}^{n} w'_{q_r} w_l |u^*_{l,r} - \xi^*_{l,r}| + |O(h^\nu_y)| + |O(h^\mu_z)| \\ &\le \gamma |u^*_{p,q} - \xi^*_{p,q}| \sum_{r=0}^{q} \sum_{l=0}^{n} w'_{q_r} w_l + |O(h^\nu_y)| + |O(h^\mu_z)|. \end{aligned}$$

Since in every Newton-Cotes formula $\sum_{r=0}^{q}\sum_{l=0}^{n} w'_{q_r} w_l = (b-a)(d-c)$,

$$|u^*_{p,q} - \xi^*_{p,q}| \leq \frac{|O(h_y^{\nu})| + |O(h_z^{\mu})|}{1 - \gamma(b-a)(d-c)}.$$

□

Inequality (5) leads to the following corollary, **corollary 2.2.** $|u^*_{p,q} - \xi^*_{p,q}|$ vanishes when h_y and h_z tend to zero.

Now, to find the approximate solution, one needs to solve nonlinear equation (4).

3 The successive numerical approach

Iterative methods are widely used for finding approximate solution of nonlinear systems of equations [21]. Borzabadi et. al. in [5] presented a successive substitution, similar to Gauss-Seidel method for solving one dimensional Fredholm integral equation. The nonlinear system of equations (4) has also a structure that permits us to approximate its solution by a similar successive iterative approach presented in [5]. Hereby we define an iterative process which leads to the sequence of matrices $\{\xi^{(k)}\}$. The components of the matrices satisfy the iteration formula,

$$\xi_{i,j}^{(k+1)} = f_{i,j} + \sum_{r=0}^{j}\sum_{l=0}^{n} w'_{j_r} w_l k(x_i, t_j, y_l, z_r, \xi_{l,r}^{(k)}), \tag{7}$$

where $i = 0, 1, \cdots, n, j = 0, 1, \cdots, m$ and $k = 0, 1, \cdots$. Though, the convergence scheme can be constructed for detecting approximate solution (4). However, we first study the conditions that guarantee the convergence of the sequence $\{\xi^{(k)}\}$.

theorem 3.1. *Considering assumptions of Proposition 2.1, the produced sequence* $\{\xi^{(k)}\}$ *from the iteration process* (7) *tends to the exact solution of* (4)*, say* ξ^**, for any arbitrary initial matrix* $\xi^{(0)}$*.*

Proof. By (4) and (7) we have,

$$\xi_{i,j}^{(k+1)} - \xi^*_{i,j} = \sum_{r=0}^{j}\sum_{l=0}^{n} w'_{j_r} w_l (k(x_i, t_j, y_l, z_r, \xi_{l,r}^{(k)}) - k(x_i, t_j, y_l, z_r, \xi^*_{l,r})),$$

and according to condition (*iii*) of Proposition 2.1,

$$\xi_{i,j}^{(k+1)} - \xi_{i,j}^{*} = \sum_{r=0}^{j}\sum_{l=0}^{n} w'_{j_r} w_l \frac{\partial k}{\partial u}(x_i, t_j, y_l, z_r, \eta_{l,r}^{(k)})(\xi_{l,r}^{(k)} - \xi_{l,r}^{*}),$$

where $\eta_{l,r}^{(k)}$ is a real number between $\xi_{l,r}^{(k)}$ and $\xi_{l,r}^{*}$ for $l = 0, 1, \cdots, n$ and $r = 0, 1, \cdots, m$. Thus one may obtain the following inequalities

$$\begin{aligned}|\xi_{i,j}^{(k+1)} - \xi_{i,j}^{*}| &\leq \max_{\substack{0\leq i\leq n\\ 0\leq j\leq m}} |\xi_{i,j}^{(k)} - \xi_{i,j}^{*}| \sum_{r=0}^{j}\sum_{l=0}^{n} w'_{j_r} w_l |\frac{\partial k}{\partial u}(x_p, t_q, y_l, z_r, \eta_{l,r}^{(k)})| \\ &\leq \gamma \max_{\substack{0\leq i\leq n\\ 0\leq j\leq m}} |\xi_{i,j}^{(k)} - \xi_{i,j}^{*}| \sum_{r=0}^{m}\sum_{l=0}^{n} w'_r w_l,\end{aligned}$$

where $i = 0, 1, \cdots, n, j = 0, 1, \cdots, m$. By setting $\lambda = \gamma(b-a)(d-c)$ we conclude that

$$\max_{\substack{0\leq i\leq n\\ 0\leq j\leq m}} |\xi_{i,j}^{(k+1)} - \xi_{i,j}^{*}| \leq \lambda \max_{\substack{1\leq i\leq n\\ 1\leq j\leq m}} |\xi_{i,j}^{(k)} - \xi_{i,j}^{*}|.$$

By mathematical induction on k, we get

$$\max_{\substack{0\leq i\leq n\\ 0\leq j\leq m}} |\xi_{i,j}^{(k+1)} - \xi_{i,j}^{*}| \leq \lambda^k \max_{\substack{0\leq i\leq n\\ 0\leq j\leq m}} |\xi_{i,j}^{(0)} - \xi_{i,j}^{*}|,$$

for each $k = 0, 1, \cdots$. Since $0 < \lambda < 1$, then, $k \to +\infty$ implies that $\max_{\substack{0\leq i\leq n\\ 0\leq j\leq m}} |\xi_{i,j}^{(k+1)} - \xi_{i,j}^{*}|$ vanishes. □

4 Algorithm of the approach

In this section, we propose an algorithm on the basis of the above discussions to solve the Volterra-Fredholm integral equation (1). This algorithm is presented in two stages, the initialization and the main steps.

Initialization
Choose $\epsilon > 0$, and equidistance partitions $\triangle^{(1)} = \{a = x_0 = y_0, x_1 = y_1, \cdots, x_{n-1} = y_{n-1}, x_n = y_n = b\}$ on $[a, b]$ with the step size $h_x = x_{i+1} - x_i,\ i = 0, 1, \cdots, n-1$, plus $\triangle^{(2)} = \{c = t_0 = z_0, t_1 = z_1, \cdots, t_{n-1} = z_{n-1}, t_n = z_n = d\}$ on $[c, d]$ with the step size $h_t = t_{j+1} - t_j,\ j = 0, 1, \cdots, m-1$ and an initial matrix $\xi^{(0)}$. Set $k = 0$ and go to the main steps.
Main steps
Step 1. Compute $\xi^{(k+1)}$ by (6), and go to Step 2.

Step 2. Compute $\max_{\substack{0\leq i\leq n\\ 0\leq j\leq m}} |\xi_{i,j}^{(k+1)} - \xi_{i,j}^{(k)}|$ and go to Step 3.

Step 3. If $\max_{\substack{0\leq i\leq n\\ 0\leq j\leq m}} |\xi_{i,j}^{(k+1)} - \xi_{i,j}^{(k)}| < \epsilon$, stop; Otherwise, set $k = k + 1$ and go to step 1.

In the next section the advantages and the influence of the proposed approach in thrilling convergence rate of the solution for the problems is demonstrated via some examples.

5 Numerical examples

Suppose $u^*(x,t)$ is the exact solution of Volterra-Fredholm integral equation (1) and $\hat{\xi}_{i,j},\ i = 0,1,\cdots,n,\ j = 0,1,\cdots,m$ is a solution obtained by applying the given algorithm with a known $\epsilon > 0$ and partitions $\triangle^{(1)}$ and $\triangle^{(2)}$. To compare the precision of the approximate solution, the discrete error function

$$e(x_i,t_j) = |u^*(x_i,t_j) - \hat{\xi}(x_i,t_j)|,\ i = 0,1,\cdots,n,\ j = 0,1,\cdots,m, \qquad (8)$$

is established.

Example 5.1. In this example, we apply the developed method to a two dimensional Fredholm integral equation as follows [13],

$$u(x,t) = \frac{1}{(1+x+t)^2} - \frac{x}{6(1+t)} + \int_0^1 \int_0^1 \frac{x}{1+t}(1+y+z)u^2(y,z)dydz.$$

This integral equation has analytical solution $u(x,t) = \frac{1}{(1+x+t)^2}$ on $[0,1]\times[0,1]$. We take $\epsilon = 10^{-6}$ and partitions with the discretization parameters $h_x = \frac{1}{100}$ and $h_t = \frac{1}{100}$. The initial matrix $\xi^{(0)} = \mathbf{0}$ is considered first to start the algorithm. In Table 1, one can see all acceptable values for error estimation (8) which is obtained by applying the developed algorithm to the illustrated equation.

Table 1: Error estimation for Example 5.1

x t	0.0	0.2	0.4	0.6	0.8	1.0
0.0	0.000	0.000	0.000	0.000	0.000	0.000
0.2	3.980×10^{-6}	3.317×10^{-6}	2.843×10^{-6}	2.488×10^{-6}	2.211×10^{-6}	1.990×10^{-6}
0.4	7.958×10^{-6}	6.631×10^{-6}	5.684×10^{-6}	4.973×10^{-6}	4.421×10^{-6}	30979×10^{-6}
0.6	1.193×10^{-5}	9.943×10^{-6}	8.522×10^{-6}	7.457×10^{-6}	6.629×10^{-6}	5.966×10^{-6}
0.8	1.590×10^{-5}	1.325×10^{-5}	1.136×10^{-5}	9.940×10^{-6}	8.835×10^{-6}	7.952×10^{-6}
1.0	1.987×10^{-5}	1.656×10^{-5}	1.420×10^{-5}	1.242×10^{-5}	1.104×10^{-5}	9.937×10^{-6}

Example 5.2. In this example, we apply our method for the following two dimensional Fredholm integral equation [2],

$$u(x,t) = xe^{-t} - \frac{1}{2}t - \frac{7}{12}x + \frac{1}{3}xe^{-1} + \int_0^1 \int_0^1 (xy + te^z)u(y,z)dydz.$$

The analytical solution of this integral equation is $u(x,t) = xe^{-t} + t$ on $[0,1] \times [0,1]$. By solving this equation, we observe that the proposed algorithm does not give rise to a convergent sequence. So, to overcome this shortcoming, we put $[0, 0.1] \times [0, 0.1]$ in place of $[0,1] \times [0,1]$, where the conditions of Theorem 3.1 hold. Then

$$u(x,t) = xe^{-t} + \frac{1799}{2000}t - \frac{43}{120000}x + \frac{9}{100}te^{-0.1} + \frac{1}{3000}xe^{-1} + \int_0^{0.1} \int_0^{0.1} (xy + te^z)u(y,z)dydz.$$

Table 2 shows that in this region of integration, approximate solution tracks the exact one, almost precise.

Table 2: Error estimation for Example 5.2

x t	0.0	0.02	0.04	0.06	0.08	0.1
0.0	0.000	3.598×10^{-11}	7.197×10^{-11}	1.080×10^{-10}	1.439×10^{-10}	1.799×10^{-10}
0.02	3.178×10^{-11}	6.776×10^{-11}	1.037×10^{-10}	1.397×10^{-10}	1.757×10^{-10}	2.117×10^{-10}
0.04	6.356×10^{-11}	9.954×10^{-11}	1.355×10^{-10}	1.715×10^{-10}	2075×10^{-10}	2435×10^{-10}
0.06	9.533×10^{-11}	1.313×10^{-10}	1.673×10^{-10}	2.033×10^{-10}	2.393×10^{-10}	2.752×10^{-10}
0.08	1.271×10^{-10}	1.631×10^{-10}	1.991×10^{-10}	2.351×10^{-10}	2.710×10^{-10}	3.070×10^{-10}
0.1	1.589×10^{-10}	1.949×10^{-10}	2.308×10^{-10}	2.668×10^{-10}	3.028×10^{-10}	3.388×10^{-10}

Example 5.3. In this example, we apply the proposed method to the following two dimensional Volterra integral equation [18],

$$u(x,t) = xsin(t)(1 - \frac{x^2 sin^2(t)}{9}) + \frac{x^6}{10}(\frac{sin(2t)}{2} - t) + \int_0^t \int_0^x (xy^2 + cos(z))u^2(y,z)dydz.$$

This integral equation has analytical solution $u(x,t) = xsin(t)$ on $[0,1] \times [0,1]$. We take $\epsilon = 10^{-6}$ and partitions with the discretization parameters $h_x = \frac{1}{100}$ and $h_t = \frac{1}{100}$. The initial matrix $\xi^{(0)} = \mathbf{0}$ is considered for starting the algorithm. Table 3 illustrates the precision of the approximate solution by showing the error criteria (7) corresponding to the given partition.

Table 3: Error estimation for Example 5.3

x t	0.0	0.2	0.4	0.6	0.8	1.0
0.0	3.906×10^{-31}	2.651×10^{-33}	1.716×10^{-33}	7.961×10^{-34}	2.432×10^{-34}	4.102×10^{-35}
0.2	3.227×10^{-33}	1.722×10^{-8}	8.025×10^{-8}	2.172×10^{-7}	4.268×10^{-7}	6.769×10^{-7}
0.4	4.711×10^{-33}	8.889×10^{-8}	2.616×10^{-7}	5.724×10^{-7}	1.025×10^{-6}	1.569×10^{-6}
0.6	1.199×10^{-32}	2.928×10^{-7}	7.087×10^{-7}	1.338×10^{-6}	2.213×10^{-6}	3.293×10^{-6}
0.8	5.513×10^{-32}	7.761×10^{-7}	1.742×10^{-6}	3.063×10^{-6}	4.852×10^{-6}	7.135×10^{-6}
1.0	3.906×10^{-31}	1.833×10^{-6}	4.003×10^{-6}	6.847×10^{-6}	1.067×10^{-5}	1.571×10^{-5}

Example 5.4. In this example, we apply our method to a Volterra-Fredholm integral equation as follows [3],

$$u(x,t) = x^2 + xt - \frac{1}{15}xt^4 - \frac{1}{16}xt^5 + \int_0^t \int_0^1 xty^2z^2u(y,z)dydz.$$

This integral equation has analytical solution $u(x,t) = x^2+xt$ on $[0,1]\times[0,1]$. We take $\epsilon = 10^{-6}$ and partitions with the discretization parameters $h_x = \frac{1}{100}$ and $h_t = \frac{1}{100}$. The initial matrix $\xi^{(0)} = \mathbf{0}$ is considered for starting the algorithm. Table 4 exhibits good error values by applying the developed algorithm.

Table 4: Error estimation for Example 5.4

x t	0.0	0.2	0.4	0.6	0.8	1.0
0.0	0.000	0.000	0.000	0.000	0.000	0.000
0.2	0.000	4.063×10^{-8}	2.567×10^{-7}	9.000×10^{-7}	2.425×10^{-6}	5.598×10^{-6}
0.4	0.000	8.126×10^{-8}	5.133×10^{-7}	1.800×10^{-6}	4.850×10^{-6}	1.119×10^{-5}
0.6	0.000	1.219×10^{-7}	7.699×10^{-7}	2.700×10^{-6}	7.276×10^{-7}	1.679×10^{-5}
0.8	0.000	1.625×10^{-7}	1.027×10^{-6}	3.600×10^{-6}	9.701×10^{-6}	2.239×10^{-5}
1.0	0.000	2.031×10^{-7}	1.283×10^{-6}	4.500×10^{-6}	1.213×10^{-5}	2.799×10^{-5}

6 Conclusions

In this paper, an iterative approach for obtaining approximate solutions for two dimensional Volterra-Fredholm integral equations, considering some special conditions on the kernel, as continuous differentiability of kernel, is proposed. Theorem 3.1 provides a sufficient condition for convergence of the approach, but it is not necessary. Therefore, Examples 5.1, 5.3, and 5.4 show that, despite the lack of conditions, convergence of the proposed method holds for a class of two dimensional Volterra-Fredholm integral equations. Also the changing in problem for holding conditions of Theorem 3.1 lead to the convergence of the method, as it is described in Example 5.2. The validity and efficiency of the proposed scheme is demonstrated on the examples included.

References

1. Atkinson, K. and Han, W. *Theoretical Numerical Analysis: A Functional Analysis Framework*, Texts in Appl. Math. 39 (2005), Springer, New York, second edition, .

2. Avazzadeh, Z., Heydari, M. and Loghmani, G. B. *A Comparison Between Solving Two Dimensional Integral Equations by the Traditional Collocation Method and Radial Basis Functions*, Appl. Math. Sciences, 5(23) (2011) 1145 - 1152.

3. Babolian, E. and Jafari Shaerlar, A. *Two Dimensional Block Pulse Functions and Application to Solve Volterra-Fredholm Integral Equations with Galerkin Method*, Int. J. Contemp. Math. Sciences, 6(16) (2011) 763-770.

4. Badr, A. A. *Block-by-Block Method for Solving Nonlinear Volterra-Fredholm Integral Equation*, Math. Problems in Engineering, Article ID 537909, doi:10.1155/2010/537909, (2010) 8 pages.

5. Borzabadi, A. H. and Fard, O. S. *A numerical scheme for a class of nonlinear Fredholm integral equations of the second kind*, Journal of Comput. and Appl. Math. 232 (2009) 449-454.

6. Brunner, H. *On the numerical solution of nonlinear Volterra-Fredholm integral equation by collocation methods*, SIAM J. Numer. Anal. 27(4) (1990) 987-1000.

7. Brunner, H. and Messina, H. *Time-stepping methods for Volterra-Fredholm integral equations*, Rediconti di Mathematica, Serie VII, 23 (2003) 329-342.

8. Chan, R. and Ng, M. K. *Conjugate gradient methods for Toeplitz systems*, SIAM Review, 38 (1996) 427-482.

9. Cherruault, Y. and Saccomandi, G. *Some, New results for convergent of Adomian's method applied to integral equation*, Math. Comput. Modelling, 16(2) (1992) 85-93.

10. Farengo, R., Lee, Y. C. and Guzdar, P. N. *An electromagnetic integral equation: application to microtearing modes*, Phys. Fluids, 26 (1983) 3515-3523.

11. Guoqiang, H. *Asymptotic error expansion for the Nystrom method for a Volterra-Fredholm integral equations*, J. Comput. Appl. Math. 59 (1995) 49-59.

12. Hacia, L. *On approximate solution for integral equations of mixed type*, ZAMM Z. Angew. Math. Mech. 76 (1996) 415-416.

13. Han, G. Q. and Wang, R. F. *Richardson extrapolation of iterated discrete Galerkin solution for two-dimensional Fredholm integral equations*, J. Comput. and Appl. Math, 139 (2002) 49-63.

14. Jerri, A. J. *Introduction to Integral Equations with Applications*, John Wiley and Sons, INC, (1999).

15. Kauthen, P. J. *Continous time collocation methods for Volterra-Fredholm integral equations*, Numer. Math. 56 (1989) 409-424.

16. Kress, R. *Linear Integral Equations*, Springer-Verlag, New York, (1989).

17. Maleknejad, K. and Hadizadeh, M. *A new computational method for Volterra-Fredholm integral equations*, J. Comput. Math. Appl. 37(9) (1999) 1-8.

18. Nadjafi, J. S., Samadi, O. N. and Tohidi, E. *Numerical Solution of Two-Dimensional Volterra Integral Equations by Spectral Galerkin Method*, Journal of Appl. Math. and Bioinformatics, 1(2) (2011) 159-174.

19. Pachpatte, B. G. *On a New Inequality Applicable to Certain Volterra-Fredholm Type Sum-difference Equations*, Tamsui Oxford Journal of Mathematical Sciences, 26(2) (2010) 173-184.

20. Rajan, D. and Chaudhuri, S. *Simultaneous estimation of super-resolved scene and depth map from low resolution defocused observations*, IEEE Transactions on Pattern Analysis and Machine Intelligence, 25 (2003) 1102-1117.

21. Stoer, J. and Bulirsch, R. *Introduction to Numerical Analysis*, Speringer-Verlage, New York, (1993).

Persian Translation of Abstracts

روشهای واسط غوطه ور مرتبه بالا برای معادله موج آکوستیک با ضرایب ناپیوسته

جواد فرضی و سید محمد حسینی

چکیده : این مقاله در مورد حل عددی معادله موج آکوستیک است که دامنه جواب شامل واسطهایی باشد. برای حل مسائل واسط باید توجه زیادی به واسطها شود تا مرتبه دقت بالا حاصل شود. در واقع، هرگونه کاربرد مستقیم یک روش تفاضل متناهی مرتبه بالا برای چنین مسائلی به جوابهای تقریبی نادقیق با نوسانات بالا در واسطها منجر می شود. با این وجود، امکان بدست آوردن روشهای مرتبه بالا برای رفع این پدیده در واسط وجود دارد. در این مقاله یک روش واسط غوطه ور مرتبه ششم برای معادله موج آکوستیک ارائه می شود. مرتبه دقت در ناپیوستگی با استفاده از شرایط پرش حفظ می شود. تعدادی بررسی عددی قرار داده شده است که مرتبه دقت و پایداری عددی روش ارائه شده را تایید می کند.

کلمات کلیدی : روشهای واسط؛ روشهای مرتبه بالا؛ روش لکس وندروف؛ ضرایب ناپیوسته؛ شرایط پرش.

حل عددی دستگاه معادلات دیفرانسیل سخت بدست آمده از واکنش های شیمیایی

غلامرضا حجتی، علی عبدی، فرشته میرزایی، و سعید بی مثل

چکیده : دستگاه های مسایل مقدار اولیه سخت در بازه های انتگرال گیری بزرگ از واکنش های شیمیایی، برای حل به روش های کارا با دقت خوب و ناحیه پایداری وسیع نیاز دارند. در این مقاله روش های خطی عمومی مشتق دوم را برای حل چند مساله سخت شیمیایی مانند آکزو نوبل شیمیایی، مساله HIRES و مساله OREGO به کار می بریم.

کلمات کلیدی : روش های خطی عمومی؛ معادلات دیفرانسیل معمولی؛ واکنش های شیمیایی؛ دستگاه های سخت.

یک روش عددی بر مبنای ماتریس های عملیاتی برای حل معادلات دیفرانسیل-انتگرال غیر خطی

احمد گلبابایی

چکیده : این مقاله یک روش محاسباتی را برای دو دسته از معادلات انتگرال دیفرانسیل بیان می کند، دستگاه غیر خطی معادله انتگرال دیفرانسیل ولترا فردهلم و معادله انتگرال دیفرانسیل غیر خطی از مرتبه کسری . ابزار مورد استفاده برای این کار ماتریس های عملیاتی انتگرال و انتگرال کسری می باشد. با این روش ، مساله داده شده تبدیل به یک دستگاه جبری می شود. مثال هایی عددی داده شده که کارایی ودقت بالای روش را اثبات می کنند.

کلمات کلیدی : ماتریس عملیاتی انتگرال؛ ولترا – فردهلم؛ دستگاه غیر خطی معادله انتگرال دیفرانسیل؛ مرتبه کسری؛ موجک لژاندر.

حل مساله معکوس برای معادله سهموی با شرایط مرزی غیر موضعی در فضای هسته بازتولید

مریم محمدی، رضا مختاری، و فرشته طوطیان اصفهانی

چکیده : در اين مقاله، الگوريتمي بازگشتي براي حل يك مساله معكوس سهموي با يك شرط مرزي غيرموضعي در فضاي هسته بازتوليد ارايه مي‌شود. جواب تحليلي مساله در فضاي هسته بازتوليد به صورت يك سري نامتناهي و جواب تقريبي از قطع كردن سري نامتناهي جواب تحليلي به دست مي‌آيد. همگرايي جواب تقريبي به جواب تحليلي نيز ثابت مي‌شود. نتايج عددي به دست آمده از روش، حاكي از آن است كه مي‌توان آن را به عنوان يك روش ساده و كارا در حل چنين مسايل معكوسي در نظر گرفت.

کلمات کلیدی : مساله معكوس سهموي؛ شرط مرزي غيرموضعي؛ فضاي هسته بازتوليد.

روش تقریبی برای حل عددی مسائل کنترل بهینه کسری تأخیری چند بعدی با استفاده از چندجملهای های برنشتاین

الهه صفایی و محمد هادی فراهی

چکیده :

در این مقاله روشی جدید برای حل مسائل کنترل بهینه کسری تأخیری که تأخیر روی تابع وضعیت و نیز تابع کنترل اعمال شده، ارائه می گردد. این روش بر اساس استفاده از چندجمله ای های برنشتاین و کنترل بازخورد می باشد. مهمترین مزیت به کارگیری کنترل بازخورد این است که می توان تأثیر چنین کنترل هایی را بر روی دستگاه دینامیکی مشاهده و خروجی را بر اساس این مشاهدات اصلاح کرد. در این مقاله از چندجمله ای های برنشتاین برای تبدیل دستگاه کنترلی کسری تأخیری با ضرایب وابسته به زمان، به یک دستگاه جبری بر حسب ضرایب مجهول تابع وضعیت و تابع کنترل در تقریب برنشتاین بهره می بریم. لازم به ذکر است که در این مقاله از مشتق کسری کپتو با درجه $0 < \alpha \leq 1$ استفاده شده است. در پایان چند مثال عددی برای نشان دادن صحت و اعتبار روش ارائه می گردد.

کلمات کلیدی : مسأله کنترل بهینه کسری تأخیری؛ مشتق کسری کپتو؛ چندجمله ای برنشتاین.

یک رهیافت تکرار متوالی برای معادلات انتگرالی والترا- فردهلم غیرخطی دو بعدی

اکبر هاشمی برزآبادی و محمد حیدری

چکیده : در این مقاله، یک روش تکراری برای بدست آوردن جوابهای معادلات انتگرالی ولترا-فردهلم پیشنهاد شده است. با در نظر گرفتن شرایطی روی هسته معادله انتگرالی که از گسسته سازی معادله انتگرالی حاصل شده، همگرایی جواب تقریبی به جواب دقیق معادله بررسی شده است. برای نمایش کارایی روش چندین مثال در نظر گرفته شده است.

کلمات کلیدی : معادله انتگرالی ولترا-فردهلم؛ روش تکراری؛ گسسته سازی؛ تقریب.

Aims and scope

Iranian Journal of Numerical Analysis and Optimization (IJNAO) is published twice a year by the Department of Applied Mathematics, Faculty of Mathematical Sciences, Ferdowsi University of Mashhad. Papers dealing with different aspects of numerical analysis and optimization, theories and their applications in engineering and industry are considered for publication.

Journal Policy

After receiving an article, the editorial committee will assign referees. Refereeing process can be followed via the web site of the Journal.
The manuscripts are accepted for review with the understanding that the work has not been published and also it is not under consideration for publication by any other journal. All submissions should be accompanied by a written declaration signed by the author(s) that the paper has not been published before and has not been submitted for consideration elsewhere.

Instruction for Authors

The Journal publishes all papers in the fields of numerical analysis and optimization. Articles must be written in English.
All submitted papers will be refereed and the authors may be asked to revise their manuscripts according to the referee's reports. The Editorial Board of the Journal keeps the right to accept or reject the papers for publication.
The papers with more than one authors, should determine the corresponding author. The e-mail address of the corresponding author must appear at the end of the manuscript or as a footnote of the first page.
It is strongly recommended to set up the manuscript by Latex or Tex, using the template provided in the web site of the Journal. Manuscripts should be typed double-spaced with wide margins to provide enough room for editorial remarks.
References should be arranged in alphabetical order by the surname of the first author as examples below:
[1] Stoer, J. and Bulirsch, R. *Introduction to Numerical Analysis*, Springer-verlag, New York, 2002.
[2] Brunner, H. *A survey of recent advances in the numerical treatment of Volterra integral and integro-differential equations*, J. Comput. Appl. Math. 8 (1982), 213-229.

Submission of Manuscripts

Authors may submit their manuscripts by either of the following ways:

a) Online submission (pdf or dvi files) via the website of the Journal at:

http://jm.um.ac.ir/index.php/math

b) Via journal's email mjms@um.ac.ir

Copyright Agreement

Upon the acceptance of an article by the Journal, the corresponding author will be asked to sign a "Copyright Transfer Agreement" (see the web site) and send it to the Journal address. This will permit the publisher to publish and distribute the work.

Iranian Journal of Numerical Analysis and Optimization

Former : MRJMS

CONTENTS Vol. 4, No.1, pp 1-104, 2014

web site : http://jm.um.ac.ir

Email : mjms@um.ac.ir

ISSN : 1735-7144